Electrospun Polymer Electrolyte Membranes for Fuel Cell Applications

by

Carlo Otaño Gracia

A thesis submitted in partial fulfillment of the requirements for the degree of

MASTER OF SCIENCE
in
MECHANICAL ENGINEERING

UNIVERSITY OF PUERTO RICO
MAYAGÜEZ CAMPUS
2012

Approved by:

_____	_____
Ricky Valentin, PhD President, Graduate Committee	Date
_____	_____
Quintero, Pedro, PhD Member, Graduate Committee	Date
_____	_____
Jia, Yi, PhD Member, Graduate Committee	Date
_____	_____
Juan, Ortiz, PhD Representative of Graduate Studies	Date
_____	_____
Gutierrez, J. Gustavo, PhD Director, Department of Mechanical Engineering	Date

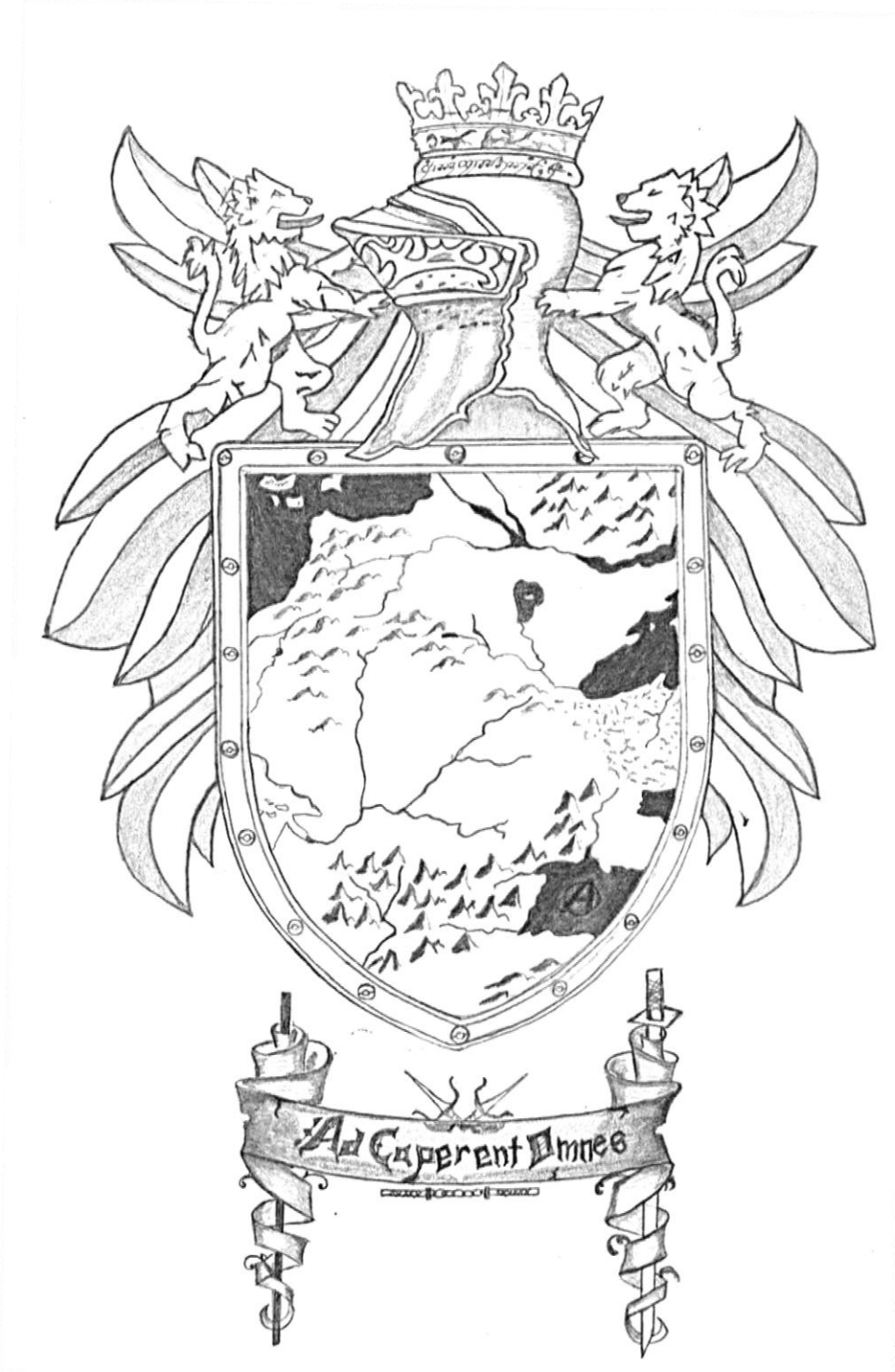
Ad Experent Omnes

Abstract:

Low temperature fuel cells have attracted a lot of attention for use as small portable power sources. The performance of the fuel cells is largely dependent on the cathode, anode and the Polymer Electrolyte Membrane (PEM). For the PEM in particular, many important characteristics are determined by the membrane morphology which is dependent on the fabrication method. Extrusion and casting are two of the most popular ones. Meanwhile, electrospinning is becoming a very popular fabrication method because it can create a woven-like membrane composed of many nano-sized fibers with very interesting morphological properties such as high surface area to volume ratio, pinhole resistance and low fuel crossover. A Nafion-Poly (Acrylic Acid) (PAA) blend was electrospun to create polymer electrolyte membranes for fuel cell applications. The membranes were pressed, heat treated, cleaned and activated. Optical and scanning electron microscopy was performed on the membranes to characterize the surface morphology, fiber orientation and fiber diameter. Different parameters were tested as a function of the compacting pressure and the annealing temperature. Water uptake and ion exchange capacity were used to characterize the water content of the membranes. The solubility and mechanical properties of the membranes were also determined. The electrospun membranes were compared to commercially available membranes. The electrospun membranes were found to have higher water content with an increase of 1,017% when compared with the commercial membranes when the water uptake and the ion exchange capacity were evaluated. The water uptake, ion exchange capacity and water content were found to be dependent on the Nafion-PAA concentration and the processing order but not on the annealing temperature and compressing pressure. The electrospun membrane's solubility was found to be dependent on the annealing temperature and the mechanical strength was found to be a function of the Nafion-PAA concentrations. The fiber diameter distribution was found to change as function of Nafion content with higher content resulting in smaller diameters and the fiber orientation was only dependant on the oscillating drum collector used in the electrospinning process.

Resumen:

Las pilas de combustión de baja temperatura han atraído mucha atención para usarse como pequeñas fuentes de energía portátiles. El rendimiento de las pilas de combustión depende en gran medida de la Membrana de Polímero Electrolítica (PEM). Muchas características importantes del PEM son determinados por la morfología de la membrana. La morfología de la membrana está determinada en gran medida por el método de fabricación como extrusión o fundición. Electrotejido es un proceso de manufactura que puede crear una membrana hecha de un tejido compuesto por nano-fibras con propiedades morfológicas muy interesantes. Estas características son: una alta razón de área de superficie en relación al volumen, resistencia a agujeros de alfiler y resistencia a la filtración de combustible. Una mezcla de Nafion y Acido (Poli Acrílico) (PAA) se unieron para crear una solución de alta viscosidad cuyo uso sea adecuado para el proceso de electrotejido. A través del electrotejido se crea una membrana que será adherida dentro de una pila de combustión. Posterior al electrotejido las membranas son sometidas a un proceso de compactación bajo presión, además se le realizan tratamientos térmicos, de limpieza y activación. La microscopia óptica y electrónica de barrido fue utilizada para caracterizar la morfología superficial, la distribución de diámetro de las fibras y su orientación. Diferentes parámetros en función de la temperatura del tratamiento térmico y de la presión de compactación fueron probados para identificar sus efectos en la membrana. La absorción de agua y capacidad de intercambio iónico fueron utilizados para analizar el contenido acuosos de las membranas. Adicionalmente se caracterizo la solubilidad y la fuerza de tensión máxima de las mismas. Las membranas producidas por electrotejido obtuvieron mayor contenido acuoso con un aumento máximo de 1,017% comparadas con las membranas comerciales al analizar la absorción de agua y el intercambio iónico. Se encontró que la absorción de agua, el intercambio iónico y el contenido acuoso dependen de la concentración de Nafion-PAA y del orden de procesamiento pero no de la temperatura de tratamiento térmico ni de la presión de compresión. Se hallo que la solubilidad tan solo es afectada por la concentración de Nafion-PAA y por la temperatura del tratamiento térmico. La distribución del diámetro varió en función del contenido de Nafion y la orientación de la fibra tan solo dependió del colector oscilatorio

Table of Contents

Table of Figures

Table of Tables

Table of Equations

1 Introduction

Fuel cell technology has the potential to greatly improve our daily lives and protect the environment. Primitive fuel cells have been around since the 1840s. Since then, fuel cells have come a long way to offer us some unique advantages: no moving parts and a high maximum theoretical efficiency without unwanted byproducts like CO_2 [1]. One of the major disadvantages of fuel cell is its high cost compared to other technologies [2]. A new Electrospun Polymer Electrolyte Membrane (EPEM) is proposed in order to improve upon the cost and manufacturability of fuel cells. The EPEM can potentially have a simple manufacturing process. This membrane can be implemented with a hybrid fuel cell in order to construct an electrospun polymer electrolyte hybrid fuel cell. This thesis will lay the ground work by establishing a fundamental understanding of the properties of this type of membrane from a morphological perspective.

1.1 Objectives

- Improve polymer electrolyte membranes by increasing the water content of the membranes.
- Use electrospinning to create polymer electrolyte membranes.
- Determine the effects of the manufacturing and processing parameters on the polymer electrolyte membrane.

1.2 Hybrid Fuel Cell

A fuel cell works as an electrochemical cell were it consumes a fuel (reactants) and produces electricity and byproducts. The main components of the fuel cell are illustrated in Figure 1. They consist of the anode, cathode and the electrolyte. Reactant and reaction products are managed in the cathode and anode, while all the chemical reactions occur at the interface between these three major components.

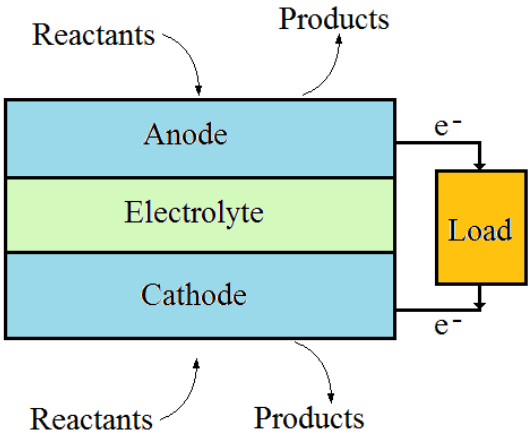

Figure 1: Major components of a fuel cell

Most fuel cells use a single electrolyte, e.g. a Proton Exchange Membrane (PEM) or an Anion Exchange Membrane (AEM), and are called Polymer Electrolyte Membrane Fuel Cells (PEMFC). A Hybrid Fuel Cell (HFC) incorporates both membranes, the PEM and AEM. The PEM allows positive ions to transverse the membrane but no electrons. The AEM allows negative ions to transverse the membrane but no electrons. This process is presented in Figure 2.

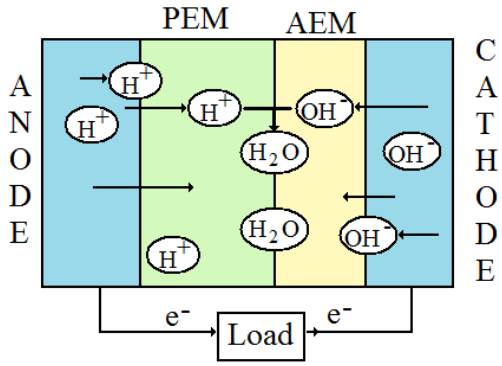

Figure 2: Hybrid fuel cell

The PEMFC typically uses perfluorinated membranes such as Nafion® manufactured by DuPont as an electrolyte. Nafion has a polytetrafluoroethylene or Teflon ™ backbone functionalized with sulfonic acid ($SO_3^-H^+$) groups. The Teflon ™ backbone gives the Nafion its mechanical strength while the sulfonic groups provide charge mobility for proton conductivity. A Nafion membrane can be manufactured using numerous techniques including extruding, recasting, die casting and electrospinning. Different techniques create different morphologies which in turn gives the Nafion different properties and characteristics.

1.3 Electrolyte Material

A major component of all fuel cells is the electrolyte. The electrolyte forms a barrier which forces electrons to go around but allows ions to pass. The electrolyte is so important that it forms the basis for fuel cell classification. Table 1 summarizes the five major types of fuel cells and their electrolytes.

Table 1: Comparison of fuel cell technologies [3].

Fuel Cell Type	Common Electrolyte	Operating Temperature	Advantages	Disadvantages
Polymer Electrolyte Membrane (PEM)	Perfluoro sulfonic acid	50-100°C	• Solid electrolyte reduces corrosion & electrolyte management problems • Low temperature • Quick start-up	• Expensive catalysts • Sensitive to fuel impurities • Low temperature waste heat
Alkaline (AFC)	Aqueous solution of potassium hydroxide soaked in a matrix	90-100°C	• Cathode reaction faster in alkaline electrolyte, leads to high performance • Low cost components	• Sensitive to CO_2 in fuel and air • Electrolyte management
Phosphoric Acid (PAFC)	Phosphoric acid soaked in a matrix	150-200°C	• Higher temperature enables CHP • Increased tolerance to fuel impurities	• Pt catalyst • Long start up time • Low current and power
Molten Carbonate (MCFC)	Solution of lithium, sodium, and/ or potassium carbonates, soaked in a matrix	600-700°C	• High efficiency • Fuel flexibility • Can use a variety of catalysts • Suitable for CHP	• High temperature corrosion and breakdown of cell components • Long start up time • Low power density
Solid Oxide (SOFC)	Yttria stabilized zirconia	700-1000°C	• High efficiency • Fuel flexibility • Can use a variety of catalysts • Solid electrolyte • Suitable for CHP & CHHP • Hybrid/GT cycle	• High temperature corrosion and breakdown of cell components • High temperature operation requires long start up time and limits

Many PEMFC use Nafion as a polymer electrolyte membrane. Nafion is an ionomer, a polymer with a neutral backbone but with ionized side chains. Nafion was the first ionomer discovered in the late 1960 by Walther Grut while working in DuPont. Nafion has excellent mechanical properties and proton conductivity. Figure 3 shows the structure of Nafion, composed of the copolymerization of a perfluorinated vinyl ether co-monomer with tetrafluoroethylene (TFE).

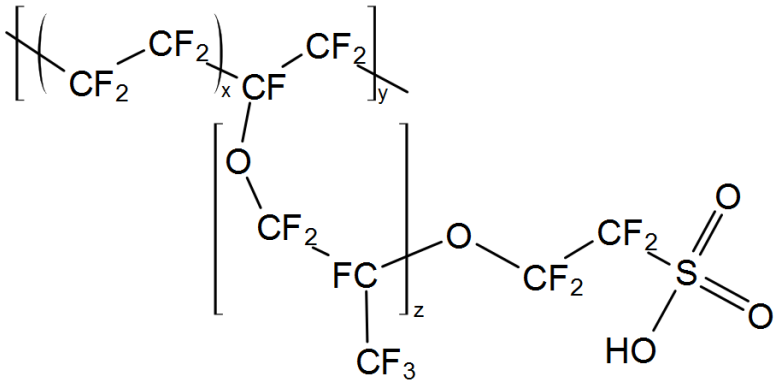

Figure 3: Nafion ionomer composed of the copolymerization of a perfluorinated vinyl ether co-monomer with tetrafluoroethylene (TFE) [4]. x = 5-13, y ≈ 1000, z = 0-3.

1.3.1 Membrane Morphology

Electrolyte material is important in determining membrane characteristics but membrane morphology also plays a crucial role. Ionomers cannot be melt-processed because of the strong

interactions between ionic groups. Traditional Nafion polymer electrolyte membranes are created in two different manners, extruded and recast membranes.

Extruded membranes are created from a precursor polymer, $-SO_2F$. The precursor can then be chemically treated with hot NaOH to change its composition to its neutral state $-SO_3Na$. The new polymer changes in composition but keeps the crystalline structure of the extruded polymer. Finally, the membrane is activated in concentrated acid to create the acid form SO_3H. The semi-crystalline nature introduced by the extrusion process gives the membranes very distinct characteristics, giving it good mechanical properties and rendering it virtually insoluble in most solvents under normal conditions. It is however soluble in an ethanol-water mix under high pressure and temperature creating a Nafion polymer solution [5].

The Nafion polymer solution can be cast (named recast membrane) by drying the solvents into many desirable geometries. At first it was assumed that the morphology of the recast films would be similar to the extruded membranes. But the recast membranes had very different properties. They are soluble in many solvents and have poor mechanical properties. Recast membranes lack any crystalline structure and are completely amorphous [6].

By using a technique known as solution processed films, Nafion membranes are obtained with the desirable properties of extruded Nafion, including the morphology. The process involves casting Nafion membranes at temperatures greater than 160 ^{o}C. This process recreates a semi-crystalline structure similar to extruded membranes. The fabrication process plays a crucial role in determining membrane characteristics. The fact that two chemically identical Nafion membranes have very different properties underscores the importance of morphology.

By using electrospinning, a new Nafion membrane fabrication process can be created. Electrospun Nafion membranes have been created in the past but none with an oscillating rotating drum. Nano-sized fibers can be used as the backbone for the Nafion membrane using electrospinning. The resulting morphology has a high surface area to volume ratio which is favorable for catalytic reactions. In addition, the resulting fiber structure has been shown to help reduce fuel crossover and pinhole losses [7].

1.4 Fuel Cells Fundamentals

In this section fuel cell fundamentals are introduced to the reader. The section starts with a basic overview of fuel cells, followed by their components, an example and finally their looses.

1.4.1 Introduction

Fuel cells work as electrochemical cells that convert internal energy into electricity (and thus produce work) similar to a battery. The main difference between a battery and a fuel cell is that batteries are a closed system while fuel cells are open systems. Once all chemicals are spent within the battery it can no longer generate any electricity. But a fuel cell with an ample supply of reactants can generate electricity for a very long time (maintenance will be required). Unlike traditional methods of converting internal energy to work, fuel cells forgo combustion. In this manner, fuel cells can be more efficient than traditional combustion power sources.

The maximum theoretical efficiency of a fuel cell is the ratio between the Gibbs free energy and the enthalpy. For a H_2-O_2 fuel cell at 25 ^oC the efficiency is 83%. The maximum efficiency of a heat expansion engine is given by the Carnot cycle. For an engine that operates at 450 ^oC

and rejects heat at 45^{o}C (generous operating parameters) the maximum efficiency will be 56%. Of course these are theoretical maximum and actual operating efficiencies will be much lower.

The only fuel cell suitable for portable applications, such as laptops or vehicles, is the Polymer Electrolyte Membrane Fuel Cells (PEMFC). PEMFC operates at low temperatures and have high power densities. For PEMFC to become competitive, and an alternate technology for every day applications, its performance must be increased. The electrospun polymer electrolyte membranes developed as part of this thesis can be used with a variety of fuels such as methanol and hydrogen. Major fuel cell parts most first be discussed to completely understand fuel cell operation.

1.4.2 Fuel Cell Components

Most fuel cells are constructed like a sandwich with all their layers stacked next to each other as seen in Figure 4. All parts are carefully designed to optimize surface area when working as a single or a stack of cells.

Major components of a fuel cell:

- Bipolar plate
- Gas Diffusion Layer (GDL)
- Membrane Electrolyte Assembly (MEA)

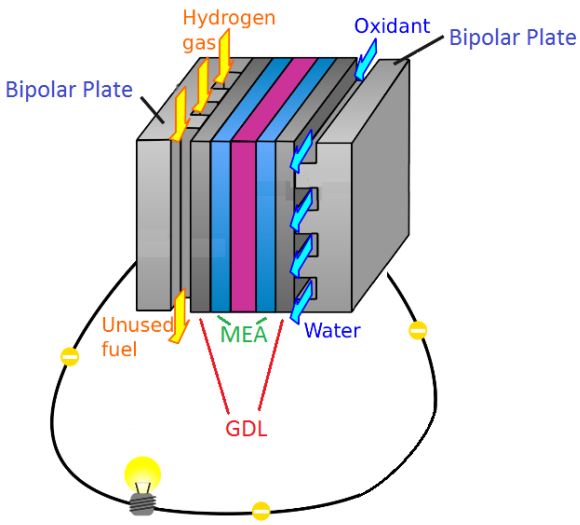

Figure 4: Major parts of a fuel cell

The bipolar plates work as an anode in one side and cathode on the other (hence their name) when the fuel cells are configured as stacks. They are electrically conductive and have flow channels constructed directly on them. The bipolar plates conduct electricity towards an external circuit and relay the reactants and products in and out of the fuel cell. The fuel cell temperature is controlled by applying heat or removing heat from the bipolar plate. They are most commonly constructed from graphite, phenol polymers and metals such as stainless steel.

The Gas Diffusion layers (GDL) helps diffuse the reactants from the flow channels towards the MEA and backwards for the products. It also conducts electricity between the catalyst and the bipolar plates. A more appropriate name would be “transport layer” since liquids, gasses and electricity pass through it. It is commonly made from carbon paper or carbon cloth.

The Membrane Electrolyte Assembly (MEA) is composed of the membrane sandwiched between tow catalyst layers, called a three layer MEA. The GDL can be directly incorporated into the MEA, being called a five layer MEA. The assembly is prepared by placing the PEM

between two appropriate catalysts and hot compressing in a press. The common catalysts used are platinum on carbon or alumina, rhodium on alumina and ruthenium.

1.4.3 Fuel Cell Operation

PEMFC have different steps required to produce electricity as shown in Figure 5. All steps can play an important part in the overall fuel cell efficiency and will be briefly discussed:

1. Reactant Transport
2. Electrochemical Reaction
3. Ionic Conduction through the electrolyte
4. Electron conduction through external circuit.
5. Product removal

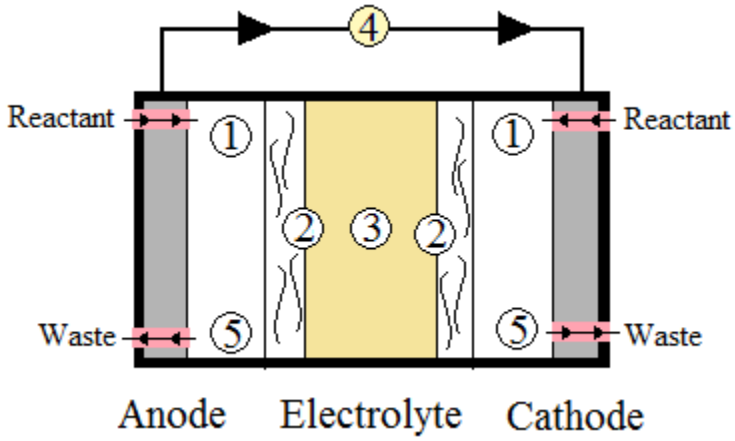

Figure 5: Major steps in fuel cell operation.

1. Reactant Transport: All fuel cells consume reactants, and a steady supply must be provided. Reactants are usually delivered through serpentine flow channels in order to improve

efficiency. The reactants then reach the Gas Diffusion Layer (GDL) where they are distributed towards the catalyst layer. Most common reactants for PEMFC are oxygen, hydrogen, methanol and air. Reactants are usually introduced with excessive water moisture to insure adequately hydrated electrolyte membrane. Without this moisture the electrolyte membrane would lose ionic conductivity do to dehydration.

2. Electrochemical reaction: This is the location where the catalyst, reactant and electrolyte coexist. The electrochemical reaction separates the electrons from the reactant and creates an ion which will then transverse the electrolyte membrane. The amount of current generated by the fuel cell is related to how fast the electrochemical reaction takes place. Careful consideration must be made when choosing a catalyst and designing the reaction zones.

3. Ionic Conduction: Ionic conduction takes place through the polymer electrolyte. Electricity can be harvested from a fuel cell by forcing the ions to go through the membrane but rejecting the electrons. Ions, even single protons, are much more massive than electrons and thus penetrate the membranes with more difficulty. The polymer electrolyte is usually made of Nafion. If the polymer electrolyte has poor ionic conductivity the fuel cell will perform poorly. Improving the properties of the polymer electrolyte is one of the focuses of this thesis.

4. Electron Conduction through external circuit: Since the electrons are rejected by the electrolyte they are forced to go through an alternate route. This detour allows the electrons to be harvested as power source. Once electrons are used, they return to the cell to complete the electrochemical reaction by combining with the ion and a reactant.

5. Product Removal: Once the electrochemical reaction is completed, a product will be generated and it must be removed. Most typical products are H_2O and CO_2. Product removal

also plays a role in water management. Without proper product removal there could be flooding and the electrochemical reaction would be "starved".

1.4.4 Example: H_2-O2 PEMFC

For a hydrogen-oxygen fuel cell the main reactants will be hydrogen and oxygen and the products will be water. The hydrogen will be supplied to the anode via a little tube. Once it reaches the bipolar plate on the anode side will flow through the channels over GDL. The GDL will help diffuse the hydrogen toward the catalyst. The same thing will be happening over the cathode bipolar plate with the oxygen molecules. Once the H_2 reaches the catalyst it will separate into two individual hydrogen atoms. The hydrogen molecule will be chemisorbed on the electrode surface and will then release an electron. The electron will go through the GDL and bipolar plate where they will be used as a current source. The proton (positive hydrogen atom) will have to go through the electrolyte. Once the proton crosses the electrolyte membrane it will combine with an electron and oxygen molecule to form water. The waste product is removed from the cell by the incoming oxygen. The whole process is shown in Figure 6 and the chemical representation is as follows:

$$H_2 \rightarrow 2H^+ + 2e^-$$

$$O + 2H^+ + 2e^- \rightarrow H_2O$$

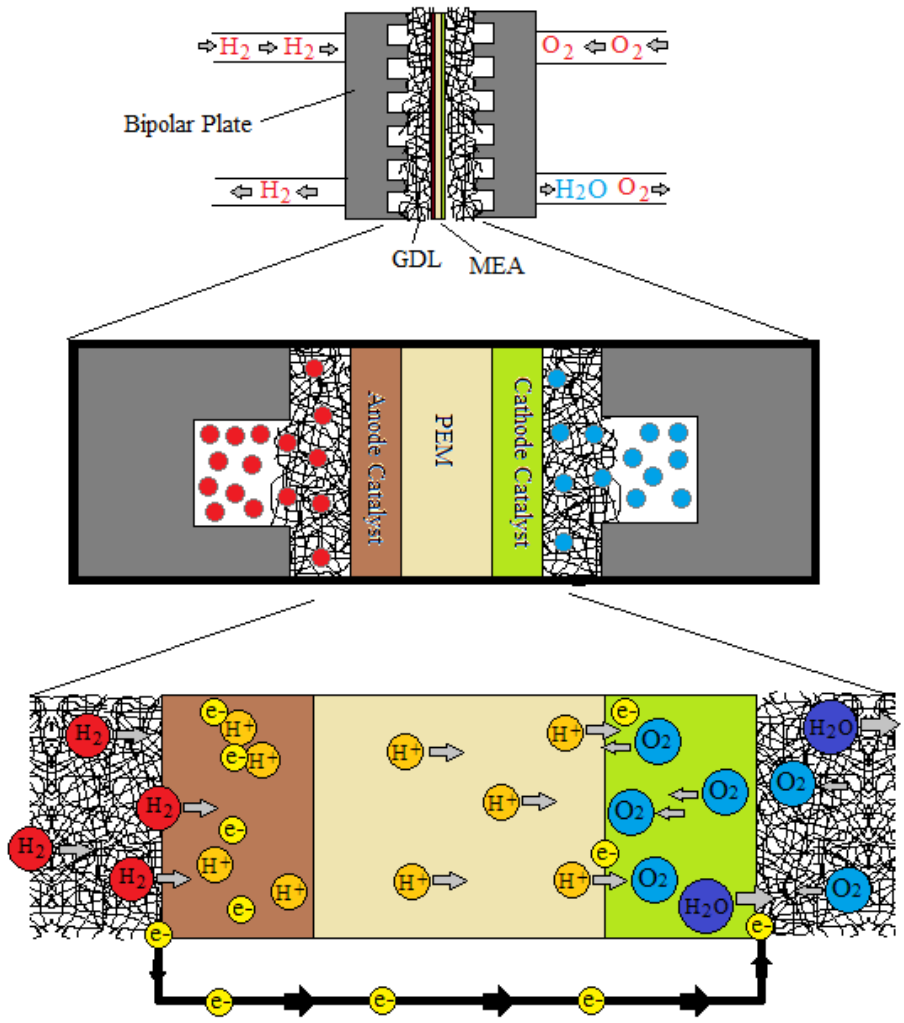

Hydrogen and oxygen enter the fuel cell through the serpentine channels at opposite ends.

The reactants diffuse though the GDL and reach the catalyst layer at the electrodes.

The hydrogen molecules react with the catalyst at the anode and dissociate in to individual protons by releasing an electron. The electron flows through an external circuit were it powers an external load. The oxygen molecules combine with the hydrogen ions and the electrons to form H_2O at the cathode side. The H_2O is discarded as a byproduct.

Figure 6: H_2-O_2 fuel cell operation

1.4.5 Fuel cell losses

While fuel cells have a high theoretical efficiency, their real life efficiency is lower. An ideal fuel cell would supply any amount of current as long as it is supplied with enough fuel without experiencing any voltage drop. In real life, the actual operating voltage would drop due to fuel cell irreversible losses. These losses decrease the operating voltage of the fuel cells as the

current drawn is increased. There are three major types of losses in a fuel cell as shown in Figure 7:

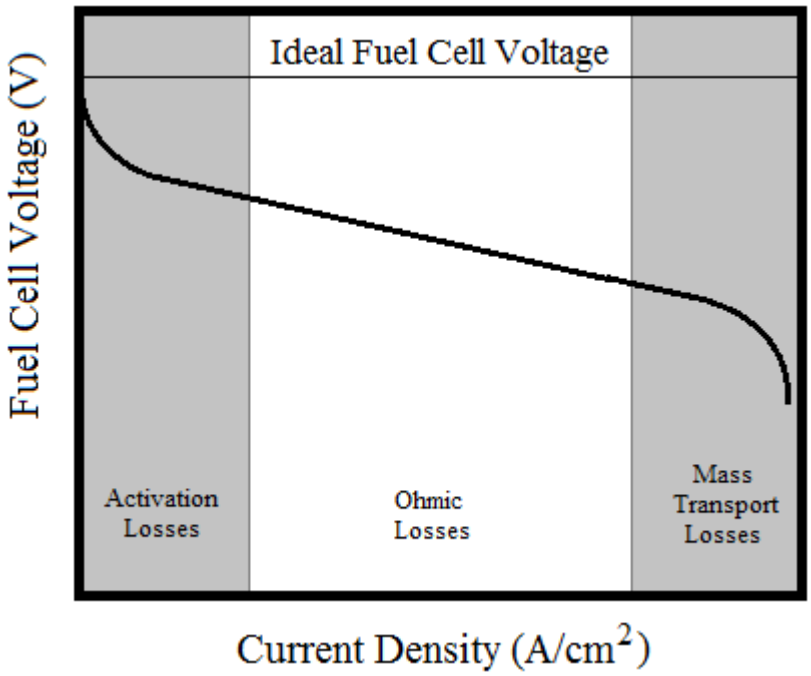

Figure 7: Fuel cell voltage drop due to activation, ohmic and mass transport losses.

1. Activation losses

   Losses associated with the electrochemical reactions. High electrochemical reaction kinetics are desired

2. Concentration looses

   Losses associated with mass transport of the reactants and products. Excessive flooding of the membranes can potentially halt mass transport.

3. Ohmic losses

   Losses associated with the ionic and electric conductivity of the membranes

All losses depend on the current drawn. At low currents, the activation losses dominate. At high currents, the concentration losses dominate. While the ohmic losses are linearly related by ohm's law.

Ohmic Losses (Membrane Resistance)

Charge transport is responsible for the ohmic losses in a fuel cell. These losses result in a voltage drop from the theoretical maximum. Like most processes, charge transport is not a frictionless process and voltage must be sacrificed to overcome resistance. The resistance of the electrolyte membrane can be calculated with Equation 1:

$$R = \frac{L}{A\sigma}$$ Equation 1: Resistance of the PEM

Where "R" (Ω) is the resistance, "L" is the thickness of the membrane (cm), "A" is the area (cm^2) and "σ" is the conductivity (Ω^{-1} cm^{-1}). Resistance is usually normalized in terms of area and known as Area-Specific Resistance (ASR) (Ω cm^2) as shown in Equation 2

$$ASR = AR = \frac{L}{\sigma}$$ Equation 2: ASR

As seen from Equation 1 and Equation 2, the resistance is independent of the current drawn and hence follows ohms law (hence homic losses). It is also very important to realize that the membrane resistance is proportional to the thickness of the membrane. Thus, minimizing the membrane thickness will reduce the resistance of the membrane.

Membranes thickness is restrained by some considerations:

- Mechanical Integrity: The membrane cannot be made too thin because it will develop pinholes or rip causing fuel and oxidants to combine. Such a combination of fuel and oxidants would render the fuel cell useless.
- Shorting. For very thin membranes, if thickness is around the same size as the electrode roughness, there is a possibility for electrical shorting. Electrical shorting will not be catastrophic but it will reduce the efficiency of the fuel cell due to current leaking.
- Fuel Crossover. The thinner the membrane becomes the higher the risk of fuel crossover loss. Some fuel crossover might be tolerated but, as the membranes get thinner and thinner, the losses become too large becoming unsustainable.

2 Literature Review and Theoretical Background

In this chapter a literature review will be performed for the most important articles regarding hybrid fuel cell, membrane morphology and water content. The theoretical background necessary to understand the research and the results are introduced in this chapter.

2.1 Literature Review

Literature review was performed for the hybrid fuel cells, membrane morphology and water content. Hybrid fuel cells were recently developed by Dr. Paul A. Kohl and his research team at Georgia Institute of Technology. A brief review of their literature will give valuable information on hybrid fuel cells. The membrane morphology section will review important aspects about the structure of Nafion at different length scales. The Water content section will examine the effect of water content on important membrane properties.

2.1.1 Hybrid Fuel Cells

Proton exchange membrane fuel cells (PEMFC) offer the highest power densities, good start up and low temperature operation. Nonetheless they have sluggish kinetics, expensive noble metal catalyst, and poor CO and S tolerance when compared to Phosphoric acid fuel cells (PAFC) and Alkaline Fuel Cell (AFC) [8]. In an attempt to overcome this, the first hybrid fuel cell with alkaline electrodes and a PEM core (AEPEMFC) was created by Unlu, Zhou and Kohl [9]. In this hybrid configuration high-pH Anion Exchange Membranes (AEM) are utilized as electrodes with a PEM core as illustrated by Figure 8. This configuration has a higher ionic conductivity than a pure AEM fuel cell (198 $m\Omega cm^{-2}$ vs. 460 $m\Omega cm^{-2}$). It also exhibits enhanced water management due to water generation a two points within the membrane electrode assembly (MEA): 1) At the PEM/cathode interface and 2) within the anode electrode. It is this

second source of water generation that eventually limits the effectiveness of the fuel cell by ultimately "drying" it up. This type of cell configuration has lower power densities than typical PEMFC (78 mW cm^2 vs 700 mW cm^2 respectively).

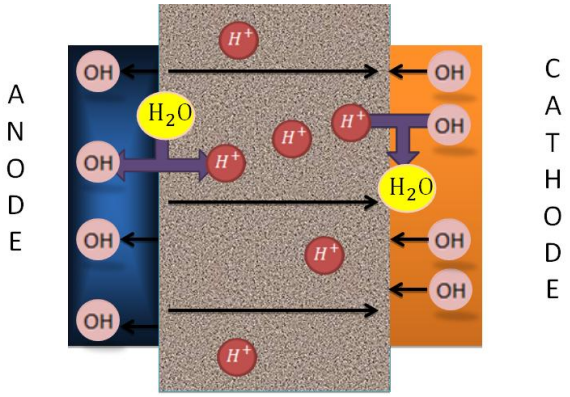

Figure 8: Hybrid fuel cell with high-pH electrodes and PEM core.

To further understand the reaction kinetics of (AEPEMFC) two semi-hybrid fuel cells were studied [10] and compared to PEMFC. The first semi-hybrid configuration was AEM cathode and a PEM anode and was termed cathode hybrid fuel cell (CHFC). The second was an AEM anode and a PEM cathode termed anode hybrid fuel cell (AHFC). Both configurations are show in Figure 9.

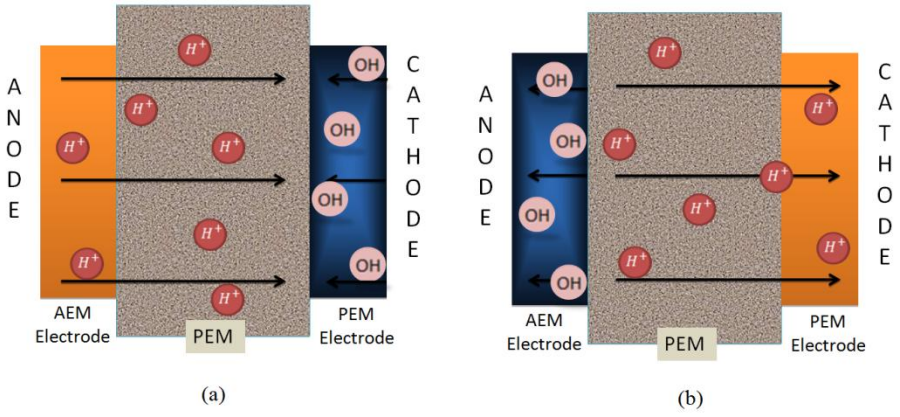

Figure 9: (a) Cathode Hybrid Fuel Cell (CHFC) and (b) Anode Hybrid Fuel Cell (AHFC).

These semi-hybrid fuel cells made it possible to identify the source of the lower power densities when compared PEMFC. In a typical fuel cell the cathodic activation looses dominate the fuel cell performance but that may not be the case for a hybrid fuel cell. For a traditional and hybrid fuel cell, the ohmic resistances due to a PEM core are similar. For both semi-hybrid fuel cells the charge transfer resistance (R_{CT}) in the AEM was orders of magnitude bigger (5x) when compared to the PEMFC. R_{CT} in the AEM stresses the importance of developing efficient AEM. The after mentioned research concentrated in changing the catalyst load to improve the AEM.

As the next step a hybrid fuel cell with both AEM and PEM electrolytes was constructed by Kohl's team at Georgia Tech [11] as shown in Figure 10. Two different configurations were constructed, one with AEM anode (a) and a second with AEM cathode (b). The resulting thickness of both configurations was 174 μm. These configurations had very small maximum power densities (0.03 mW/cm^2 (a) and 0.64 mW/cm^2 (b) vs 300-1000 mW/cm^2 for conventional PEMFC at 100% RH). The reasons stated for low performance are non-optimized fabrication methods and the large membrane thickness causing high resistance.

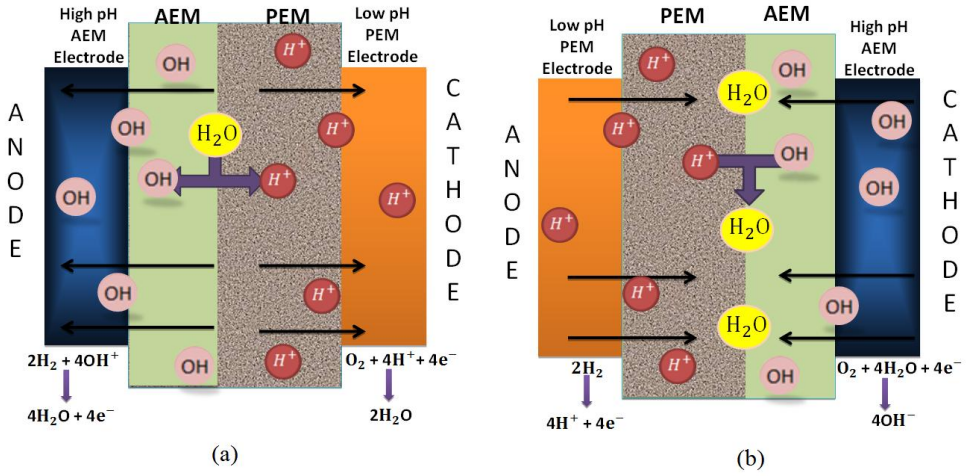

Figure 10: Hybrid fuel cell with PEM and AEM electrolytes in a) AEM anode/PEM cathode and b) AEM cathode/PEM anode.

Another type of hybrid fuel (semi-hybrid) cell was examined in the same article with only one electrolyte, the same as illustrated in Figure 9. These configurations had higher maximum power densities 15.3 mW/cm^2 (a) and 22 mW/cm^2 (b) at 100% RH. The configuration with the AEM anode (a) could not be run with significant loads (drawn current) this is due to inadequate water at the AEM anode-PEM junction. Water is dissociated at the AEM anode-PEM junction to provide protons and hydroxide ions for the reaction. Inadequate flux of water to the junction "dries" the membrane interface and starves the reaction of the needed ions. The AEM cathode (b) configuration had significant improvement in water management. For this configuration water is generated at the AEM cathode-PEM junction, which gives the fuel cell self-hydrating properties. Water hydration is critical at the PEM to maintain the ionic conductivity. When the fuel cell is operated at dry conditions the power density increases with a maximum of 63 mW/cm^2 at 37% RH and 52 mW/cm^2 at 0% RH. When compared to a traditional PEMFC the self-hydrating hybrid fuel cell can outperform it under high temperature dry conditions ($T > 65$ C^o and 0% RH). PEMFC can self-hydrate through back-diffusion of water produced at the cathode up to certain critical temperature (about 60 C^o but depends on operating conditions). After the critical temperature the fuel cell starts "drying" and eventually decays in performance. Additionally the AEM cathode/PEM anode configuration does not require expensive platinum catalyst at the AEM cathode.

Based on the discussed results Kohl and team further evaluated the performance of the most successful hybrid fuel cell, the self-hydrating AEM cathode/PEM anode semi-hybrid fuel cell [12]. As mentioned before the performance of the hybrid fuel cell is limited by the AEM cathode electrode. These limitations caused inadequate Oxygen mass transfer in the AEM cathode. These impediments where investigated by changing the ionomer content of the AEM

cathode electrode and by changing the flow rate of the reactants. Oxygen flow is obstructed either by water or by high ionomer content in the AEM cathode.

The hybrid fuel cell generates twice the amount of water in the PEM-AEM cathode junction than is consumed at the cathode. Excessive flooding of the junction decreases the oxygen diffusion. This can be mitigated by increasing the flow rate of the oxygen supply at the cathode. Typical PEMFC with low RH can't be run on high flow rated because produces excessive evaporation, drying the membranes. But for the hybrid fuel cell it actually helps solve the problem of excessive water in the membranes. When the flow rate of Oxygen was increased from 2 sccm to 8 sccm the mass transfer resistance dropped by 250%. This drop in resistance was even obtained if the flow rate was increased by adding nitrogen instead of oxygen. The drop in mass transfer resistance is caused by increased evaporation of water at the cathode. This also explains why the hybrid fuel cell has poor performance at high RH, because of the excessive water flooding.

The ionomer content in the AEM electrode can also physically obstruct oxygen and water mass transfer but mainly affects the latter. High ionomer content (0.5 mg cm^{-2}) (MEA-L) and low ionomer content (0.3 mg cm^{-2}) AEM cathode electrode (MEA-H) where compared. The MEA-H decreased the evaporation rate off water at the AEM electrode which gave it superior performance at low RH and low currents (low water production). But as current increased (over 125 mA cm^{-2}) or RH increased (over 25% RH) excessive flooding decreased oxygen transfer and greatly decreased the performance (effectively stopping the fuel cell). The MEA-L had higher evaporation rate which slightly decreased the performance (less than 6 % decrease in current density) at very dry conditions (low currents and lo RH). The article concludes that a hybrid fuel

with low ionomer content and high oxygen flow rates can outperform a typical PEMFC operating under dry conditions.

While Kohls research is highly impressive, no mention is made of changing the production methods of the membranes. By using electrospinning a highly diffusive AEM cathode electrode could be manufactured greatly increasing the performance of the hybrid fuel cells [13]. Electrospinning can not only help with water management it can also increases ionic conductivity on the membranes and thus reduce the ohmic losses.

Table 2: Summarized types of hybrid fuel cell

Type of Fuel cell	Illustration	Advantages	Disadvantages
Typical PEMFC		• High power densities	• CO_2 Poisoning • Expensive catalyst • Can't operate at low RH
Hybrid fuel cell with alkaline electrodes and a PEM core	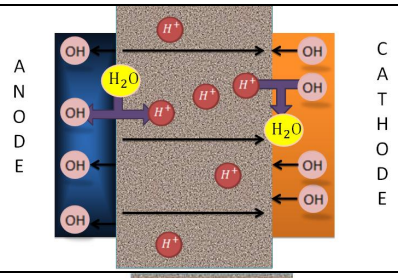	• No expensive catalyst required • Higher ionic conductivity than AEMFC	• Low power densities • Water management problems at the AEM electrode-PEM junction
Semi-Hybrid AEM anode/PEM cathode	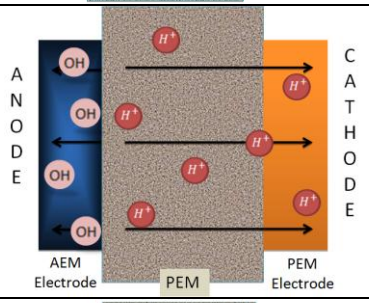	• Anode electrode does not require expensive catalyst	• Water management problems at the AEM anode electrode-PEM junction • Not practical for implementation
Semi-Hybrid AEM cathode/PEM anode	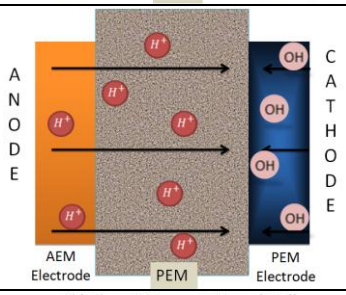	• Self-Hydrating properties allow operations under dry conditions • Can outperform PEMFC under dry conditions • Cathode electrode does not require expensive catalyst	• Low power densities
Hybrid AEM/PEM electrolyte AEM cathode/PEM anode	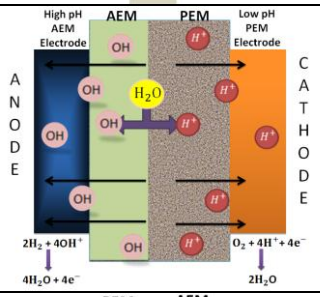	• Anode electrode does not require expensive catalyst	• Very low power densities • Water management problems at the AEM anode electrode-PEM junction • High ohmic resistance • Not practical for implementation
Hybrid AEM/PEM electrolyte AEM anode/PEM cathode	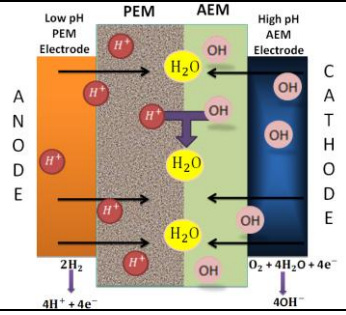	• Self-Hydrating properties allow operations under dry conditions	• Very low power densities • High ohmic resistance • Not practical for implementation

2.1.2 Membrane Morphology

Ionomers can have multiple levels of morphology depending on the scale that is being considered as shown in Figure 11. All levels can have an impact on the macro-properties of the membrane.

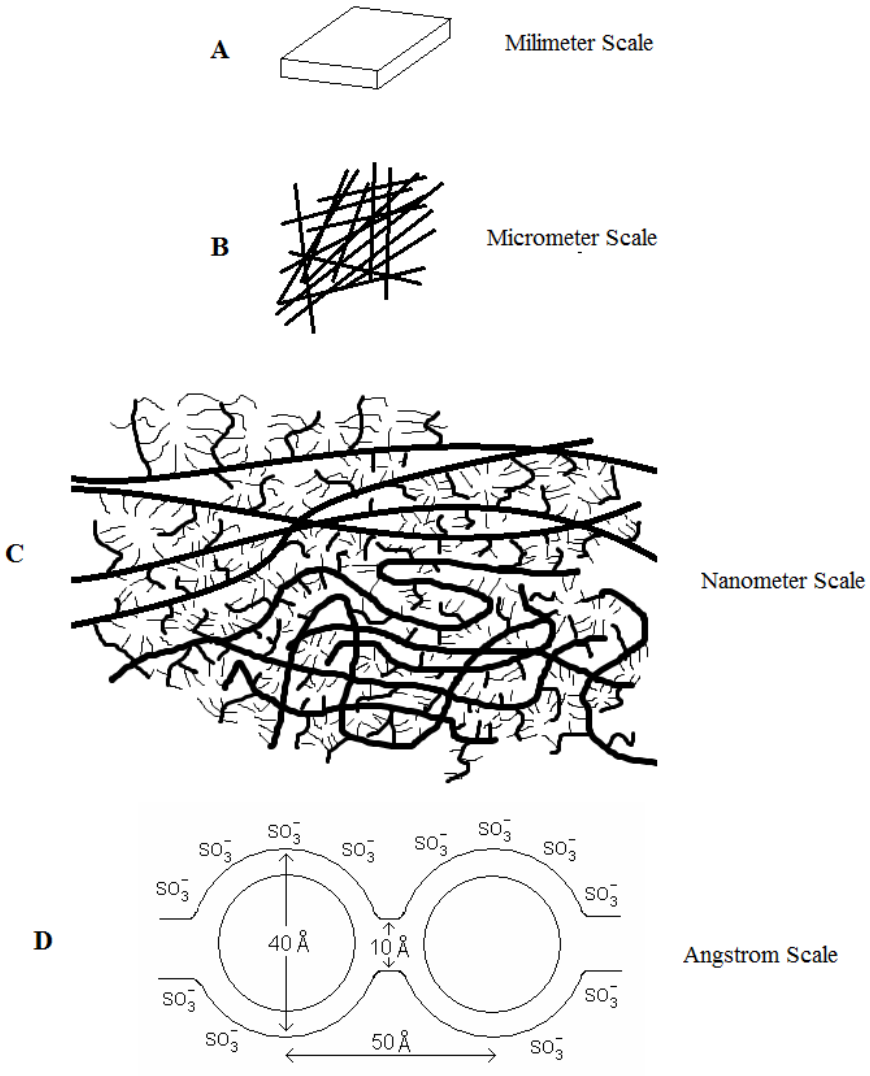

Figure 11: Membrane morphology a different length scales. A) At the millimeter length scale a membrane can be 2" x 2" in size. B) At the micrometer length scale the nano-fibers that compose the membrane can be observed. C) At the nanometer length scale the polymer backbone and the side chains can be observed. D) At the angstrom length scale the inverted micelles can be observed.

Angstrom Length Scale

There is currently a lot of debate about the structural nature of Nafion. Many different models have been proposed to explain Nafion's different characteristics. One of the oldest models shown to have withstood the test of time was proposed by Gierke and is known as the cluster network model [14]. In this model the structure of Nafion is characterized by inverted micelles as shown in Figure 12. The inner structure of the micelles is composed $-SO_3^-$ provided by the end of the side chains of the polymer. Depending on the number of monomer repetitions (x, y, m, and n) one single repetition of copolymer can have between 2,000 and 18,000 $-SO_3^-$ groups. The structure is adopted even if there is ionic repulsion, to minimize repulsive interactions between water and the fluorocarbon backbone. The inverted micelles attract water inside the structure and maximize solvation of the $-SO_3^-$ groups. It is within these structures that cationic conduction takes place by H^+ hopping from one site to the next. While this model is very successful in describing ionic cluster it does not consider the macromolecular crystalline structure of Nafion.

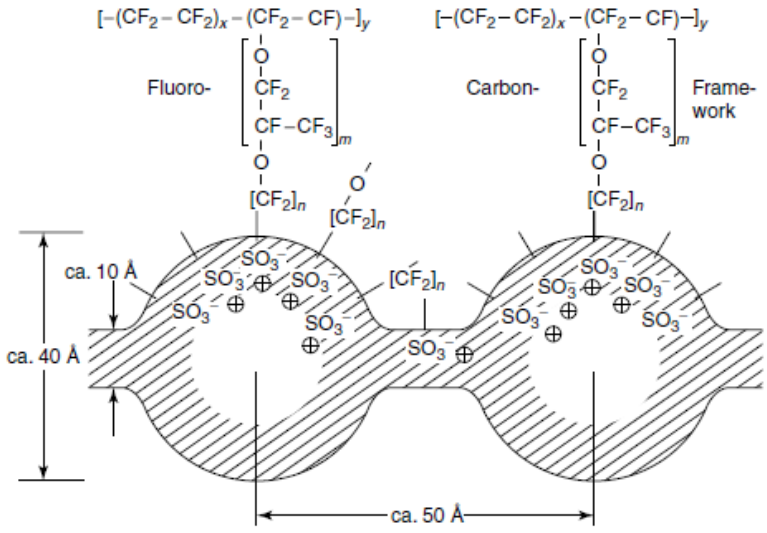

Figure 12: Cluster network of inverted micelles connected by channels.

Nanometer Length Scale

It is known that as received membranes and recast films have different properties. This difference is do to the lack crystalline structure in the recast film. R. B. Moore et al. studied the morphological properties of solution cast Nafion [6]. In the study three different types of membranes and their morphologies were studied:

1. As received commercial membranes bought from DuPont. This membranes are partially crystalline

2. Recast membranes created by casting Nafion polymer solutions at room temperature. These membranes lack any sort of crystallinity

3. Solution Process membranes created by casting at high temperatures. These membranes have the same partial crystallinity as commercial membranes.

The difference in crystallinity is attributed to the processing temperature. Recast films are cast at room temperature. Without sufficient temperature there is not enough mobility in the polymer chains to rearrange the structure in semi-crystalline fashion. In the solution process membranes the mobility is provided by thermal excitation. The partial crystallinity of the polymer strengthens the membrane by providing secondary crystalline bonds (similar to cross-linking). This additional strength helps reduce water swelling. There is also reduced solubility because the crystallinity retards access of the solvent to the bulk of the membrane. The casting temperature was determined for different types of solvents as summarized in Table 3.

Table 3: Minimum temperatures required obtain insoluble membranes

Solvent	Casting Temperature ^{o}C
Dimethylformamide	124
Dimethyl sulfoxide	164
Ethylene glycol	185

Even though there is not enough thermal excitation when membranes are cast at room temperature to provide mobility for the main polymer chains, there is enough excitation to mobilize the side chains. Recast membranes where still able to create the ionic cluster morphology seen in all membranes.

Micrometer Length Scale

Ionomers have been electrospun in the past for fuel cell applications. Jonghyun Choi et al. electrospun a 25 wt % sulfonated poly(arylene ether sulfone) in dimethylacetamide solution[15]. The fibers were collected in a rotating oscillating collector. The average fiber diameter was 110 nm. The electrospun membranes where then compacted and welded to create the final membrane. Compacting was performed by applying 13000 psi for 3 minutes at 25 ^{o}C. Welding was achieved by exposing the fiber membrane to DMF vapor at 25 ^{o}C for 18 minutes. In addition the fiber membranes were impregnated by an internetwork filler. The filler was created by impregnating the membrane in Norland Optical Adhesive (NOA).

The proton conductivity was found to have a maximum of 0.086 S/cm for the composite fiber membrane vs 0.09 S/cm for Nafion 117. Compacting played a crucial role in increasing the ionic conductivity of the membrane. There is linear relationship between compacting and ionic conductivity. By doubling the density of the fiber membrane from 20% to 40% there was

increase in ionic conductivity from 22 S/cm to 45 S/cm. The welding also increased the ionic conductivity by 10% but that maybe within experimental error for ionic conductivity measurements.

Another very important property is full cross over. The electrospun membranes were found to have oxygen permeability of 0.18 barrers (0.53 for regular homogenous membrane), an oxygen barrier property 50 times bigger than that of Nafion 117 at 9.4 barrers. This means thinner membranes could be used to create PEM. No mention is given as to why the electrospun membranes have superior permeability properties than an homogenous regular membrane.

Hong Chen et al successfully electrospun a Nafion and Poly(Acrylic Acid) (PAA) blend using a stationary collector [13]. At first a pure Nafion solution was used with a variety of solvents and different concentrations to try to perform electrospinning but there was insufficient viscosity in the solution. The lack of viscosity was attributed to insufficient chain entanglement in the Nafion solution. To increase the viscosity a Nafion-PAA blend was successfully used to increase the viscosity and perform electrospinning. A minimum of 16% wt PAA 88% wt Nafion was determined to be required for defect free fibers.

Water stability was significantly enhanced by thermal treatment at 140 ^{o}C for ten minutes. The research team made significant progress in promoting the importance of viscosity in electrospinning solutions but left a few unanswered questions. No ionic conductivity, water uptake and ion exchange measurements were reported. Membrane quality could be greatly increased by employing an oscillating rotating collector in the electrospinning process.

2.1.3 Water Content

Many important properties of the Polymer Electrolyte Membrane (PEM) are a function of water content. Some of these properties are mechanical strength, water diffusivity and ionic conductivity. Water content (λ) is defined as the ratio between water molecules and exchanges sites as shown by Equation 3

$$\lambda = \frac{mol\ H_2O}{mol\ SO_3^-}$$ Equation 3: Water Content

Water content has profound effect on the PEM morphology. G Gebel studied the structure of Nafion at different hydration levels [16]. The water fraction volume (volume of water per volume of Nafion) was varied from 3% up to 93%. Small Angle X-ray and Neutron Scattering (SAXS and SANS) was performed to investigate the structure of the polymer. Nafion was placed in a pressure vessel to undergo water uptake. The structure of Nafion was found to change with water content as seen in Figure 13.

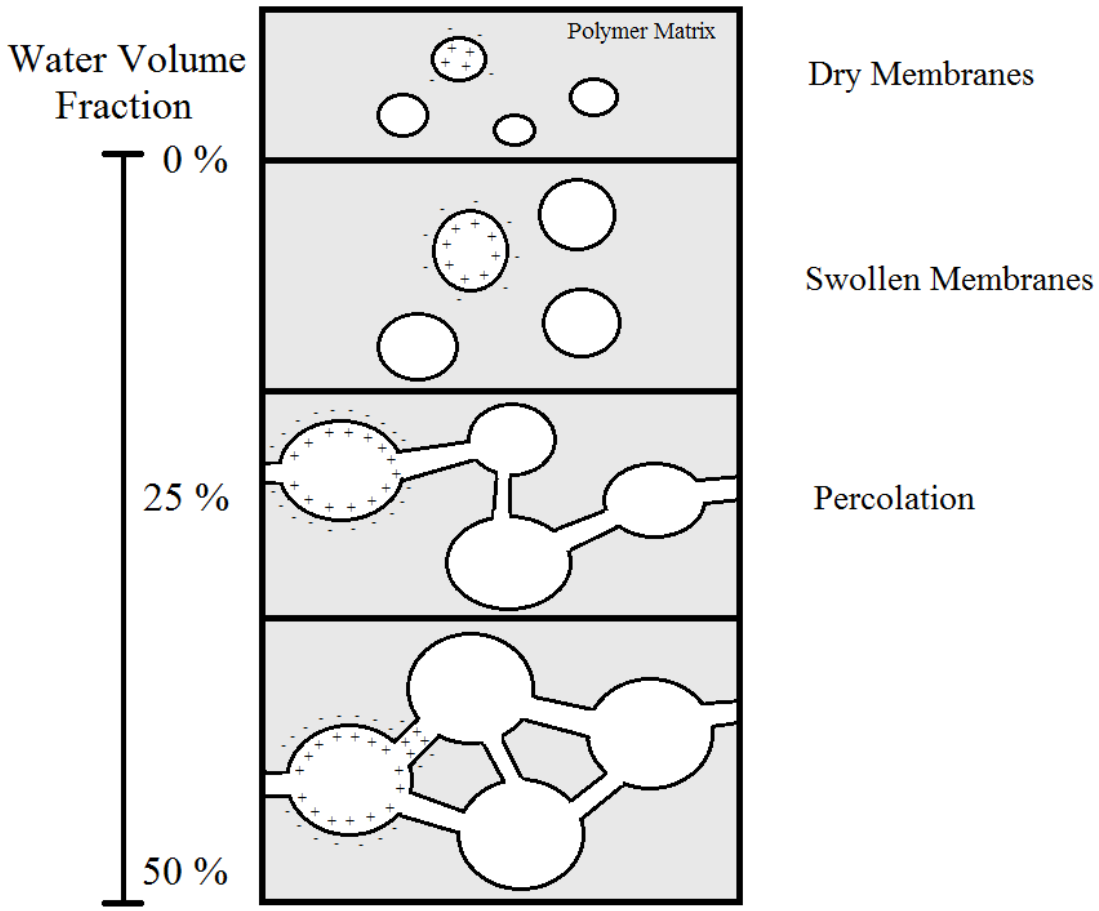

Figure 13: Structural evolution of Nafion with water content.

Dry membranes were found to consist of isolated spherical ionic clusters. They have very poor conductivity because they have no water to dissolve the protons in the sulfonated groups and the great distance between ionic clusters. In its dry sate Nafion clusters are 15 Å in diameter and separated from each other by 27 Å. As water content increases the ionic clusters grow absorbing water within the spherical structure. The amount of spherical ionic clusters decreases, while the amount of ionic groups within each cluster increases. Above a volume fraction of 20% ionic conductivity greatly increases as the clusters grow in size to 40 Å. Between 30% and 50% water volume fraction, the ionic clusters are connected by cylinders with water dispersed in the polymer matrix. During this phase not only does cluster size increase to

50 Å but so does the connectivity and size of connecting cylinders. As the clusters increase in size and connectivity so does the ionic conductivity of the PEM. After water volume fraction of 50% the membranes starts to partially dissolve and the structure of the polymer changes to rod-like polymer aggregates. At this point the membrane looses mechanical strength and becomes unmanageable.

Beattie et al. studied different factors that help predict ionic conduction in proton exchange membranes [17]. Four different series of membranes with different equivalent weights were studied:

1. Sulfonated abb-trifluorostyrene-*co*-substituted-abbtrifluorostyrenes (BAM®)
2. Sulfonated styrene–(ethylene–butylene)–styrene triblock copolymers (DAIS)
3. Nafion® 117 (E-form and N-form)
4. Ethylenetetrafluoroethylene-*g*-polystyrene sulfonic acid membranes (ETFE)

The membrane's ionic conductivity was correlated with water uptake, Equivalent Weight (EW), water content and proton concentration (ion exchange). Proton conductivity was determined by electrochemical impedance spectroscopy. Proton concentration was determined by ion exchange titration. In the case of Nafion, DAIS and ETFE the conductivity did increase as function of water content but not for the BAM membrane. It was determined that by itself none of the four factors could help predict the ionic conductivity. Only by comparing proton concentration and water content can the membrane's ionic conductivity be successfully trended.

The conclusion from the group is that since water content is determined as ratio of water molecules to exchange sites it can be artificially ballooned. For two membranes with the same

amount of water uptake the membrane with lower exchange sites will have the higher water content (and supposedly higher ionic conductivity). In fact a membrane with no exchange sites will have an infinite amount of water content. For two membranes with similar proton concentration the membrane with the highest water uptake will in fact have the higher ionic conductivity. Thus it is only by first comparing proton concentration (ion exchange capacity) and then water content that correct expectation can be drawn about the membrane's ionic conductivity.

2.2 Theoretical Background

In this section the theoretical background necessary to understand the results are discussed. Charge transport in the fuel cell is first discussed followed by the Springer fuel cell model.

2.2.1 Charge Transport through the Electrolyte Membrane

For a fuel cell to work correctly it must effectively conduct electrons to an external circuit and ions through the electrolyte membrane. Conductivity is the ability of material to allow the transport of a charge when driven by an electric field. The higher the conductivity the easier it will be for charge to transverse the material. The conductivity of a material is determined by two factors:

- How many carriers are available.
    - Carrier concentration can vary among different materials and microstructure.
- Mobility of the carriers in the material.
    - Mobility depends on both the charge carrier and the transport medium. Even though electrons are transported much more readily than ions in metals they cannot transverse an electrolyte.

Equation 4 defines conductivity. Where "Z_i" is charge number for the carrier (e.g., Z_i = -1 for e^-), "F" is faradays constant, "c_i" is the molar concentration of charge carriers and "u_i" is the mobility of the charge carriers in the material.

$$\sigma_i = (|Z_i|\ F)\ c_i\ u_i$$ Equation 4: Conductivity

Ionic Conduction

Ionic conduction dominates ohmic losses because electronic conduction is readily achieved in comparison to ionic conduction. Electrons are of a much smaller mass and easily transported through carbon, and metal. Even small ion like hydrogen are still huge and heavy.

The mobility of ions in polymer electrolyte can be calculated with Equation 5. Where "F" is Faradays constant, "R_g" the gas constant, "D" the diffusivity and "Z_i" the charge number of the ion.

$$u = \frac{|Z_i|\ F\ D}{R_g T}$$ Equation 5: Ion mobility

The diffusivity can be calculated with Equation 6. Where "D_0" is the attempt frequency, "R_g" is the gas constant, "ΔG" is the activation barrier for the process and "T" the temperature (k).

$$D = D_o\ e^{\left(-\frac{\Delta G}{RT}\right)}$$ Equation 6: Diffusivity

By combining Equation 4, Equation 5 and Equation 6 we obtain Equation 7

$$\sigma_i = \frac{(Z_i\ F)^2}{RT}\ c_i\ D_o\ e^{\left(-\frac{\Delta G}{RT}\right)}$$ Equation 7: Ionic Conductivity (Expanded)

Equation 7 has many constants (Z_i, C_i) than can be readily calculated by experiments except for the diffusivity component (D_0, ΔG). The reason for this difficulty is given by the fact

that for a polymer electrolyte such as Nafion the diffusivity is not only a function of temperature but also a function of water content.

2.2.2 Springer Fuel Cell Model

There are numerous models for water and charge transport trough the proton exchange membrane [18]. Springer et. all. developed a one dimensional diffusion based model with all variables held as function of water content. Proton conductivity was studied and empirical formulas, constant and coefficients were obtained by curve fitting [19]. The Springer model considers electro-osmotic drag from the anode to the cathode, water back diffusion from the cathode to the anode and water generation at the cathode as responsible for the difference in the water content throughout the membrane. The model can be used described an entire cell or just the electrolyte membrane.

The model first predicts the water content of the membrane based on the water vapor activity of the incoming fuel (e.g. hydrogen). There is no incoming fuel when considering only the electrolyte membrane and since the water content of the membrane was directly measured this step is not necessary. The model then predicts the ionic conductivity at 30 ^{o}C based on the water content. The ionic conductivity at 30 ^{o}C is then used as a constant to determine the ionic conductivity as function of temperature. For the moment being there is no interest in calculating the ionic conductivity as function of temperature, only in comparing the ionic conductivity to the commercial membranes. Equation 8 calculates the ionic conductivity of the membrane as function of water content and Equation 9 calculates the ionic conductivity as function of temperature.

$$\sigma_{30} = 0.005139\lambda - 0.00326$$

Equation 8: Ionic conductivity as function of water content

$$\sigma_T = \sigma_{30} \times e^{\left[1268\left(\frac{1}{303}+\frac{1}{273+T}\right)\right]}$$

Equation 9: Ionic conductivity as function of temperature

The Springer model does have some limitations. It is can only be used with 1100 EW Nafion membranes and is not very accurate at low hydration levels. When calculating the water content for use with the Springer model the equivalent weight used should be the one specified by the manufacturer (EW 1100).

In essence the Springer model is approximating the diffusivity of the electrospun membrane. By rearranging Equation 7 and comparing to Equation 9 some resemblance of the equations can be observed as summarized in Table 4.

Table 4: Summary of important equations.

Formula:	**Equation:**
$D = D_o\, e^{\left(-\frac{\Delta G}{R\,T}\right)}$	Equation 6: Diffusivity
$\sigma_i = (Z_i\, F)^2\, c_i\, D_o\, e^{\left[-\left(\frac{\Delta G}{R\,T} + \ln\,(RT)\right)\right]}$	Equation 7: Ionic Conductivity
$\sigma_{30} = 0.005139\lambda - 0.00326$	Equation 8: Ionic conductivity as function of water content
$\sigma_T = \sigma_{30} \times e^{\left[1268\left(\frac{1}{303} + \frac{1}{273+T}\right)\right]}$	Equation 9: Ionic conductivity as function of temperature

The water content is then responsible along with temperature for the ionic conductivity of the membrane. The ionic conductivity at a constant temperature is only dependant on the water content of the membrane. This implies that the water content is increasing the diffusivity of the membrane. By using the Springer model the ionic conductivity of the electrospun membranes was compared to the commercial membranes.

3 Methodology

3.1 Introduction

In this chapter the procedures for fabricating, processing, characterizing and analyzing different membranes are discussed. This chapter is divided in three segments that follow the research process as seen in Figure 14.

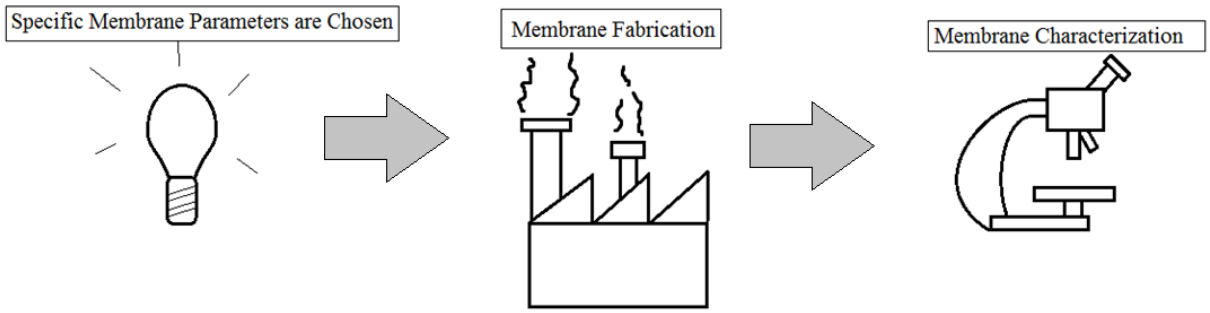

Literature review is performed and important parameters are identified. A design of experiment is implemented.	Polymer solutions are prepared and then electrospun. Electrospun membranes are then processed with specific parameters.	Membranes are characterized and analyzed using different techniques.

Figure 14: Flowchart of research process.

Important parameters which might affect the properties of the membranes were first identified. These parameters include variables related with the fabrication process known as electrospinning. Other parameters might be related with the electrospinning precursor polymer solutions. Other parameters are related to the membrane processing parameters of the electrospun membranes such as press pressure and annealing temperatures. Some parameters

where modified while exploring and then fixed as in the case with the electrospinning fabrication process parameters and the precursor solutions. The post electrospinning processing parameters such press pressure, annealing temperature had to be tested with a Design of Experiment (DOE).

Membrane fabrication can be subdivided into three steps, precursor solutions, electrospinning and membrane processing. The precursor polymer solutions composed of a Nafion- Poly (Acrylic Acid) blend were required for use in the electrospinning process. A Nafion polymer solution was mixed with Poly (Acrylic Acid) (PAA) polymer solution because a pure Nafion solution had insufficient viscosity for use in electrospinning. The electrospinning process uses an electric field to stretch the polymer blend solution in to small micro-to-nano sized fibers. These fibers accumulate in specialized collector eventually forming an electrospun membrane. These electrospun membranes with no additional processing parameters are known as non-processed electrospun membranes.

The membranes are processed by performing three additional steps; compacting, annealing, cleaning and activation. Compacting is performed subjecting the membranes to pressure under a press. Annealing was performed by heating the membrane in a vacuum oven. Cleaning and activation is single step where the membrane is cleaned by removing any organic contaminants and the membrane is chemically treated to their acid state.

Characterization was used to look at important membrane characteristics. Scanning Electron Microscopy (SEM) and optical microscopy was used to evaluate fiber diameter distribution, fiber orientation and fiber-void fractions. Water uptake was used to evaluate water absorption by the membranes. Ion Exchange Capacity (IEC) gave valuable information on ion accessibility to the sulfonated exchange sites within the membrane. Water content was used to

evaluate the ionic conductivity of the membranes. Tensile strength and solubility was performed on select membranes.

3.2 Specific Membrane Parameters

Important parameters such as polymer concentration, press pressure, annealing temperature and processing order were identified. DOE with three samples per data point was created to study these important membrane fabrication and processing parameters. Water uptake, IEC and water content were performed to characterize the membranes with the DOE:

- Polymer Blend Concentration
    - Nafion is mixed with PAA to increase the viscosity for use with the electrospinning process. Others polymers such polyethylene glycol, polyvinyl alcohol and polyvinyl pyrrolidone have been successfully reported in the literature to increase the viscosity of the Nafion polymer solutions for use in the electrospinning process [20][21]. But PAA is a polyelectrolyte like Nafion and will have better functional compatibility than other non-polyelectrolyte polymers. Without the addition of the PAA electrospinning would not be possible [13].
    - DOE parameters:
        - 85% Nafion 15% PAA
        - 80% Nafion 20% PAA

- Compacting Pressure
    - Compacting pressure was identified in the literature as an important parameter having an effect on the ionic conductivity of the electrospun sulfonated poly(arylene ether sulfone) membranes [22]. The authors found that the ionic conductivity increased

linearly with the fiber volume fraction. The authors increased the fiber volume fraction by compacting the fibers under pressure from 700 psi to 13,000 psi.

- DOE parameters:
  - 5,000 Psi
  - 14,000 Psi

- Annealing Temperature
  - Nafion has been known to increase in crystallinity when subjected to an annealing processes above the glass transition temperature of 110 ^{o}C [23][5]. The increased crystallinity gives Nafion better mechanical properties and reduces the solubility of the membrane. Two temperatures, one above and one below the glass transition temperature of Nafion were used in the annealing process.
  - DOE parameters:
    - 70 ^{o}C
    - 120 ^{o}C

- Compacting and Annealing Order
  - Compacting and annealing processes are found in conjunction as processing parameters in the literature. But there are no reports in the literature on the effect of changing the processing order. Usually compacting is first performed followed by the annealing process. The compacting and annealing process were interchanged in order to determine their effect on the electrospun membranes.
  - DOE parameters:
    - Compact first, anneal second (order 0)
    - Anneal first, press second (order 1)

Table 5 shows the different membranes prepared and their fabrication parameters. It is important to note that it is not just the parameter which was evaluated but also the order in which

they are carried out. Polymer blend concentration was always chosen first but the annealing and compacting steps can be interchanged in order.

Membranes created via electrospinning but without any processing parameters (annealing, pressure, cleaning and activation) are known as non-processed electrospun membranes. For the sake of simplicity the concentration of the membranes by weight might be abbreviated by only stating the concentration of the Nafion component. For example instead of writing "80% Nafion-20% PAA membrane" it might be written as "80% Nafion membrane". The concentration of the Poly (Acrylic Acid) (PAA) is implied since Nafion is always mixed with PAA.

Table 5: Samples prepared and their fabrication parameters. Samples with order = 1 are first annealed and then compacted. Samples with order = 0 are first compacted and then annealed.

Global #	Nafion-PAA concentration (wt %)	Order	Heat Treatment Temperature (^{o}C)	Press Pressure (KSI)
1	80-20	1	70	5
2	80-20	1	70	14
3	80-20	1	120	5
4	80-20	1	120	14
5	80-20	0	70	5
6	80-20	0	70	14
7	80-20	0	120	5
8	80-20	0	120	14
9	85-20	1	70	5
10	85-15	1	70	14
11	85-15	1	120	5
12	85-15	1	120	14
13	85-15	0	70	5
14	85-15	0	70	14
15	80-15	0	120	5
16	85-15	0	120	14

3.3 Membrane Fabrication Process

The fabrication process can be subdivided in to three parts: Precursor solution preparations, electrospinning, and membrane preparation. Figure 15 illustrates a flow chart of the membrane fabrication process.

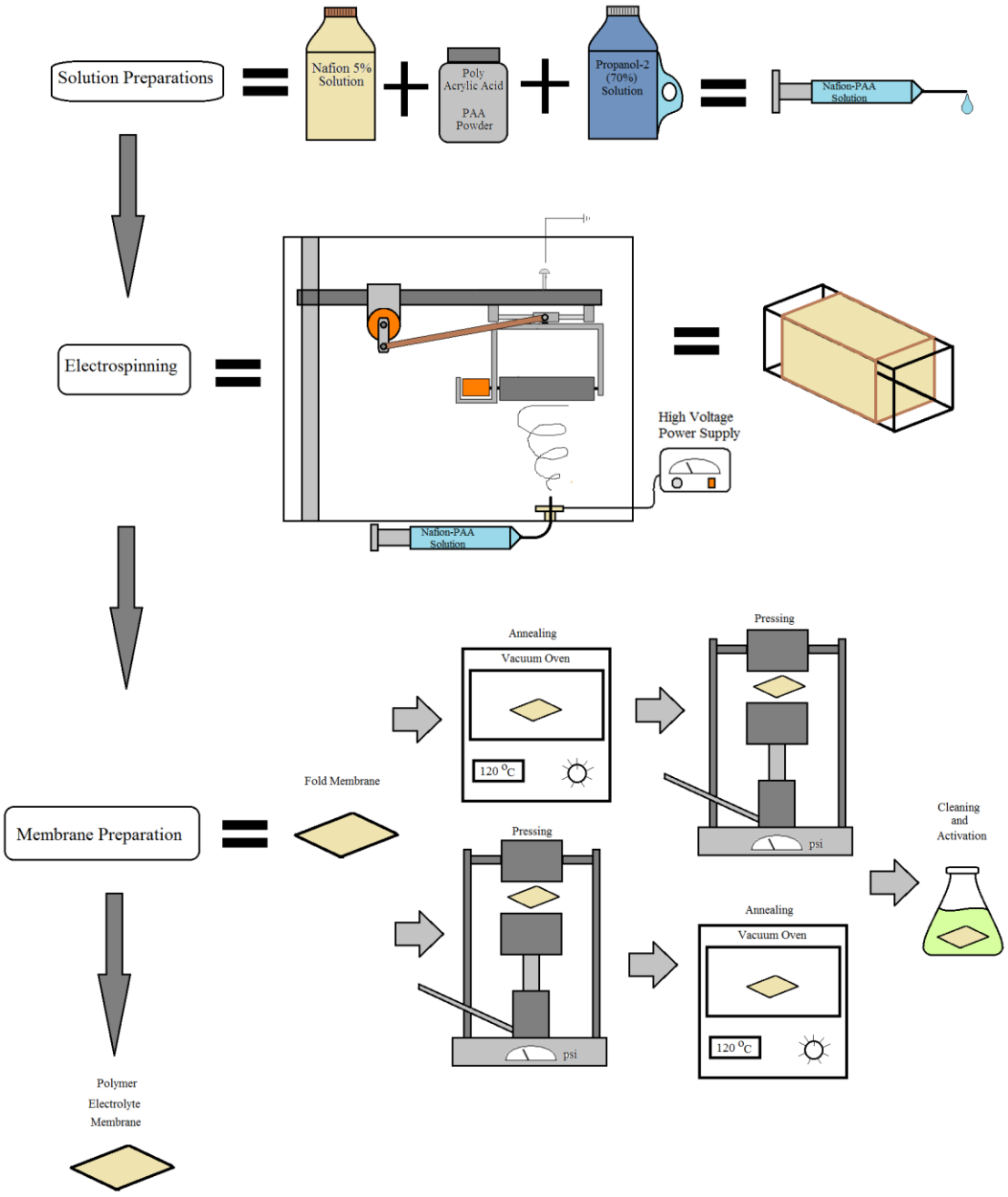

Figure 15: Membrane fabrication process flow diagram

3.3.1 Solution Preparation

A solution had to be prepared for the electrospinning process. Figure 16 illustrates how the solutions were prepared. Preparing the solution requires two main ingredients, dry Nafion and PAA solution, prepared in six steps. The precursor solutions are created by blending Nafion and PAA with concentrations determined by weight.

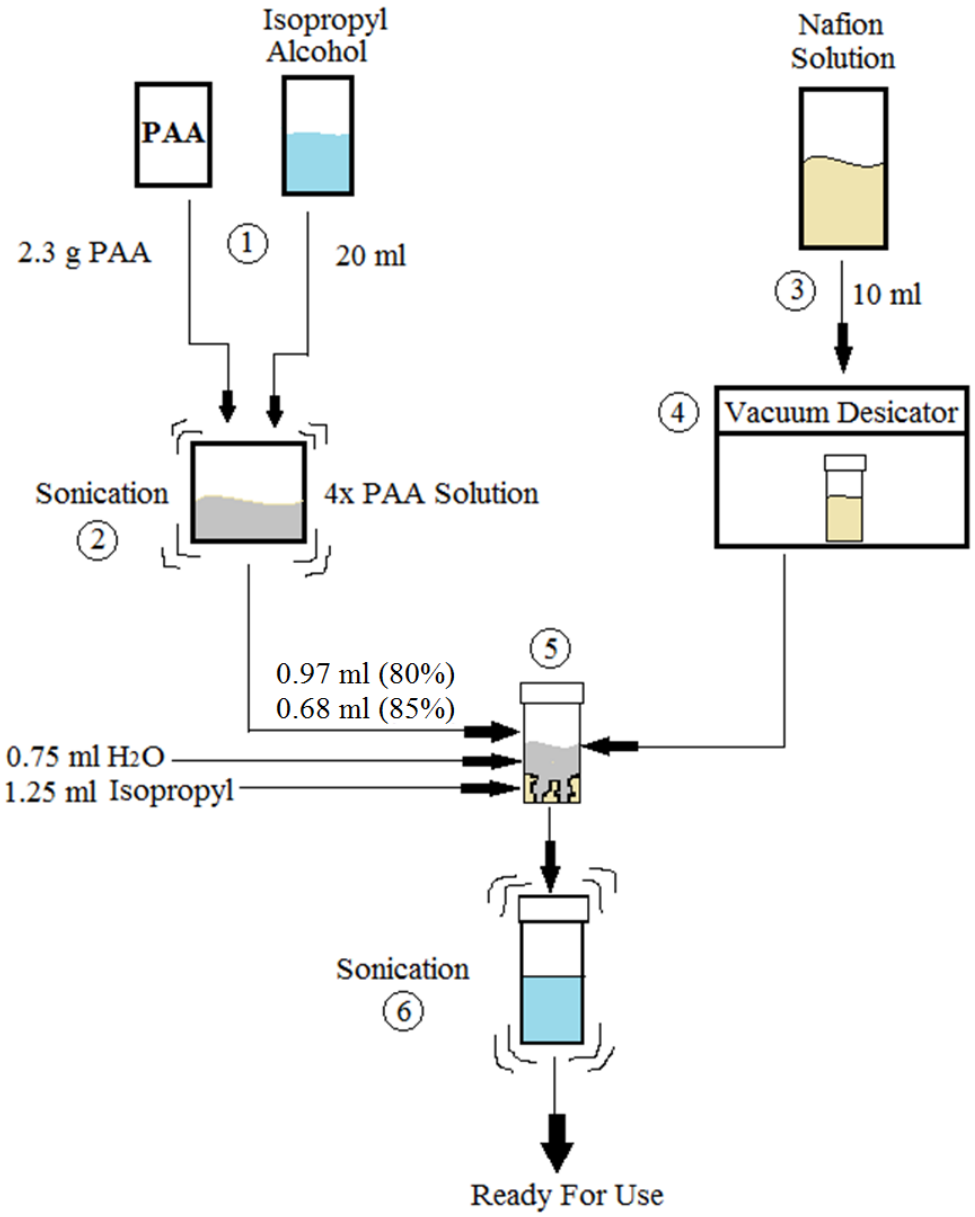

Figure 16: Steps used to successfully create a solution for use in electrospinning.

PAA Solution

1. Combine ingredients
    a. Measure 20 ml of Propanol-2 (70%) and place in a 100 ml beaker.
    b. Place magnetic stirrer in the beaker and begin stirring.
    c. Slowly add 2.3088 grams of Poly (Acrylic Acid) to the beaker. This process should be done in three minutes.

2. Mix ingredients
    a. Stir for 72 hours. Interrupt stirring only for the following steps:
        i. Every 12 hours manually stir with a spatula for one minute.
        ii. After 36 hours sonnicate every 8 hours for thirty minutes (30 min)
    b. After 72 hours the solution should be inspected for inconsistencies. Should more time be necessary keep repeating steps 2.a.i and 2.a.ii.

Dry Nafion

1. A separate Nafion material is prepared by first collecting 10 ml of commercial Nafion solution.

2. The solution is placed in a vacuum dessicator for 24 hours. The result is dried Nafion

Combining Nafion and PAA

3. PAA solution is placed with the dried Nafion material. In addition 0.75 ml of deionized water and 1.25 ml of Isopropyl (70%) is added to the dried Nafion. The water can be substituted by Isopropyl resulting in 2 ml of just isopropyl.

4. The combined solutions are sonicated for a day with one hour intervals and hand mixing.

3.3.2 Electrospinning

Electrospinning is a simple, inexpensive and robust process which creates micro-to-nano sized fibers from a polymer solution. Authors have reported using electrospinning to create composite and electrospun membranes for fuel cell applications with Non-Nafion polymers with very attractive properties such as low methanol fuel crossover and increased ionic conductivity [24][25].

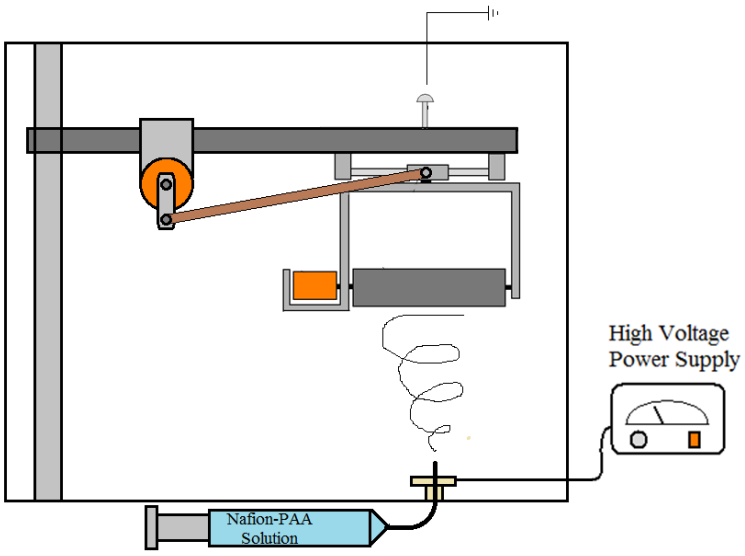

Figure 17: Electrospinning equipment setup.

Figure 17 shows an advance electrospinning setup. A polymer solution with the desired membrane or electrode material is placed in a syringe at the bottom of the electrospinning box. A high voltage supply crates an electrostatic field which pulls on the polymer solution as it is pumped through a needle. As the polymer solution is stretched in the air it spins (hence electrospinning) towards the grounded collector. This process evaporates the solvent and micron-to-nano sized fibers land and accumulates at the grounded collector. The collector is an oscillating rotating drum. This enables the fibers to be collected evenly on the surface of the collector. With this technique it is possible to create an electrospun polymer electrolyte membrane.

A rectangular wire frame collector will collect the fibers (hence the name) as shown in Figure 18. This technique allows for easy processing of the fibers into a uniform rectangular membrane. It also avoids the problem of fibers adhering to the cylinder.

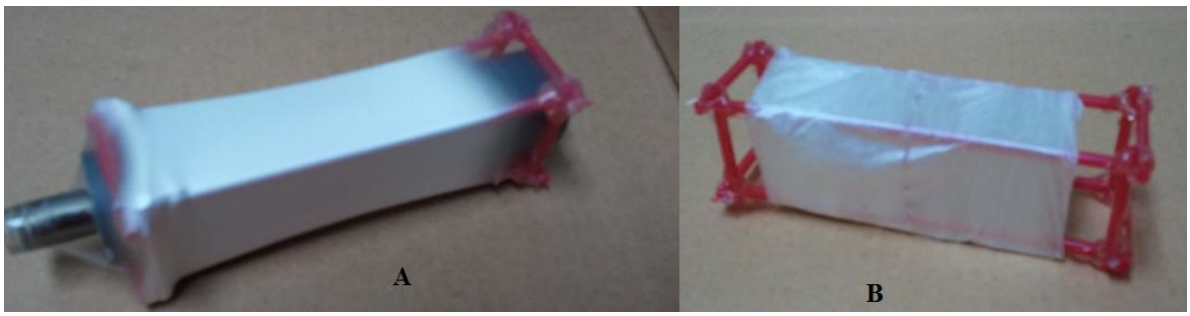

Figure 18: Fibers as collected during electrospinning (A) and after been prepared for removal and processing into a membrane (B).

Electrospinning parameters:

1. Working distance: 21.5 cm

The working distance is the length between the collector and the needle

2. Voltage: 35 kV

   The voltage is the strength of electric potential between the needle and the grounded segment. It is responsible for stretching the polymer solution from the needle tip.

3. Flow rate: 0.2 mL/h

   The flow rate is the volumetric flow rate of the polymer solution through the syringe tip.

4. Relative Humidity: 54%-64%

   If the relative humidity is outside the critical range the polymer solution will solidify and obstruct the flow of the polymer solution.

5. Both motors operate counterclockwise

   Two motors drive the motion of the drum collector and the oscillating mechanism.

6. Temperature: 74.8 ^{o}F -76.4 ^{o}F

   The ambient temperature of the research area oscillates between 74.8 ^{o}F -76.4 ^{o}F.

7. Time: 1 hour.

   The fibers can be collected for different amounts of time to change the thickness of the membranes.

The rectangular frame was not electrically grounded to successfully collect the fibers in the collector. The collector has to be located in an intercepting manner as depicted in Figure 19. The ground is located on the arm that connects to the box.

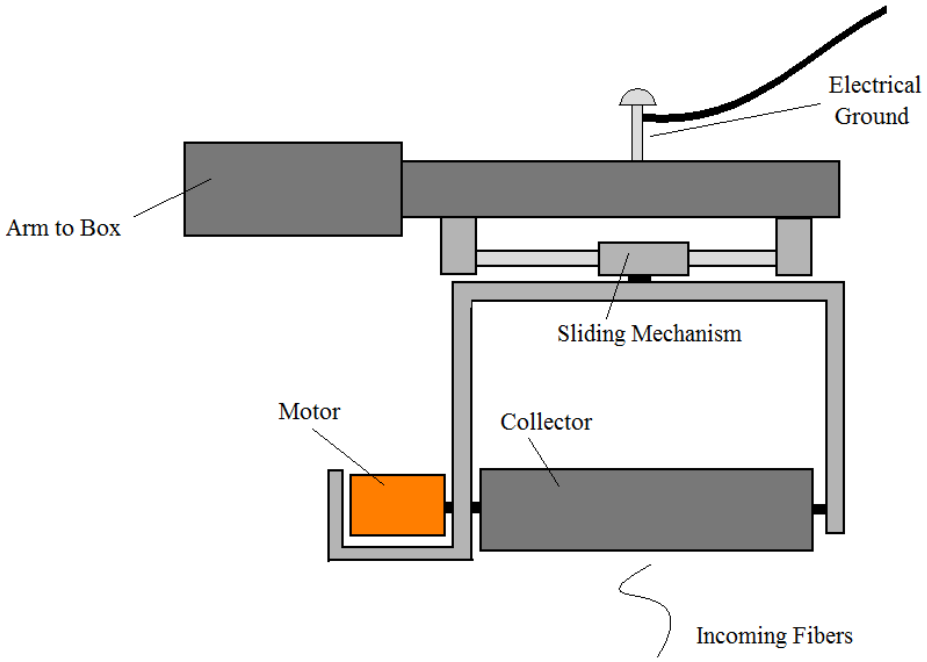

Figure 19: Correct location of electrical ground.

Membranes were cut from the rectangular wire frame and folded into a square as show in Figure 20. From there on the membranes were processed by pressing and heating or vice versa.

Figure 20: A folded non-processed electrospun membrane removed from the collector.

3.3.3 Membrane Processing

Membranes are said to be processed if after they are collected they are annealed, compacted, cleaned and activated. Cleaning and activation are considered a single step which is always the last step performed.

Compacting

Pressing was achieved by locating the fiber membranes between two Teflon sheets. The sheets are then placed between two Bakelite cylinders with a one inch diameter. 5,000 or 14,000 psi is then applied for five minutes (5 min.). The fibers go from white to transparent after pressing. Uneven pressing causes the membranes to have regions which are not transparent.

Annealing

Fibers are heated in a vacuum oven at 70 ^{o}C or 120 ^{o}C for 15 minutes. This procedure is performed at vacuum.

Fiber Cleaning and Activation Procedure

Membrane cleaning and activation procedure varies from laboratory to laboratory. In some cases the membranes are directly placed in an activation process with nitric acid by skipping a cleaning process with hydroxide peroxide[23][26][15].The hydroxide peroxide helps remove impurities within the membrane. Since electrospun membranes are more likely to introduce impurities, cleaning with hydroxide peroxide should not be omitted. But the traditional step of boiling the membrane for one hour cannot be used. Boiling the membranes

severely compromises its mechanical strength. Instead the membrane will be placed with hydroxide peroxide at room temperature. When it comes to activating the membranes in nitric acid there are also different procedures. Different times and temperatures are applied by different researchers [27]. The temperature has to be fixed at room temperature to avoid degradation but the time can be varied from 20 minutes to 48 hours [28]. A reasonable time of 24 hour at room temperature seems sufficient to allow for proper activation.

Cleaning and Activating Procedure

1. Individually submerge the membranes in 10 ml of Hydroxide Peroxide 3% for 1 hour at room temperature.
2. Wash membranes by placing in 130 ml deionized water and gently stir for one minute.
3. Submerge the membranes in 10 ml of concentrated nitric acid (70%) for 24 hours at room temperature.
4. Wash membranes three times with deionized water until all acid residues are removed.
    a. Place in 130 ml of deionized water and gently stir for one minute. Repeat Once
    b. Place in 130 ml of deionized for one hour.
5. Store accordingly as needed.

3.4 Characterization

Various characterization techniques were used to determine important membranes properties. A design of experiment with 16 different membranes with 3 repetitions per membrane was used to determine water uptake, ion exchange capacity and water content. SEM and optical microscopy was performed on all 16 different membranes (48 membranes if repetitions are counted). Fiber diameter distribution, and fiber orientation analysis was performed on non-processed membranes only. Solubility and tensile strength was performed on selected membranes only. Most results except for SEM and optical microscopy were compared with commercial membranes made by DuPont. They had the same equivalent weight (Eq: 1100) as the Nafion polymer solution and had a thickness of 0.005 inches. No processing was necessary for the commercial Nafion membranes but the exact same cleaning and activation procedure of the electrospun membranes were used with the commercial membranes.

3.4.1 Scanning Electron Microscope (SEM) and Optical Microscopy

SEM microscopy revealed important information about porosity, fiber size distribution, fiber defects and fiber orientation. It was used to determine membrane thickness. An optical microscope was used to verify fiber diameter size and measure membrane thickness.

Membrane Orientation

MatLab software was used to draw a line diagonally at 45^{o} along the photograph and the fibers that intersected the line were measured. Membrane orientation was measured by drawing a vector along the directions of the fibers. The angle between the direction perpendicular to the

nominal direction (direction of the rotating drum) and the individual fibers was measured. Each fiber angle was divided by the nominal angle (1 being perfect orientation and zero being a perpendicular direction) and the average calculated. The average fiber orientation was also calculated.

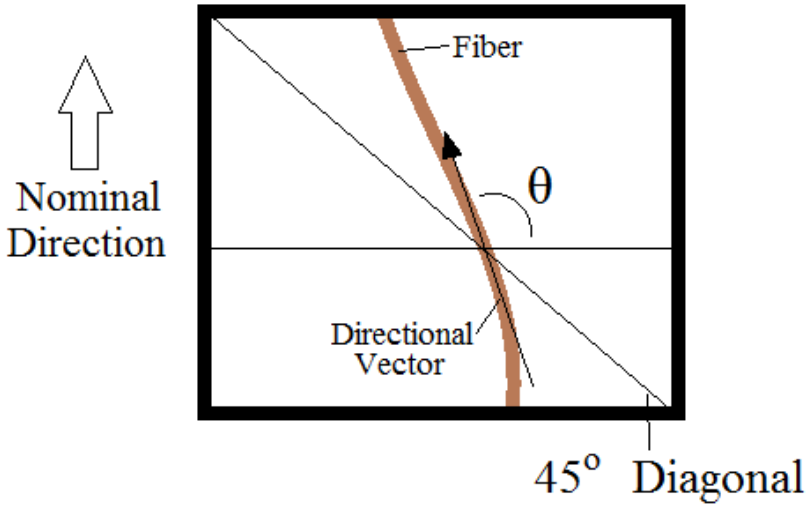

Figure 21: Angle (θ) calculated between direction perpendicular to the nominal direction and the directional vector.

Membrane Diameter

The fiber diameter was measured using Image J software. Three diagonal lines at 45° were drawn on the photograph and at each intersection between lines and fibers the diameter was measured. Histograms and average fiber diameter were calculated.

Fiber-Void Fraction

The fiber-void fraction was calculated using Image J software. The SEM photographs were passed through Fast Fourier Transfer filter to reduce spot size noise from the image. Binary color threshold was used to differentiate between the fibers and the voids. The area

fraction feature of Image J was used to calculate fiber-void fraction. There is a level subjectivity when applying the threshold differentiation. Three measurements are taken with a low, medium and high threshold value. That's why the Fiber-Void fraction is given as range and an average.

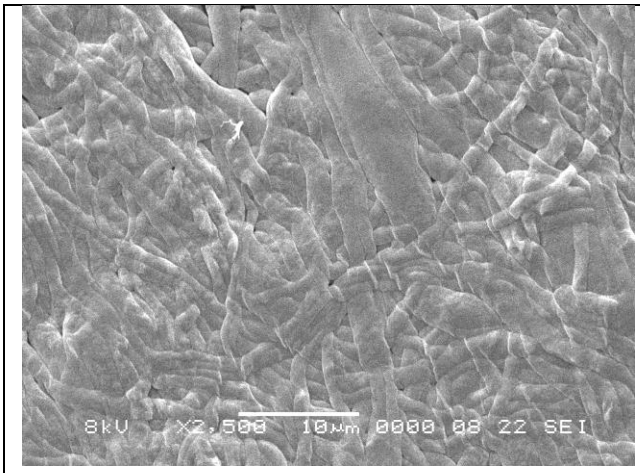

A. Original SEM photograph

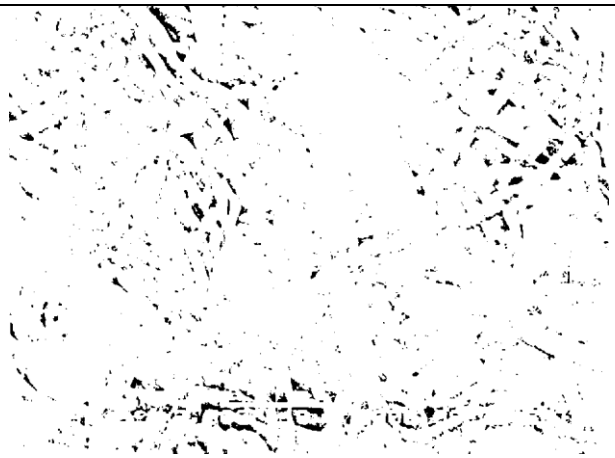

B. Low Threshold Value

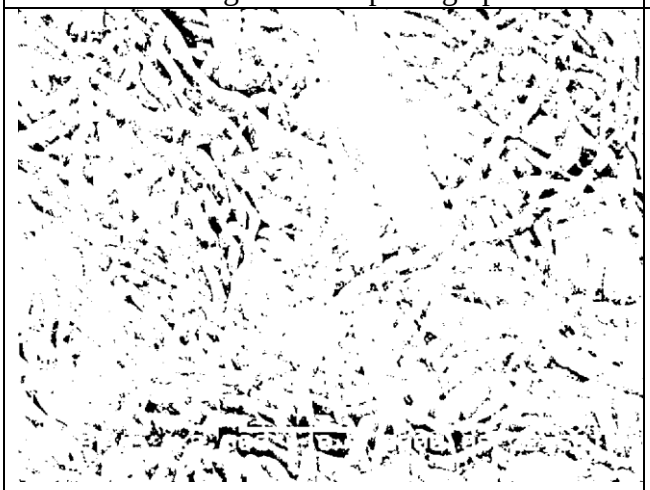

C. Medium Threshold Value

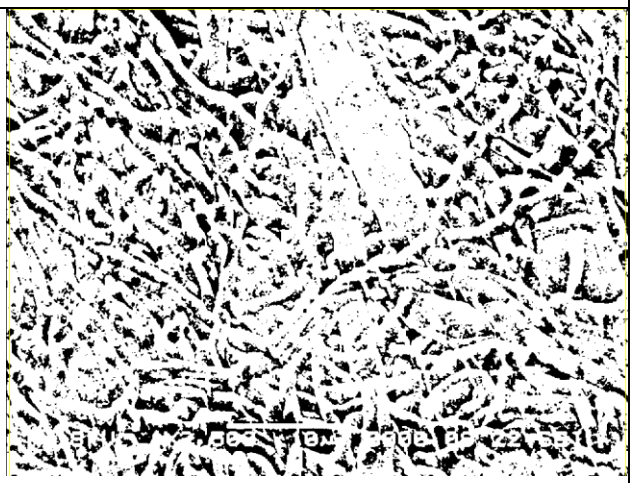

D. High Threshold Value

Figure 22: Fiber-void fraction calculations with binary differentiation with different threshold values

3.4.2 Water Uptake

In order for membranes to function properly they must be adequately hydrated. The dependence of Nafion's ionic conductivity on the level of hydration is well documented [29]. Water uptake characterization will give precise information on the level of hydration of the membrane.

Procedure for Water Uptake Characterization

1. Dry membranes in vacuum desiccators for one hour with relative humidity between 10-20%.
2. Carefully weigh the membranes (weight at zero hours). All membranes must be weighted within five minutes after removal from the vacuum desiccator.
3. Submerge the membranes in deionized water and begin timing. Measure the temperature and relative humidity.
4. Carefully weigh the membranes after 24 hours.
    a. When weighing the membranes, they should first be blotted of any water.
    b. Then they should be superficially dried with a kimwipe to remove any latent water.
        i. Place the membrane on top of kimwipe and place a second kimwipe on top of the membrane.
        ii. Gently press on the kimwipe to lightly compress membrane between the kimwipes.
        iii. Carefully ensure that the pliers are dry.
        iv. Measure the weight of membranes.

c. Membranes should be re-submerged for 15 seconds (15 s), and step 4 repeated a total of three (3) times.

Water uptake should be analyzed as percent change in weight according to Equation 10. Where "w_o" is the initial weight and "w_n" the final weight.

$$Water\ Uptake = \frac{(W_n - W_0)}{W_0} \times 100$$ Equation 10: Water Uptake

3.4.3 Ion Exchange Capacity Characterization

Ion Exchange Capacity (IEC) determines how many sulfonate exchange sites are available for ion exchange. The morphological properties of electrospun membranes should outperform recast and commercial membranes by exposing more sulfonated exchange sites. These sites tend to be buried in the fluorocarbon phase in the case of recast and commercial membranes [28]. IEC is critical for establishing a comparison basis along with water content to determine the ionic conductivity of the membranes. The ion exchange capacity was determined via the titration method.

Procedure for Ion Exchange Capacity

1. Fully cleaned and activated membranes should be dried in a vacuum desiccator for one hour at a relative humidity between 5%-15%.
2. Weigh membranes.
3. Place membranes in 10 ml of NaCl 3 M for 12 hours

4. Add one drop of Fenolftaleina in the NaCl Solution
5. Begin titration with NaOH 10 mM using a micropipette.
    a. Add 30 ul of NaOH with each increment.

The ion capacity is given by Equation 11:

$$IEC\left[\frac{mmol}{g}\right] = \frac{v \times C_{NaOH}}{m_{dry}}$$ Equation 11: Ion Exchange Capacity

Were "v" is the end volume of NaOH added in ml, "C_{NaOH}" is the concentration of NaOH solution in mmol/ml and "m_{dry}" is the weight of the polymer sample.

3.4.4 Water Content

Water content (λ) is defined as the ratio between water molecules and exchange sites and can be calculated experimentally with Equation 12.

$$\lambda = \frac{mol\ H_2O}{mol\ SO_3^-} = (wt) \times \frac{1}{(W_{mg})} \times \frac{1000}{(IEC)}$$

Equation 12: Water Content Calculation

Were "wt" is the water uptake, "W_{mg}" is the molecular weight of water (18.02 g/mol) and "IEC" is the ion exchange capacity (mmol/g) (1000 to convert mmol to mol). Some researchers use the Equivalent weight given by the manufacturer instead of the IEC.

Water content is a very important propertied because it has been linearly related with ionic conductivity of the PEM. This means the higher the water content the higher the ionic conductivity.

3.4.5 Membrane Solubility

It is important to determine if the membrane will dissolve under normal operating conditions. Commercial Nafion membranes are very resistant to chemical attacks and are virtually insoluble in any solvent at regular operating conditions. Recast Nafion membranes with low crystallinity will dissolve on in water and other solvents making them unviable for use in fuel cells. Annealing the recast films above the glass transition temperature will impart a higher degree of crystallinity to membranes decreasing the solubility. Electrospun membrane will are

expected to have a higher degree of crystallinity than the recast membranes due to electrospinning.

The solubility of the electrospun membrane was determined for annealed and untreated membranes to determine the effect of the annealing temperature. The electrospun membranes were found to be virtually insoluble in water at ambient conditions. A more aggressive approach was used with a propanol-2 (70%) solvent and ultrasonic shaker. Four membranes with two different Nafion concentration and two different annealing temperatures were used with the more aggressive approach. Two additional non-processed electrospun membranes with different Nafion concentrations were also tested. All the membranes were first compacted at 5 ksi and then annealed (order 0).

Solubility Characterization Procedure

1. Fully cleaned and activated membranes should be dried in a vacuum desiccator for one hour at a relative humidity between 5%-15%.
2. Weigh membranes.
3. Submerge membranes in 20 ml of propanol-2 (70%)
4. Shake membranes with ultrasonic shaker every 8 hours for 30 minutes
5. After 48 hours remove the membranes from the propanol-2 bath and dry the membranes in a vacuum desiccator for 24 hours at a relative humidity between 5%-15%.
6. Weigh membranes

The solubility of the membranes can be calculated with Equation 13. Values from Equation 13 will be negative indicating that there is a reduction in weight. A result with 100% solubility means that the membranes completely dissolve in the solution. A result with 0%

solubility means that the membrane is insoluble or will not dissolve in any way while in the solution.

$$Solubility\ [\%] = \frac{W_f - W_i}{W_i}$$ Equation 13: Solubility

3.4.6 Tensile Strength

The tensile strength of the electrospun membranes and commercial membranes were determined with ESM301 with a series 5 load cell as shown in Figure 23. Four Non-processed electrospun membranes (two 80% and two 85%) and a commercial membrane were cut in to strips of approximately15 mm by 8 mm. The thickness of the membranes was measured with an optical microscope. The test station was programmed with an up speed of 380 mm/min (1.5 in/min). The maximum load was recorded and the maximum tensile strength calculated with Equation 14.

Equation 14: Maximum Tensile Strength

$$MTS = \frac{L_{max}}{A_{cross}}$$

Were "MTS" is the maximum tensile strength, "L_{max}" is the maximum load and "A_{cross}" is the cross sectional are of the sample.

Figure 23: ESM301 with series 5 load cell tensile strength testing station

Humidity was carefully controlled by placing the membranes in vacuum desiccator for two hours. Afterwards the membranes were placed in the testing room at 75% relative humidity for four hours. The membranes were folded four times with fibers folded perpendicular as seen in Figure 24.

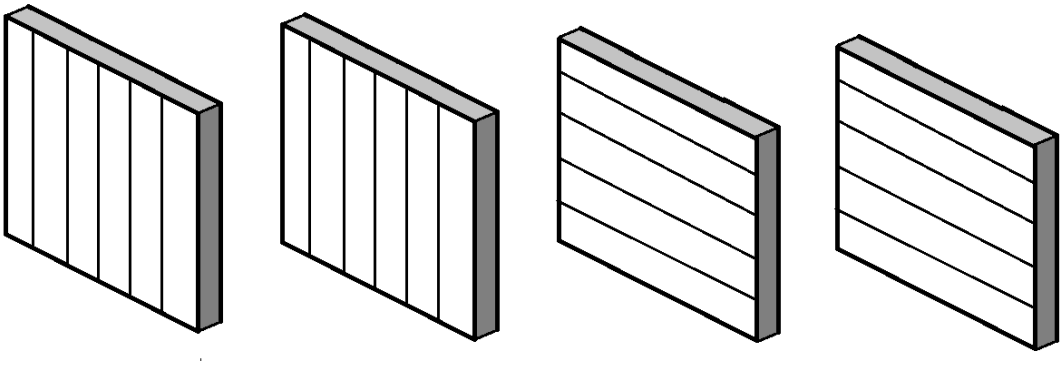

Figure 24: Fiber orientation when membranes are folded

The direction of the fiber is important because the tensile strength will change if the membrane is stretched in the direction of the fiber or the perpendicular direction.

4 Results

In this chapter characterization results and analysis are presented. Characterization and analysis results include fiber diameter distribution, fiber orientation, water uptake, IEC, water content, tensile strength and solubility. Water content is analyzed with IEC to trend ionic conductivity. The Springier fuel cell model is used to calculate the ionic conductivity of the electrospun polymer electrolyte membranes.

4.1 Scanning Electron Microscopy

Electrospinning has conferred desirable properties to the electrospun fibers such higher fiber-void fraction, orientation and less defects such as beads and tangles. As seen in Figure 25 fibers collected with the oscillating drum collector show greater fiber density and fewer defects than those collected with a stationary collector. Fiber mats created with the oscillating drum collector are also more homogenous than those collected with a stationary collector.

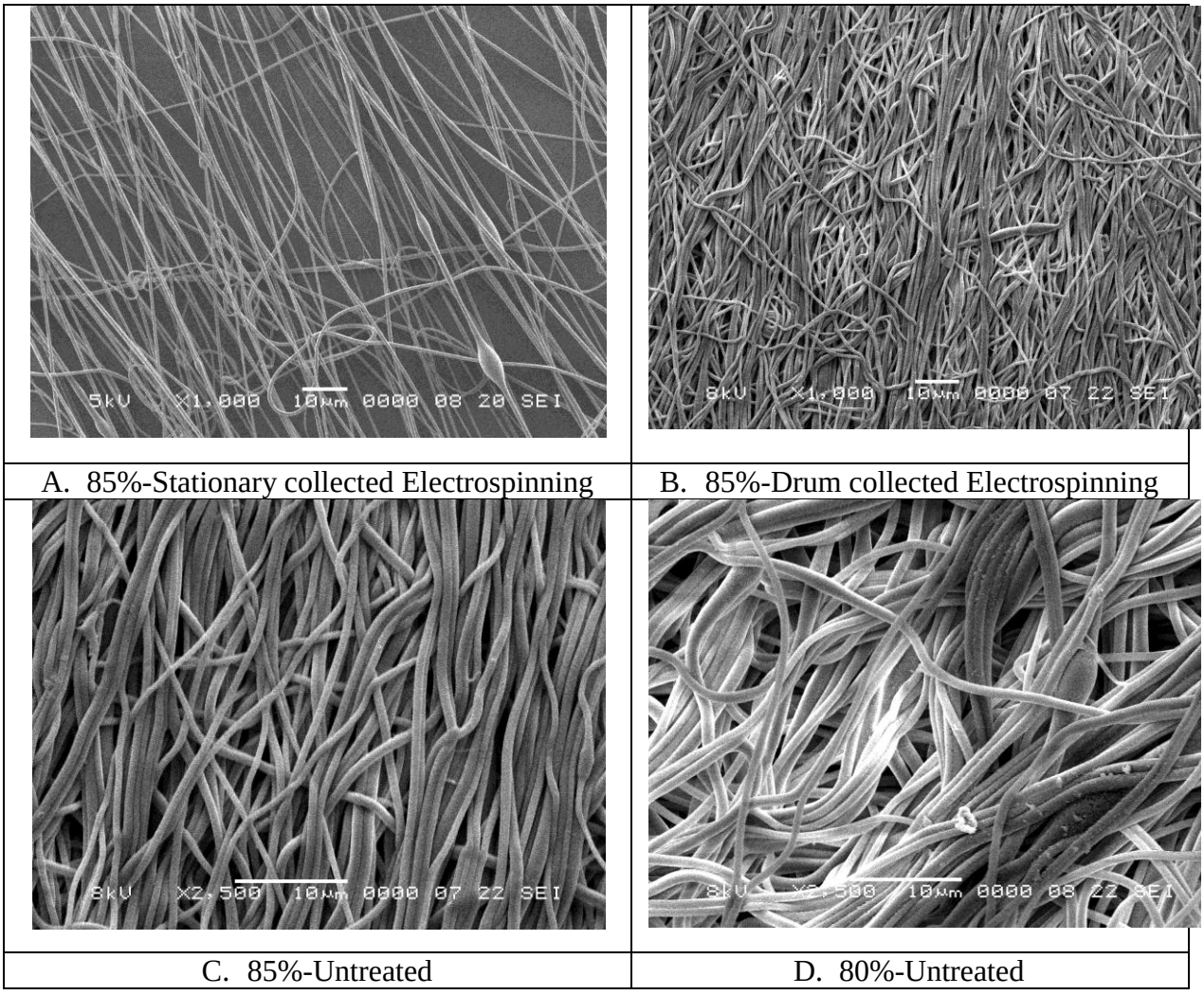

A. 85%-Stationary collected Electrospinning

B. 85%-Drum collected Electrospinning

C. 85%-Untreated

D. 80%-Untreated

Figure 25: Electrospun membranes without any processing. Zoom 2,500 times.

SEM: Nafion 85%-PAA 15%

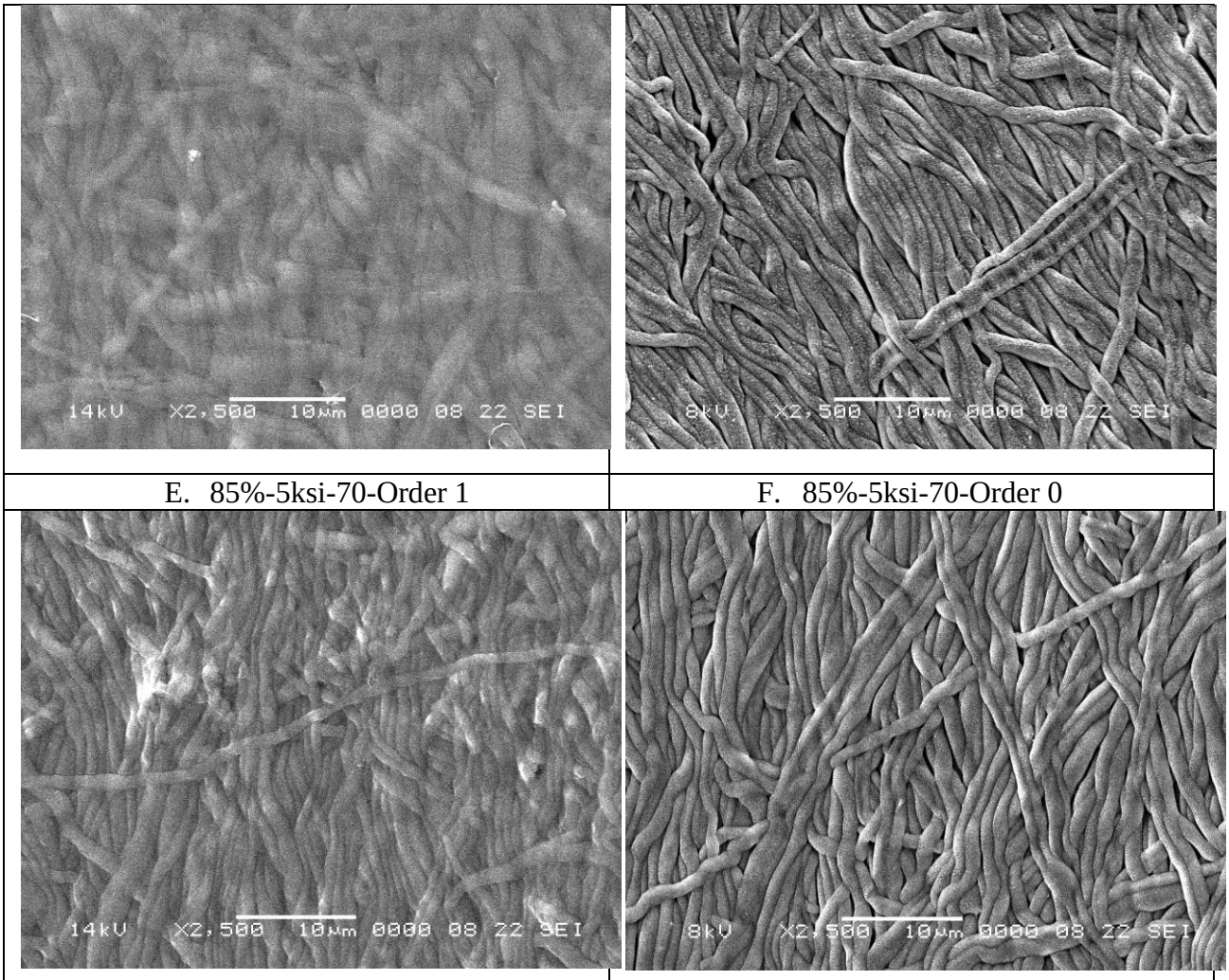

E. 85%-5ksi-70-Order 1	F. 85%-5ksi-70-Order 0
G. 85%-5ksi-120-Order 1	H. 85%-5ksi-120-Order 0

Figure 26: 80% Nafion processed at 5 ksi with different parameters. 2,500 X.

Figure 26 shows membranes prepared with 85% Nafion 15% PAA processed with different parameters. There is a difference between membranes due to the processing order. Membranes pressed first and annealed second are less defined than those with the opposite order. Fiber orientation is visible in all photographs.

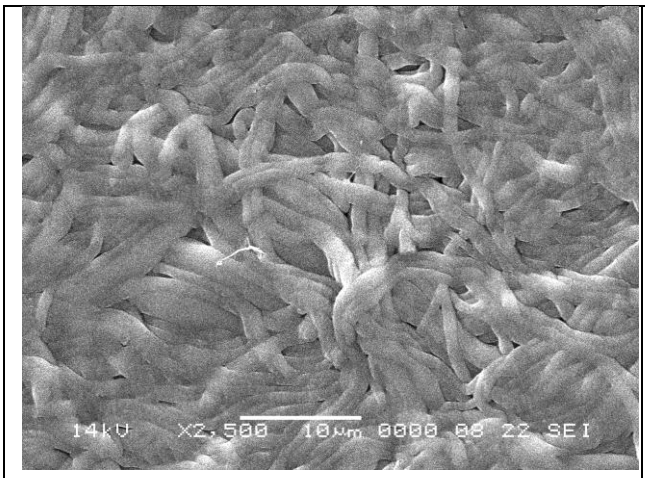

A. 85%-14ksi-70-Order 1

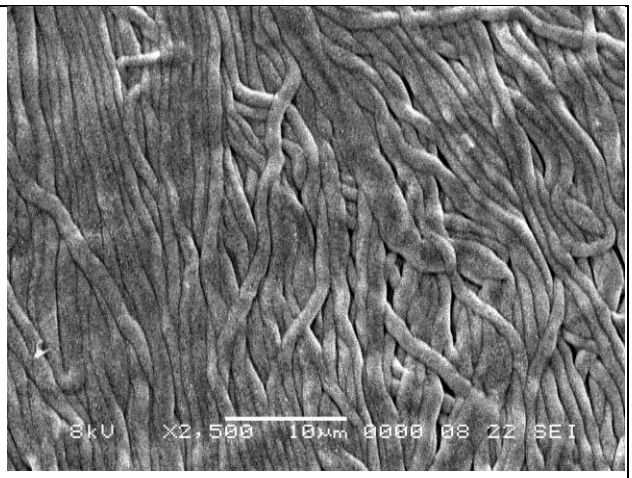

B. 85%-14ksi-70-Order 0

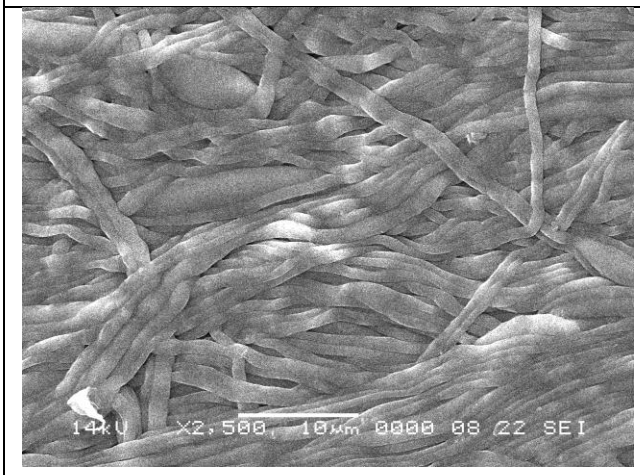

C. 85%-14ksi-120-Order 1

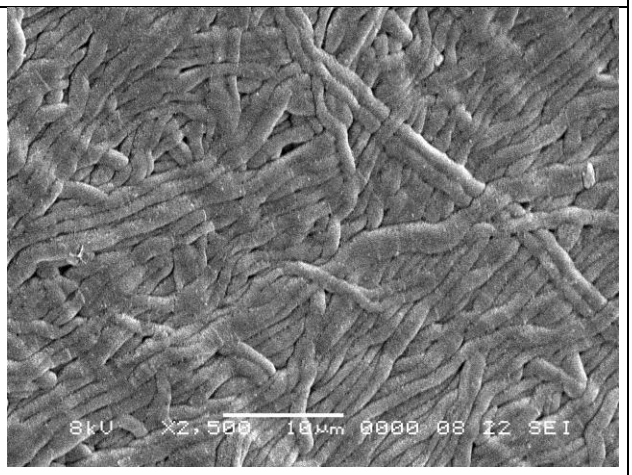

D. 85%-14ksi-120-Order 0

Figure 27: 85% Nafion processed at 14 ksi with different parameters.

Figure 27 shows membranes prepared with 85% Nafion 15% PAA processed with different parameters. There is a difference between membranes due to the processing order. Membranes pressed first and annealed second are less defined than those with the opposite order. Fiber orientation is visible in all photographs

SEM: Nafion 80%-PAA 20%

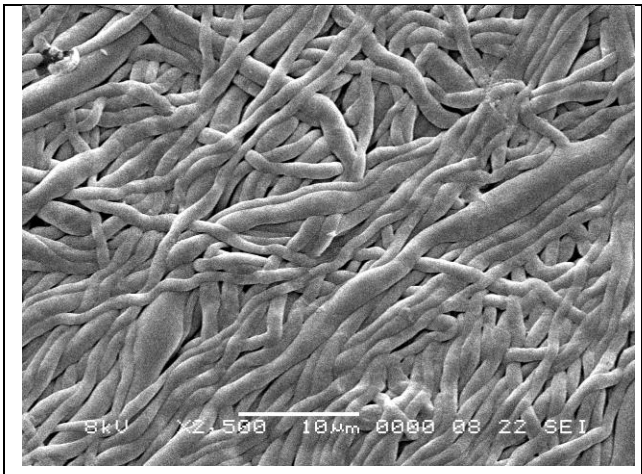

E. 80%-5ksi-70-Order 1

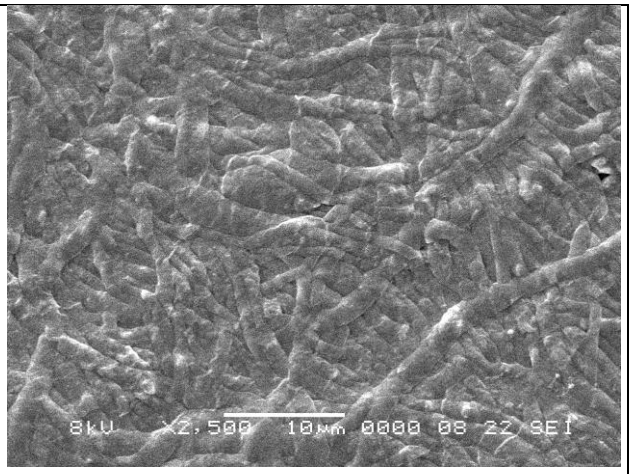

F. 80%-5ksi-70-Order 0

G. 80%-5ksi-120-Order 1

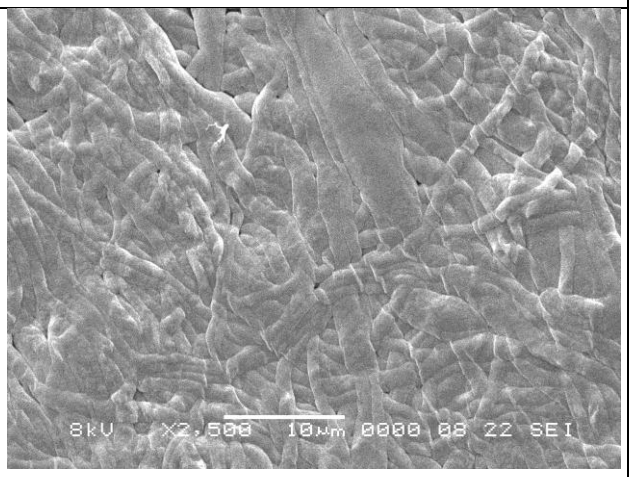

H. 80%-5ksi-120-Order 0

Figure 28: 80% Nafion processed at 5 ksi with different parameters.

Different that Nafion 85%, fibers with 80% Nafion are less defined when annealed first and pressed second as seen in Figure 28. Fiber orientation is visible in all photographs. Order 1 membranes have slightly more space between the fibers than the order 0 membranes. Fiber-void fraction for Figure 29 (C) is 83%-94% with an average of 88%, while Figure 30 (D) has 89%-97% with an average of 96%.

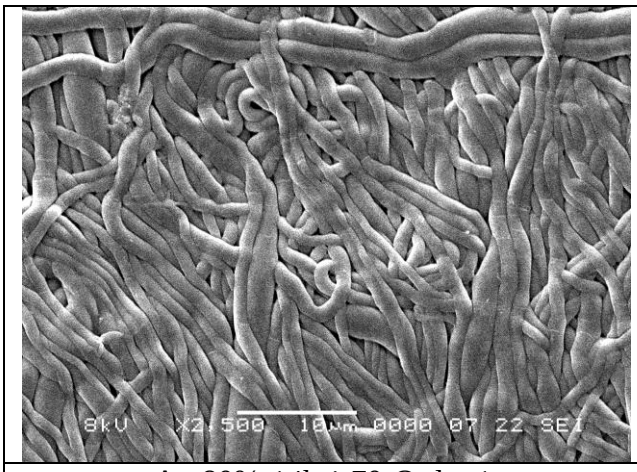

A. 80%-14ksi-70-Order 1

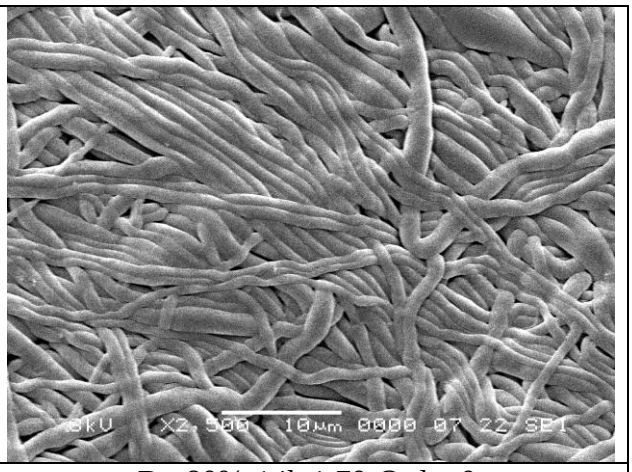

B. 80%-14ksi-70-Order 0

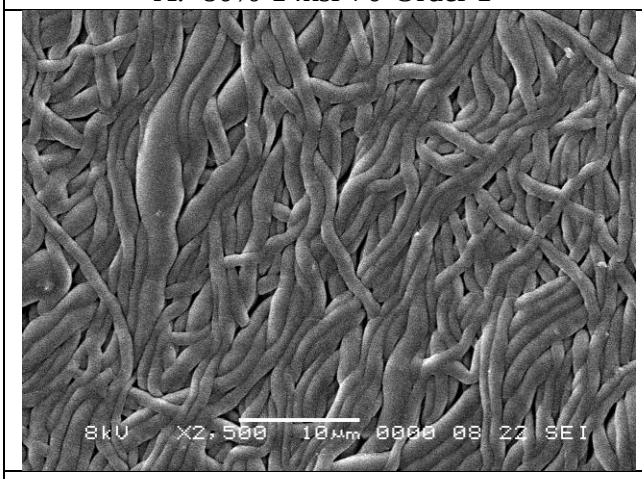

C. 80%-14ksi-120-Order 1

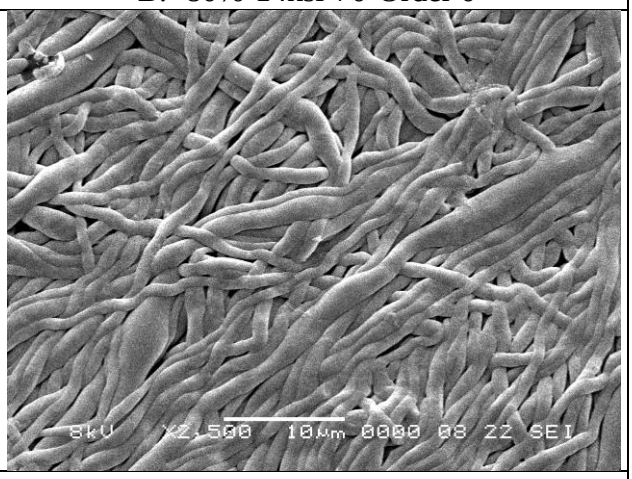

D. 80%-14ksi-120-Order 0

Figure 29: 80% Nafion processed at 14 ksi with different parameters.

As seen in Figure 29 there seems to be no difference due to the processing order for membranes with 80% Nafion processed at 14 ksi. Fiber orientation is visible in all photographs. All membranes have similar levels of porosity between the fibers. The fiber-void fraction varies between 92%-89% with an average of 90.3% for Figure 29 (C) and 93%-82% with an average of 87.6% for Figure 29 (D).

Membrane Fiber Diameter

The fiber diameter was measured using Image J software for Nafion-PAA concentrations of 80%-20%, 85%-15%, and 90%-10%. The frequency of the distribution of the fibers was plotted, the average and standard deviations was calculated. The fiber orientation was measured for the non-processed Nafion-PAA fibers with concentrations of 80%-20% and 85%-15%.

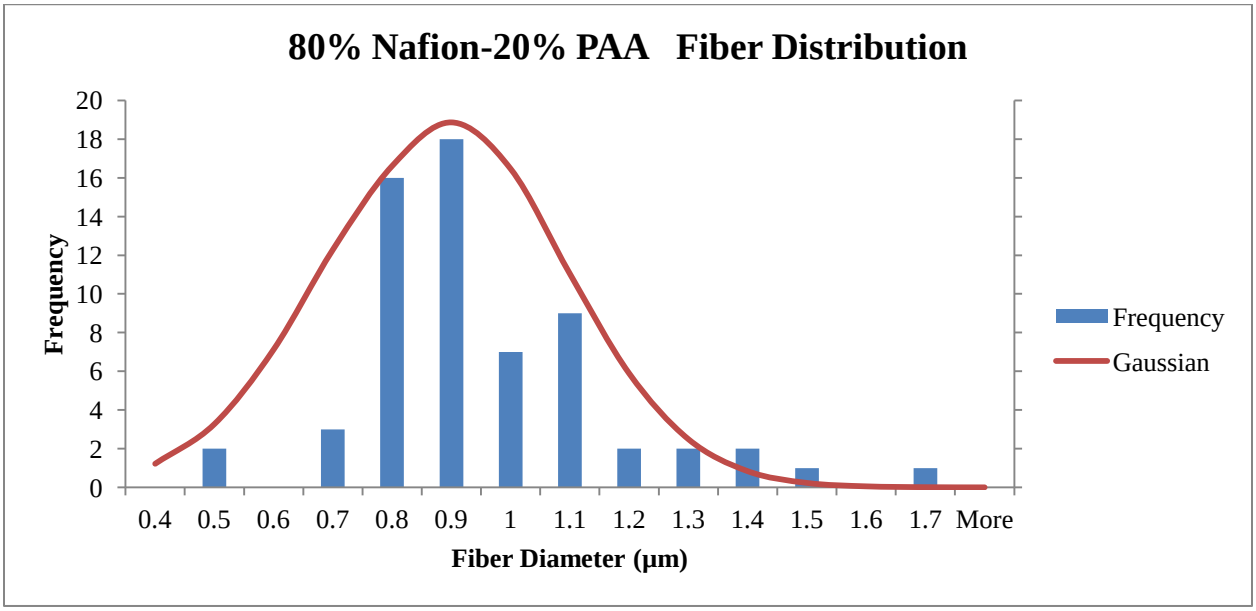

Figure 30: Histogram for fiber distribution of 80% Nafion – 20% PAA of non-processed electrospun fibers

Membranes with 80% Nafion have a larger diameter with an average of 897 nm and standard deviation of 212 nm. The fiber diameter distribution largely follows a normal distribution as seen Figure 30. Fibers with larger diameters than the average are more common than fibers with smaller diameter than the average.

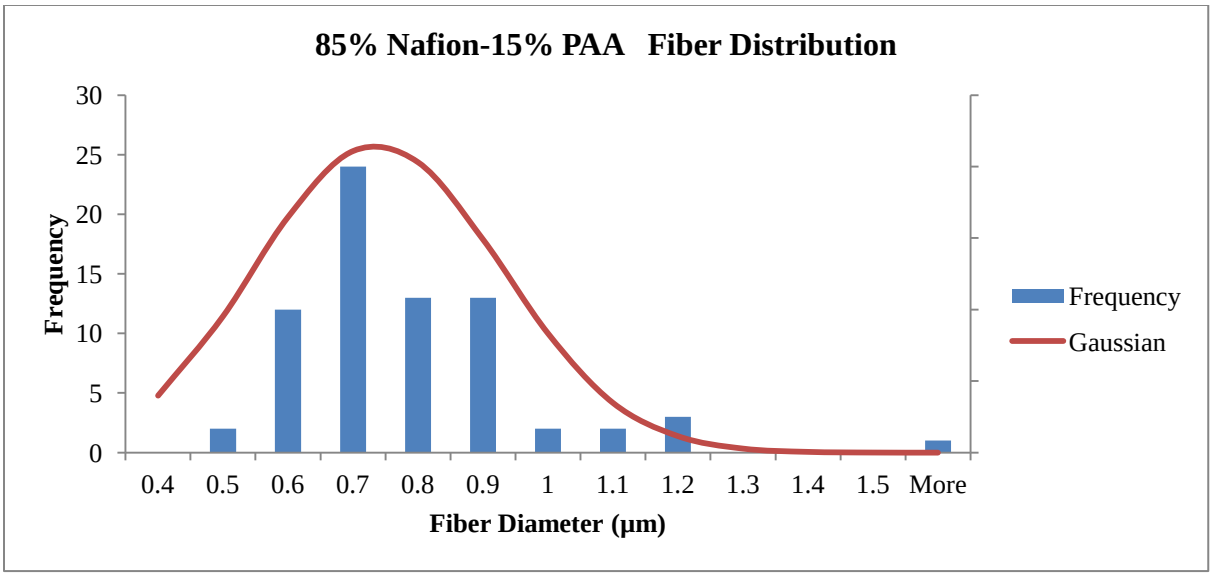

Figure 31: Histogram for fiber distribution of 85% Nafion – 15% PAA of non-processed electrospun fibers

Membranes with 85% Nafion have an average diameter of 736 nm and standard deviation of 182 nm. The fiber diameter distribution largely follows a normal distribution as seen Figure 31.

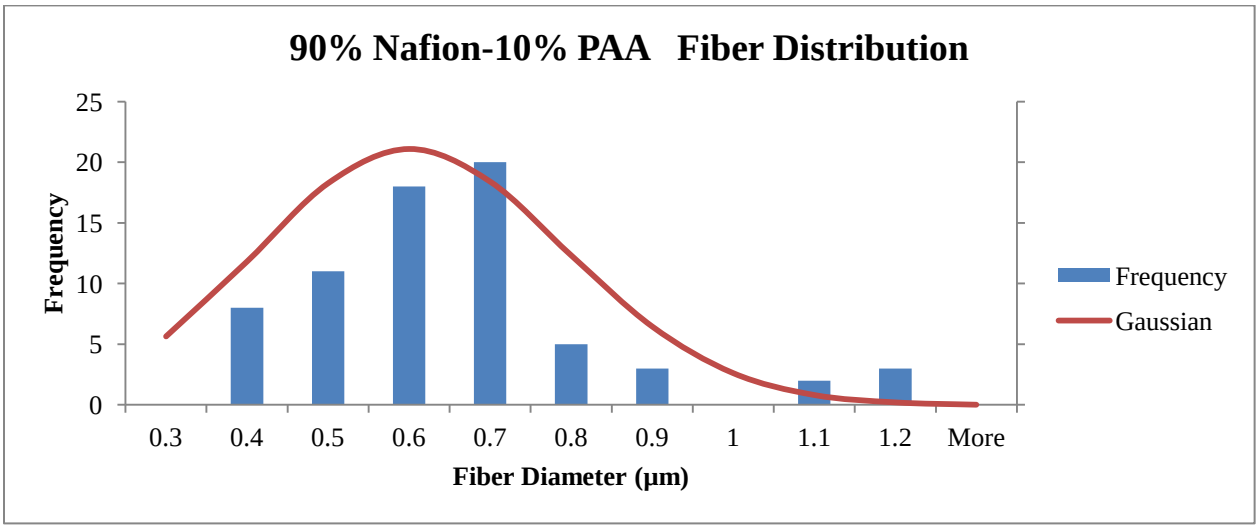

Figure 32: Histogram for fiber diameter distribution of 90% Nafion – 10% PAA of non-processed electrospun fibers.

The higher the conductivity of the polymer solution, the smaller the fiber diameter will be when created by electrospinning. Nafion has a higher conductivity than PAA and thus the higher the concentration of Nafion the smaller the fiber diameter. That's why the 80% Nafion solution has fibers bigger than the 90% Nafion Solution. Table 6 summarizes the fiber diameter, fiber diameter standard deviation and conductivity of different polymer solutions. Conductivity measurements were taken from the literature [13].

Table 6: Summary of fiber diameter and conductivity

	Nafion-PAA Concentration (%wt)				
	80%	85%	90%	0%	100%
Average Fiber Diameter (nm)	897	736	607	Na	Na
Standard Deviation (nm)	212	182	185	Na	Na
Conductivity (μS) [13]	220	280	320	100	450

Fiber Orientation

The fiber orientation was measured for non-processed Nafion-PAA concentrations of 80%-20% and 85%-15%. The average percent of alignment with respect to the nominal direction (as referenced in Chapter 3) was calculated along with the average fiber orientation.

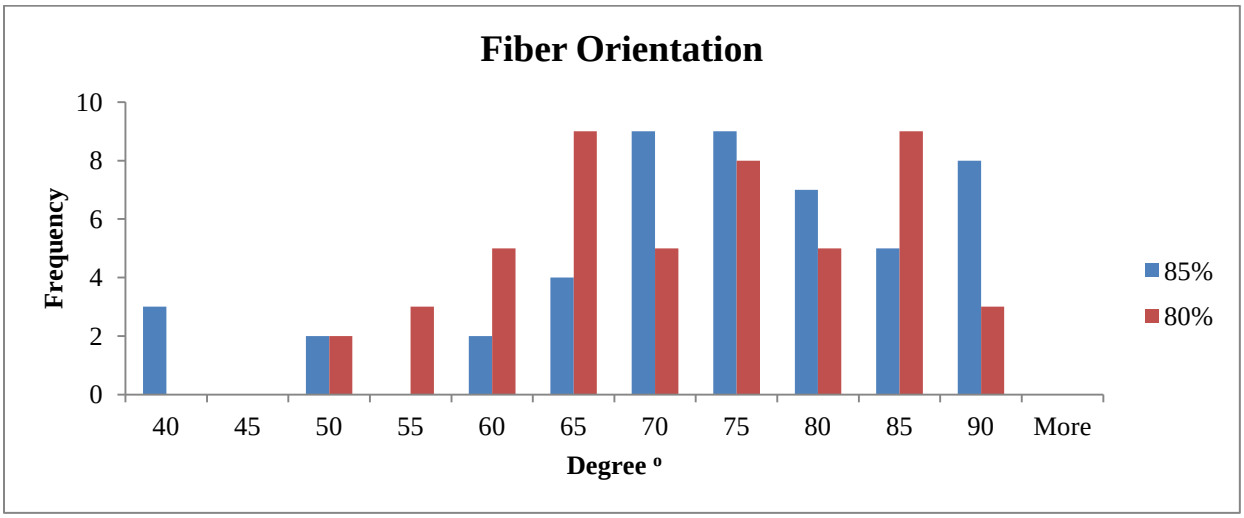

Figure 33: Histogram for fiber orientation distribution for 80% Nafion–20% PAA and 85% Nafion-15% PAA of non-processed electrospun fibers.

Table 7: Summary of fiber orientation for 80% and 85% Nafion concentration

Concentration	Percent of Alignment (%)	Average Angle (°)	Standard Deviation	Median Angle (°)
80	77.2	69.49	11.16	70.2
85	78.8	70.98	13.00	71.27

Non-processed membranes with 80% Nafion 20% PAA had an average fiber orientation 0f 69.5° and an average percent of alignment of 77.2%. Non-processed membranes with 85% Nafion 15% PAA had an average fiber orientation 0f 70.9 and an average percent of alignment

of 78.8%. Figure 33 shows the distribution of both 80% and 85% Nafion with similar distributions. The standard deviation for the angles is 11.16 and 13.00 for Nafion 80% and 90% respectively.

Fiber orientation results are very similar for both 80% and 85% Nafion concentration as summarized in Table 7. This indicates that fiber orientation is determined solely by the electrospinning parameters, in this case use of oscillating the drum collector. Nafion concentration plays a significant role in fiber diameter distribution but has no effect on fiber orientation.

4.2 Water Uptake

Water uptake indicates how much water is absorbed by the membrane. Some polymers like PAA are known to absorb many times their weight in water. Other polymers like Teflon will not absorb any amount of water. As discussed in sec 2.1.3 Water Content, water uptake is crucial in determining the water content. Water uptake measurements was performed for all 16 data points according to the DOE and a commercial membrane with three repetitions per data point

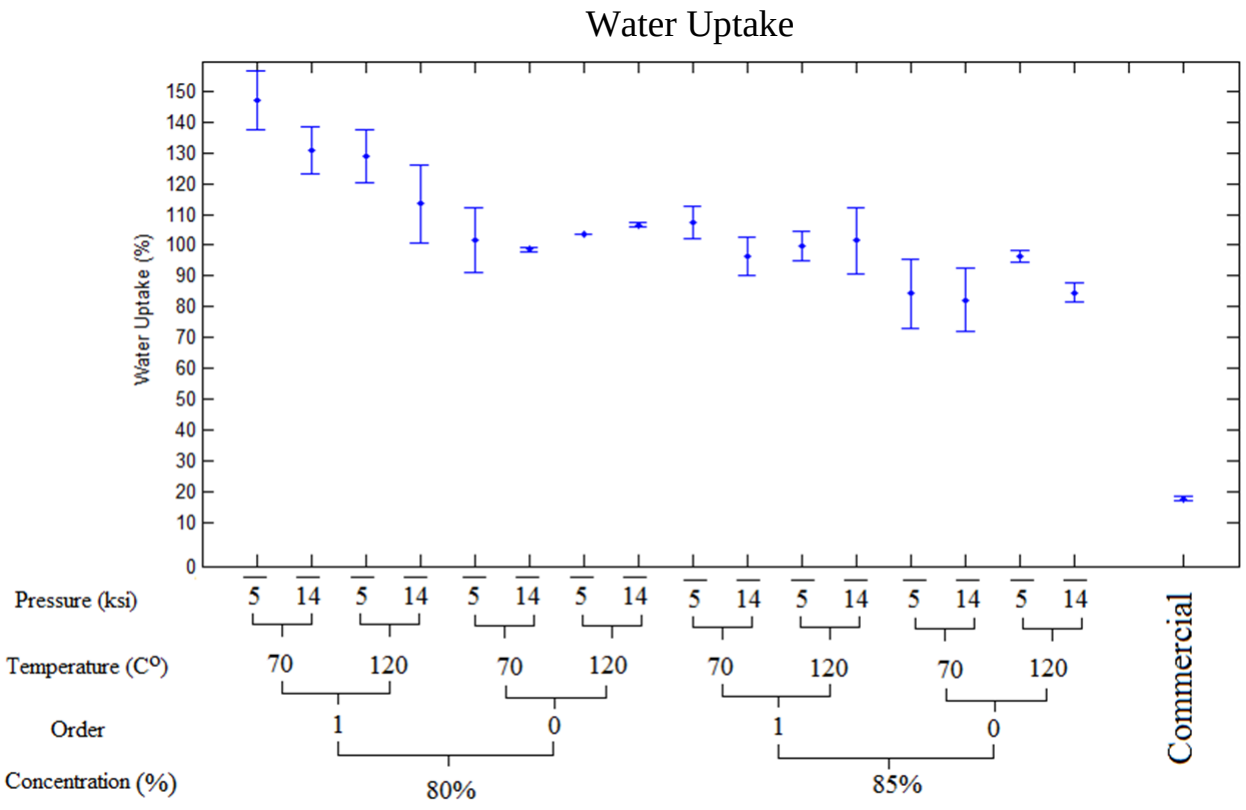

Figure 34: Water uptake with standard deviation

Membranes with lower Nafion content have higher water uptake than those with lower Nafion content. Poly Acrylic Acid (PAA) gives the membrane additional capacity to absorb water. PAA can absorb many times its weight and it is sometimes used in disposable diapers for that reason. But not all the additional water uptake is due to additional PAA. Electrospun membranes are known to swell in water when compared to non-electrospun bulk material [22]. Since the individual fibers have a high surface to area to volume ratio there is easier access to water molecules. In addition, there is no bulk material to mechanically restrict the swelling of the membranes. For such reasons electrospun membranes have increased water uptake when compared to commercial membranes.

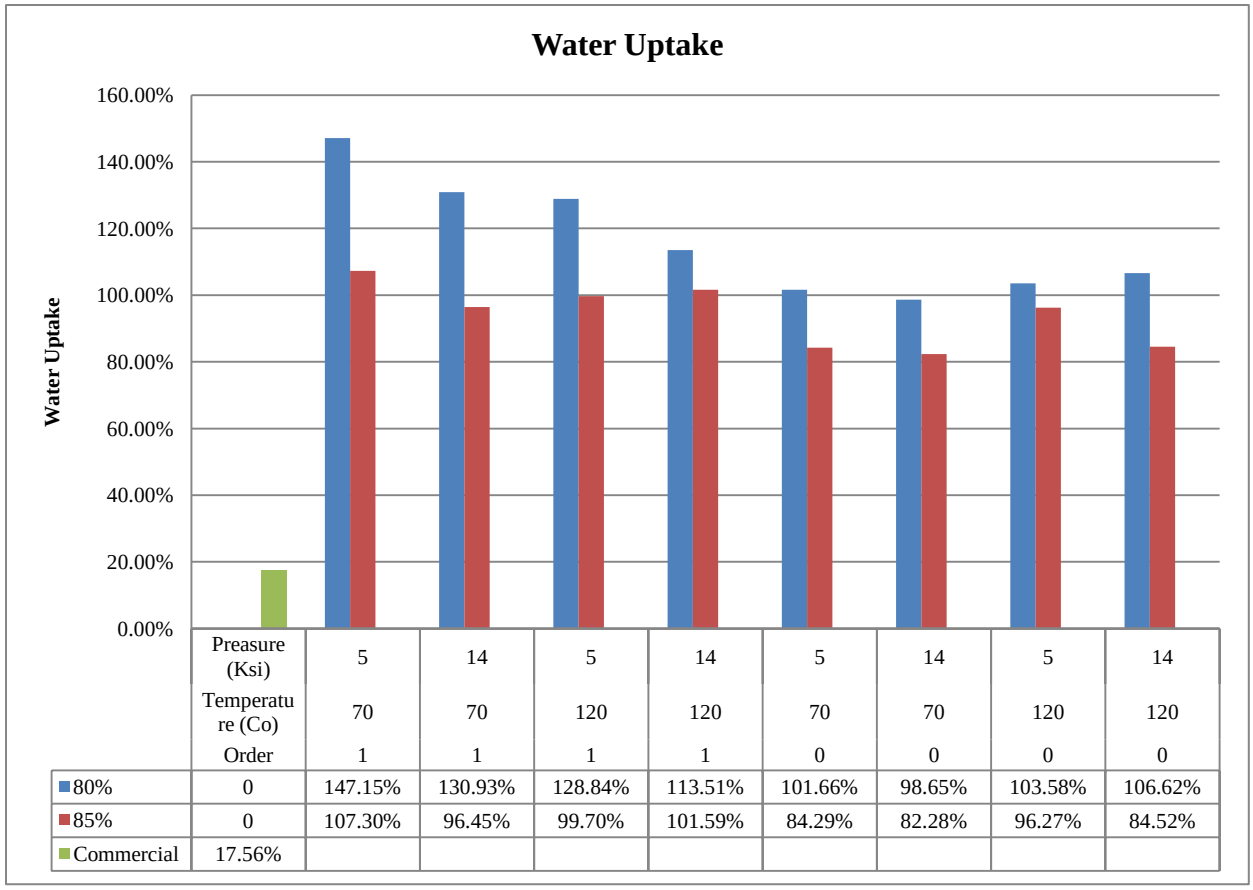

Preasure (Ksi)		5	14	5	14	5	14	5	14
Temperature (Co)		70	70	120	120	70	70	120	120
Order		1	1	1	1	0	0	0	0
80%	0	147.15%	130.93%	128.84%	113.51%	101.66%	98.65%	103.58%	106.62%
85%	0	107.30%	96.45%	99.70%	101.59%	84.29%	82.28%	96.27%	84.52%
Commercial	17.56%								

Figure 35: Average water uptake

Figure 35 shows the average water uptake of the electrospun membranes and commercial Nafion. For both 80% and 85% the maximum water uptake is for the 5 ksi, 70 ^{o}C, and order 1. It is also interesting to note that membranes annealed first and pressed second (order 1) have all higher water uptake than their respective order 0 membranes. Annealing temperature and pressure were found to have little effect on the water uptake.

The electrospun membranes can absorb at least 4.8 times the amount of the commercial membrane. The commercial Nafion membranes absorb a lot less water with only 17.56% water uptake. These values for the commercial membranes are consistent with those reported in the literature[16][8].

4.3 Ion Exchange Capacity

Ion exchange capacity gives valuable information on the ion's accessibility to the membranes exchange site. Membranes can have copious amounts of ion exchange sites but in practice they could be inaccessible. Ion exchange capacity was determined for all 16 data points according to the DOE and a commercial membrane with three repetitions per data point.

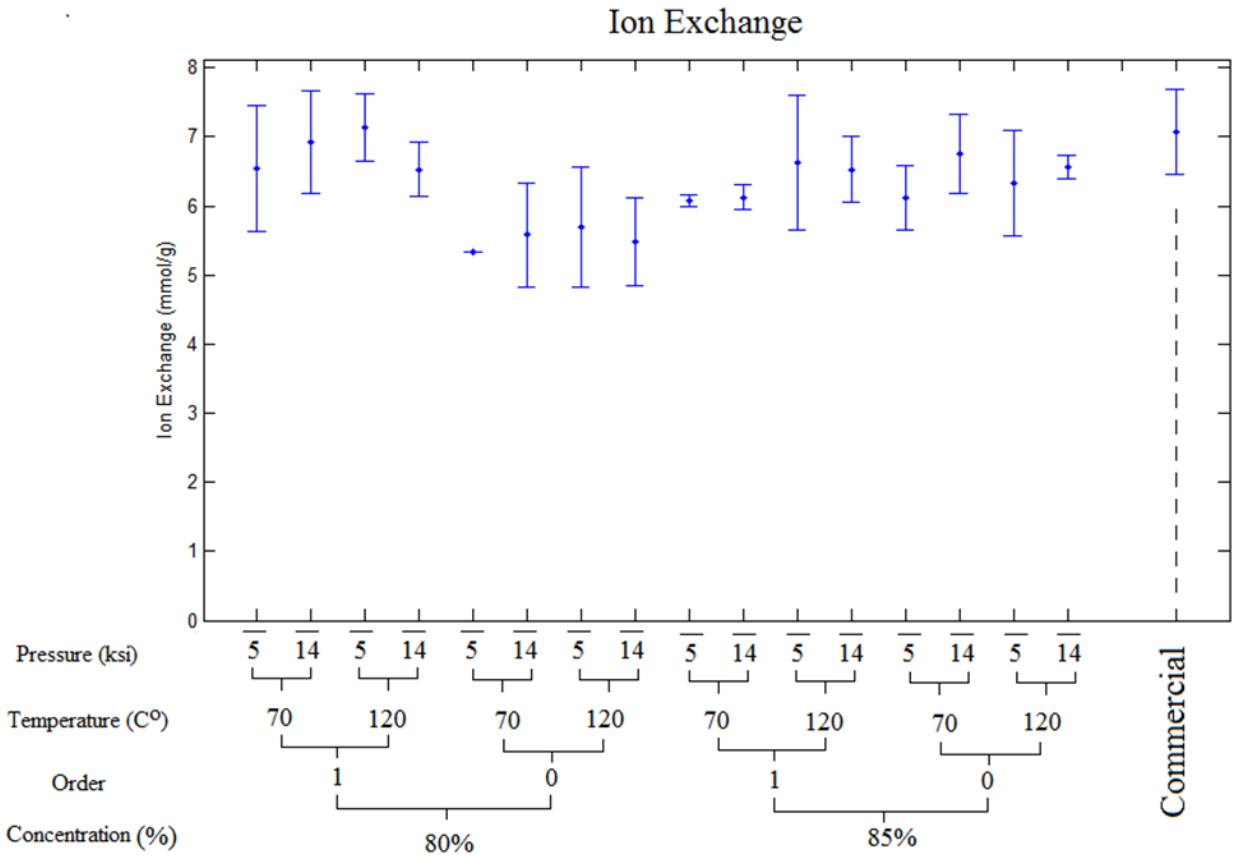

Figure 36: Ion exchange with standard deviation

All membranes have similar ion exchange capacity (IEC) including the commercial membranes with the biggest difference between membranes being 33%. This means that with ample time all membranes have roughly the same amount of accessible exchange sites. For membranes with 80% Nafion all order 1 membrane posses higher IEC than order 0 membranes.

In the case of 85% Nafion there is no clear difference between the order and the IEC. For order 1 membranes the 80% Nafion membranes have higher IEC. In the order 0 membranes the 80% Nafion membranes have lower IEC when compared to the 85% Nafion membranes.

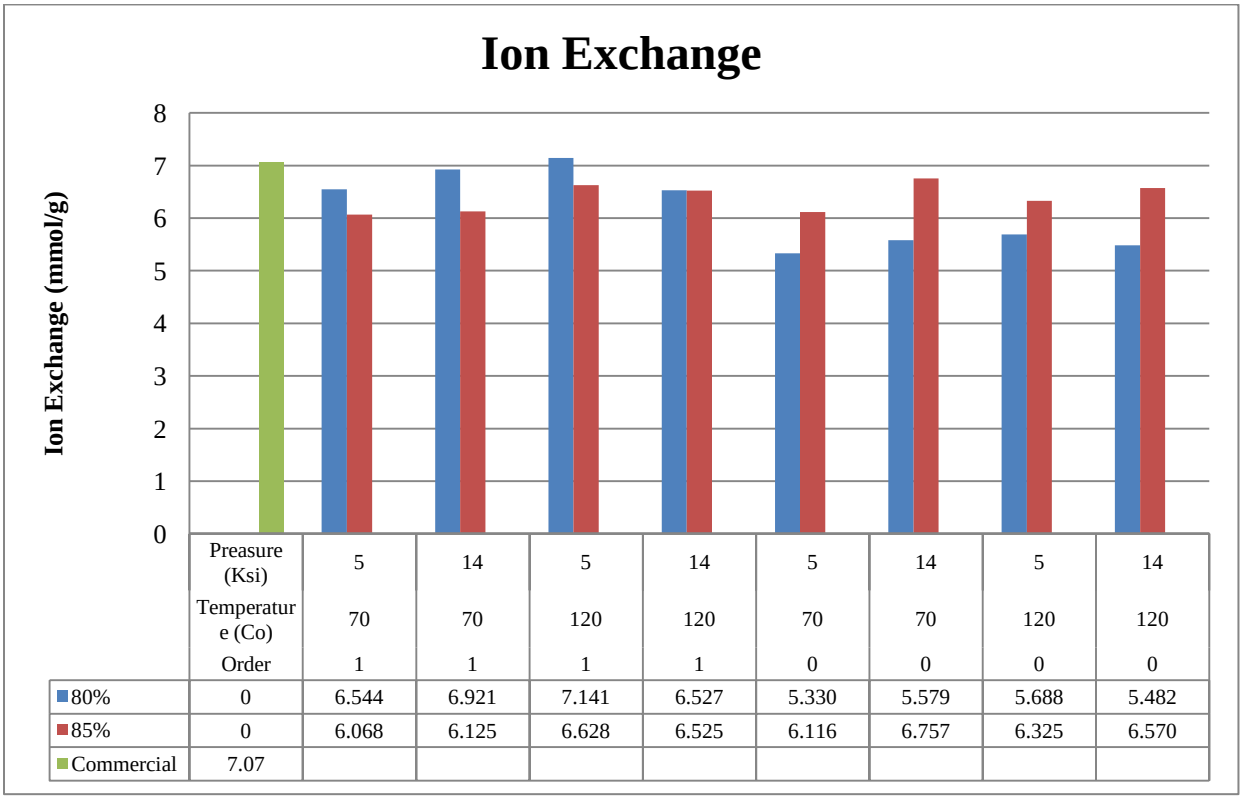

Preasure (Ksi)		5	14	5	14	5	14	5	14
Temperature (Co)		70	70	120	120	70	70	120	120
Order		1	1	1	1	0	0	0	0
80%	0	6.544	6.921	7.141	6.527	5.330	5.579	5.688	5.482
85%	0	6.068	6.125	6.628	6.525	6.116	6.757	6.325	6.570
Commercial	7.07								

Figure 37: Ion exchange capacity for electrospun and commercial membranes

The highest IEC is for 80% Nafion-20% PAA, 120 ^{o}C, 5 ksi, order 1 membranes with 7.141 mmol/g. The lowest IEC belongs to 80% Nafion-20% PAA, 70 ^{o}C, 5 ksi, order 0 membrane with 5.33 mmol/g. The commercial Nafion membranes have an average IEC of 7.07 mmol/g.

The IEC results are very important for establishing a comparison basis. If the IEC of the membranes are very similar, which is the case for the electrospun and commercial membranes, it

is possible to compare the water content to establish superiority in ionic conduction. With similar IEC the difference between better or worst ionic conduction will be determined by the water content of the membranes.

4.4 Water Content

Water content was one of the most important characterizations performed on the membranes since it is related with the ionic conductivity. Water content was determined for all 16 data points according to the DOE and a commercial membrane with three repetitions per data point.

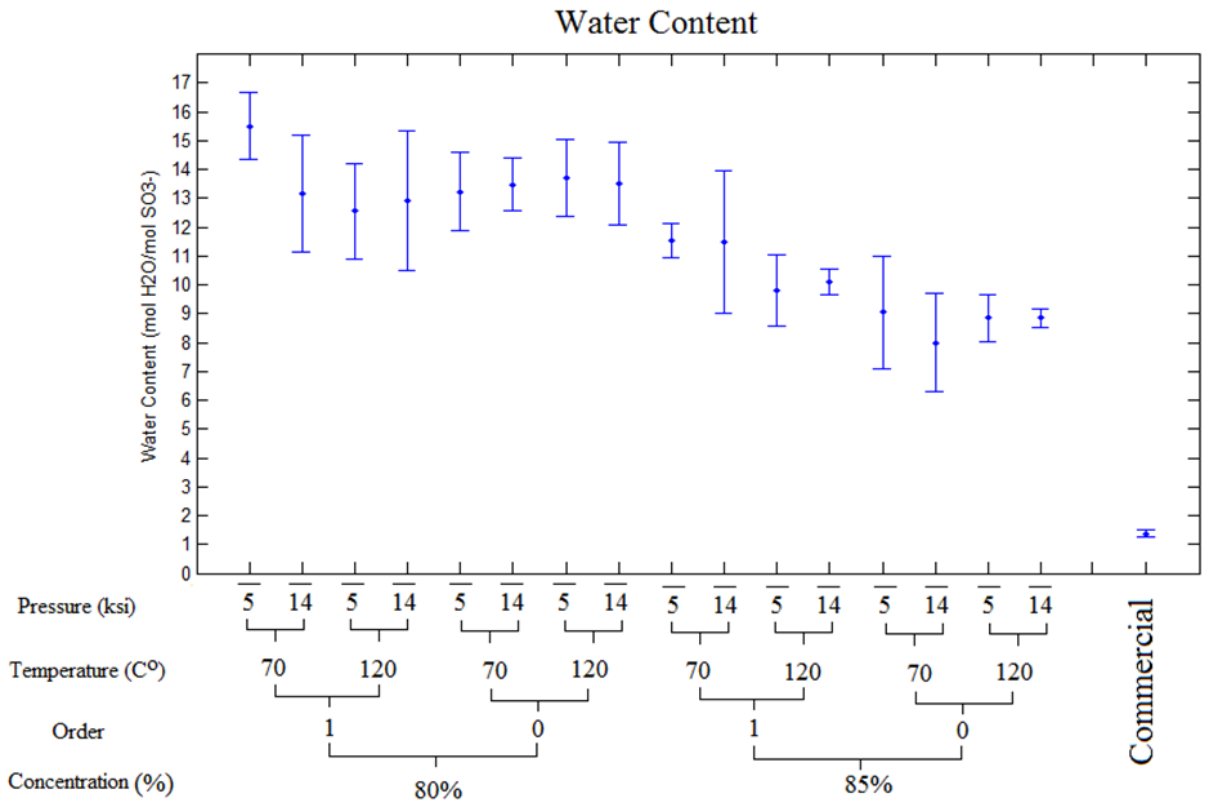

Figure 38: Water content with standard deviation of the electrospun and commercial membranes

Figure 38 shows the water content of the electrospun and commercial membranes. Water content is defined as the ratio between water molecules and exchange sites (see sec 2.1.3 Water Content). All 80% Nafion membranes have higher water content that the 85% Nafion membranes. That is because even though they have similar IEC, 80% Nafion membranes can

absorb more water. The commercial membranes have very low water content because they can't absorb as much water as the electrospun membranes. Pressure and temperature have no significant effects on the water content. Water content has the highest standard deviation because it combines errors from both water uptake and IEC.

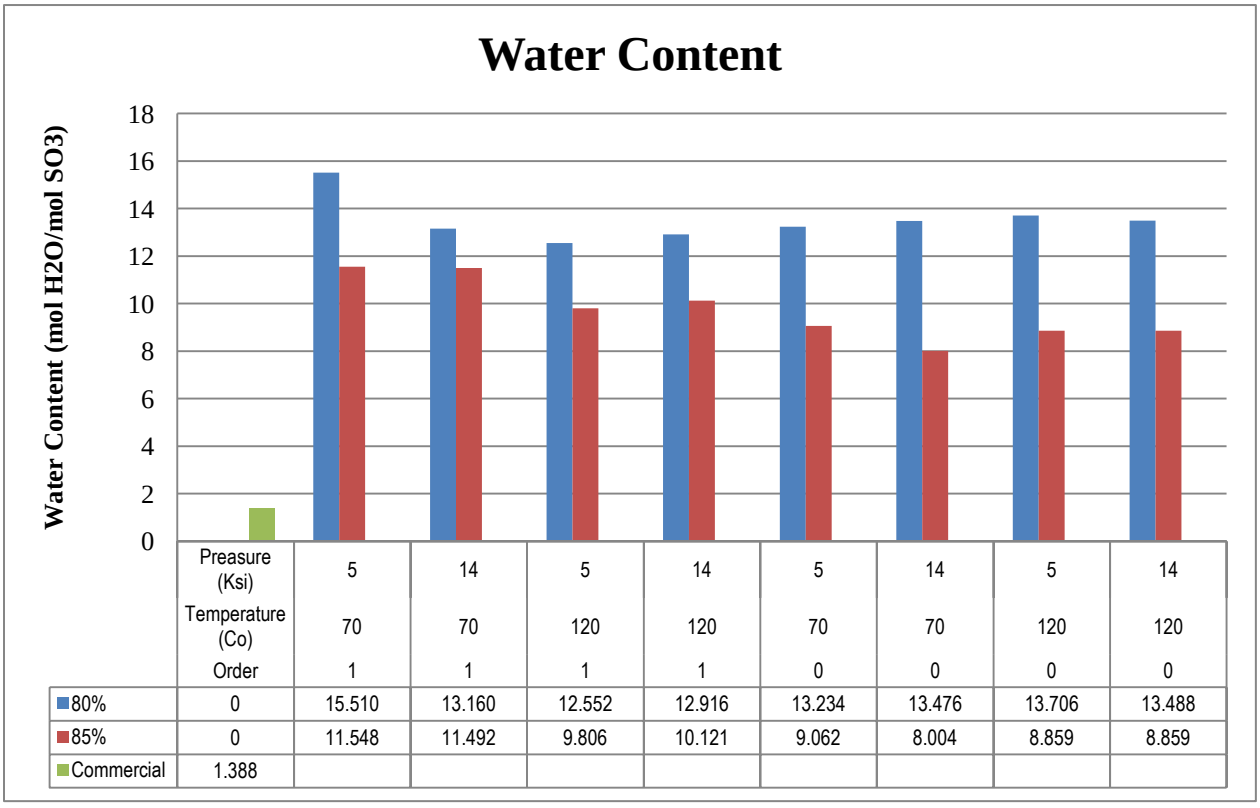

Preasure (Ksi)		5	14	5	14	5	14	5	14
Temperature (Co)		70	70	120	120	70	70	120	120
Order		1	1	1	1	0	0	0	0
80%	0	15.510	13.160	12.552	12.916	13.234	13.476	13.706	13.488
85%	0	11.548	11.492	9.806	10.121	9.062	8.004	8.859	8.859
Commercial	1.388								

Figure 39: Water content for electrospun and commercial membranes

The membrane with the highest water content is the 80% Nafion-20% PAA, 70 ^{o}C, 5 ksi, order 1 with 15.510 H2O/ $SO3^{-}$. The lowest water content is the 85% Nafion-15% PAA, 70 ^{o}C, 14 ksi, order 0 with 8.004 H2O/ $SO3^{-}$. The commercial membrane's water content is 1.388 H2O/ $SO3^{-}$, which is 82.6% smaller than the smallest electrospun membranes. The electrospun membrane will have superior ionic conductivity when compared to the commercial Nafion because of the increased water content.

4.5 Ionic Conductivity (Springer Model)

Using the Springer model and the water content of the electrospun and commercial membranes the ionic conductivity was determined. When using the Springer model the water content should be determined with the equivalent weight specified by the manufacturer (EW 1100) instead of the ion exchange capacity. The maximum reported water content of 22 (H2O/SO3) for a regular Nafion membrane was also used to calculate the ionic conductivity [17][8]. Figure 40 shows the ionic conductivity of the electrospun and commercial membranes.

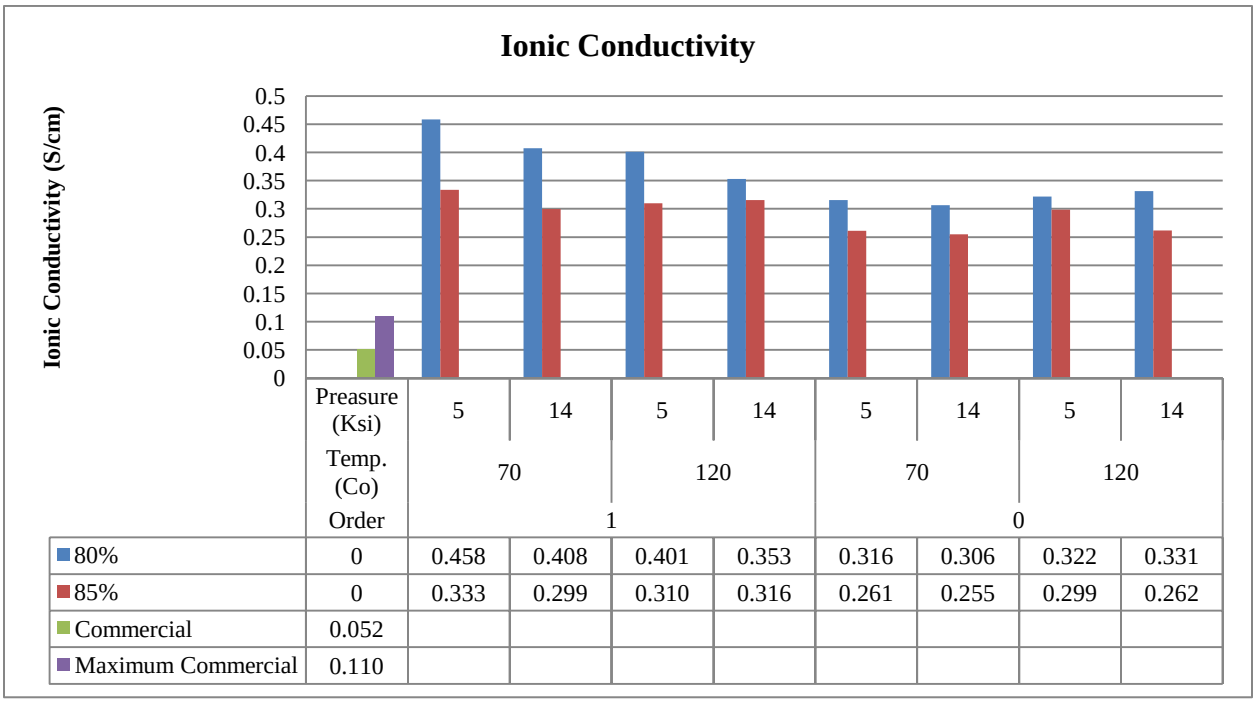

Preasure (Ksi)		5	14	5	14	5	14	5	14
Temp. (Co)		70		120		70		120	
Order		1				0			
80%	0	0.458	0.408	0.401	0.353	0.316	0.306	0.322	0.331
85%	0	0.333	0.299	0.310	0.316	0.261	0.255	0.299	0.262
Commercial	0.052								
Maximum Commercial	0.110								

Figure 40: Ionic conductivity according to the Springer Model

Based on the water content, the commercial membrane would have an ionic conductivity of 0.052 (S/cm). Using the maximum reported water content, commercial membranes have an ionic conductivity of 0.110 (S/cm). The difference between the levels of water content for the commercial membrane and those reported in the literature is due to the cleaning and activation

process. As part of the activation procedure membranes are usually boiled in water, a step known to increase water uptake and water content.

The maximum ionic conductivity for the electrospun membranes was for the 80% Nafion-20% PAA, 70 oC, 5 ksi, order 1 with 0.458 (S/cm), an increase of 784.21 % over the commercial membrane. The increased water content is a consequence of the increased water uptake as mentioned in the previous section. It is important to remember that these results are based on a model and should not be taken as the actual ionic conductivity of an operational fuel cell. These results help gage the potential of the electrospun membranes for fuel cell application.

4.6 Solubility

The electrospun membrane's solubility was tested in water by immersing the membranes in water for three weeks. The membranes were found to virtually insoluble in water at ambient conditions. The membranes are highly stable in water and in ambient conditions showing no sign of decomposition even after six months. Since water had no effect, the membranes were tested with more a hostile solvent, propanol-2 with ultrasonic vibrations. The membranes were submerged in propanol-2 (70%) for 48 hour the solubility was determined for two 80% Nafion-20% PAA membranes annealed at 70 ^{o}C and 120 ^{o}C respectively. The same thing was done for 85% Nafion-20% PAA membranes annealed at 70 ^{o}C and 120 ^{o}C . Non-processed membranes were also tested to determine their solubility.

Table 8: Solubility of Electrospun Membranes

Nafion %	Heat Treatment Temperature (Co)	Solubility
80	70	-86.49%
85	70	-81.25%
85	120	-43.05%
80	120	-44.00%
Non-Processed 80%	0	-83.05%
Non-Processed 85%	0	-80.25%

Figure 41 plots the solubility and Table 8 summarizes the solubility results for the electrospun polymer electrolyte membranes. Although annealing temperature was found to have no significant effect on the water uptake, IEC and water content of the membranes it does seem to have an effect on the solubility of the membranes. Membranes with annealing at 120 ^{o}C were found to 190% less soluble than those with annealing at 70 ^{o}C or those with no annealing. Membranes with Nafion concentrations of 80% were found to be slightly more soluble than those with 85% Nafion concentration. This is expected due the level of solubility of PAA, which

can completely dissolve in water in a matter of hours. An additional test was carried out on a single 80% Nafion membrane with increased temperature of 130 ^{o}C and dwell time of 1 hour to determine if the increased time and temperature had any effect on the solubility. The membrane had a solubility of -84.72% very similar to the other membranes, showing no improvement.

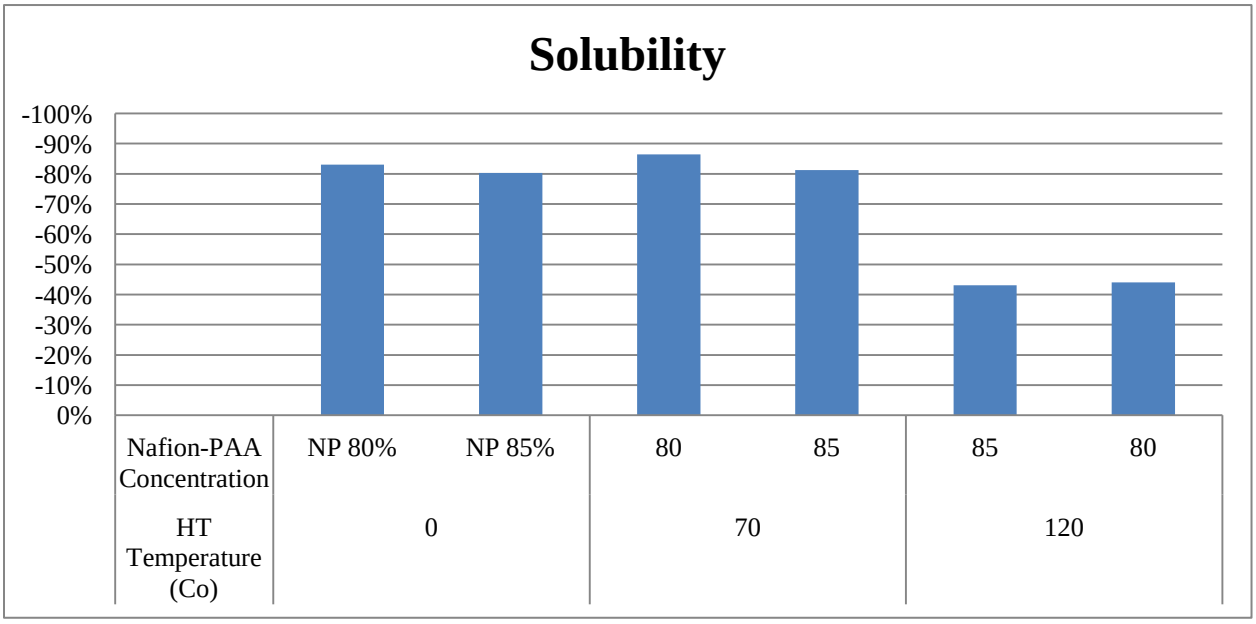

Figure 41: Solubility of electrospun membranes. HT= heat treatment, NP= non-processed electrospun membranes

Membranes heated over the Glass Transition (T_g) temperature of Nafion (110 ^{o}C) have less solubility than those with no heat treatment or with heat treatment below the T_g. That's because the glass transition temperature provides more mobility to the polymer chain allowing the polymer to rearrange its chains in semi-crystalline structure. The semi-crystalline structure provides secondary crystalline bonding. It is this secondary bonding that gives the membranes added resistance against dissolving.

All electrospun membranes are insoluble in water while recast membranes are soluble in water. This implies that the electrospun membranes have some level of crystallinity. The stretching mechanism associated with electrospinning process is imparting some level crystallinity to the membranes. Polymers are known to acquire some level of crystallinity while being drawn [30]. The same phenomenon is responsible for decreased solubility of the electrospun membranes in water.

4.7 Tensile Strength

It is of great importance that the membranes have enough mechanical strength to be used for fuel cell operations. The membranes have to withstand pressure gradients and compression while within the fuel cell. The Maximum Tensile Strength (MTS) was determined for four non-processed electrospun membranes and one commercial membrane as summarized in Table 9. The tensile strength of the membranes was then compared to the commercial membranes.

Table 9: Maximum Tensile Strength (MTS)

Nafion Concentration	Order	Temp (^{o}C)	Pressure (ksi)	MTS (Kpa)
80	N/A	N/A	N/A	11.73
80	N/A	N/A	N/A	11.40
85	N/A	N/A	N/A	16.85
85	N/A	N/A	N/A	17.12
Commercial	N/A	N/A	N/A	18.09

The 80% Nafion membranes have similar results with an average of 11.56 kpa. The 85% Nafion membranes have an average of 16.98 kpa. The commercial membrane can withstand 18.09 kpa which is 56% stronger than the average 80% Nafion membranes and 6.5% stronger than the 85% Nafion membranes. DuPont reports Nafion commercial membranes at 50%

relative humidity with maximum tensile strengths of 43 kpa in the machine direction and 32 kpa in the transverse direction. Membranes with higher levels of relative humidity will have lower MTS.

Membranes with the higher Nafion concentration are stronger because of the added Nafion content. Nafion has tetrafluoroethylene backbone similar to Teflon. This gives Nafion added mechanical strength and resistance to corrosive environments. Poly (Acrylic Acid) has lower melting point than Nafion and poor mechanical properties. Membranes made of pure PAA are very brittle. Although the electrospun membranes are not as strong as the commercial membranes they have sufficient mechanical strength to be used for fuel cell applications.

5. Conclusions

This chapter is divided in to four sections: summary of thesis, conclusions, future work and acknowledgements.

5.1 Summary of thesis

A new type of polymer electrolyte membrane was created with the electrospinning process. The electrospun polymer electrolyte membrane was composed of a Nafion-Poly (Acrylic Acid) blend. Two different blends of Nafion-PAA concentrations were created with the electrospinning process:

1. 80% Nafion- 20% Poly (Acrylic Acid)
2. 85% Nafion- 15% Poly (Acrylic Acid)

The electrospinning process was performed using an oscillating rotating drum collector with the same operating conditions for all membranes:

1. Working distance: 21.5 cm
2. Voltage: 35 kV
3. Relative Humidity: 54%-64%
4. Both motors operate counterclockwise
5. Temperature: 74.8 ^{o}F -76.4 ^{o}F
6. Time: 1 hour.

The electrospun membranes were then processed by performing compacting, annealing, cleaning and activation steps. A design of the experiment was implemented to evaluate the effects of the processing parameters:

- Compacting Pressure
  - 5,000 Psi
  - 14,000 Psi
- Annealing Temperature
  - 70 ^{o}C
  - 120 ^{o}C
- Pressure and Annealing Order
  - Press first, anneal second (order 0)
  - Anneal first, press second (order 1)

Characterization was performed on the membranes to determine important properties such as fiber orientation, fiber diameter distribution, water uptake, ion exchange capacity, water content, solubility and tensile strength. The results were analyzed and important information was determined as summarized in Table 10.

Table 10: Summary of characterization techniques and results

Characterization	**Determines**	**Results**
Fiber Orientation	The average alignment percentage and average fiber orientation	Fiber orientation is only determined by the collecting mechanism
Fiber Diameter Distribution	Distribution, average and standard deviation of fiber diameter	The higher the Nafion content the smaller the fiber diameter
Water Uptake	How much water is absorbed by the membrane	Electrospun membranes absorb significantly higher levels of water
Ion Exchange	How accessible are the ion exchange sites within the membranes	Electrospun membranes have comparable ion exchange sites with commercial membranes
Water Content	The ratio between water molecules and sulfonated exchange sites	Electrospun membranes have superior water content and thus superior ionic conductivity when compared with commercial membranes.
Solubility	How well do the membranes withstand dissolution in a hostile environment.	Partial crystallinity is obtained through electrospinning and solubility is decreased by annealing above T_g
Maximum Tensile Strength	How strong are the membranes when stretched	Electrospun membranes are weaker than commercial membranes but still have enough strength for use in fuel cell applications.

5.2 Conclusions

Electrospun polymer electrolyte membranes for fuel cell application were created and characterized. All electrospun membranes were found to have higher water uptake and water content than the commercial membranes. The 80% Nafion-20% PAA polymer blends were found to have higher water uptake and water content than the 85% Nafion-15% PAA polymer blends. Since all the membranes, including the commercial ones, have similar ion exchange capacity those with the highest water content will have superior ion conductivity. Membranes annealed first and compacted afterwards (order 1) where found to have higher water uptake, ion exchange capacity and water content than membranes with the opposite order. Annealing temperature and compacting pressure were found to have little effect on the water uptake, ion exchange and water content of the membranes. Membranes created with 80% Nafion-20% PAA blend annealed first and compacted afterwards will have the highest water content.

The annealing temperature had no effect on the water content of the electrospun membranes but did increase their crystallinity and reduced their solubility. Electrospun membranes annealed at 120 ^{o}C will have less solubility than those annealed at 70 ^{o}C. All electrospun membranes were found to possess some degree of crystallinity acquired through the stretching mechanism inherent to the electrospinning process. The stretching has the same similar effect as drawing which is known to increase the crystallinity in polymers.

The maximum tensile strength of the electrospun membranes was higher for membranes with increased Nafion content. Nafion has a tough Teflon-like backbone which gives it durability and strength. Reducing the Nafion content to levels below 80% will at some point compromise the mechanical strength of the electrospun membranes to unacceptable levels. The compacting pressure had no effect in any of the characterization results. This implies that there

is a level of compacting pressure below the minimum used in the experiments (5ksi) which will have an effect on the characterization results.

The oscillating drum collector was found to reduce the defects and create more homogeneous membranes. The average percent of fiber orientation and the average fiber orientation were found to be dependent only on the oscillating drum collector mechanism. The fiber diameter distribution was found to be related to the percent of Nafion content in the precursor polymer solution. The higher the Nafion content in the polymer solution the higher the conductivity of the polymer blend. The higher the conductivity in the electrospinning polymer solutions the thinner the fibers when electrospun.

Considering all the results, the best membrane for fuel cell applications would be the 80% Nafion-20% PAA, annealed first at 120 ^{o}C, and compacted after that at 5 ksi with an increase in water content of over 1,017%. The overall parameters and their effect on the electrospun membranes are summarized in Table 11.

Table 11: Summary of the overall parameters and their effects on the electrospun membranes

Parameter:	**Effects:**
Polymer blend Concentration	• Fiber diameter Size • Water uptake, IEC and water content • Maximum tensile strength
Processing Order	• Water uptake, IEC and water content
Annealing temperature	• Solubility
Compacting pressure	• None
Oscillating drum collector	• Fiber orientation

5.3 Future Work

Electrospun polymer electrolyte membranes have shown very good potential for use in Polymer Electrolyte Membrane Fuel Cells (PEMFC). Short term future work will focus on using the electrospun membranes in actual fuel cell applications. In situ characterization should be performed on PEMFC with methanol-air and hydrogen-oxygen as fuels. Characterization should look at the ionic conductivity and the fuel crossover of the electrospun membranes as well as power density curves. Detail studies on the maximum tensile strength could be performed to investigate the effect of relative humidity and membrane processing parameters on the mechanical properties of the membranes. The minimum compacting pressure threshold can be determined with additional experiments in order to optimize manufacturing processes.

Medium term future work should focus on adding electrospun catalysts and electrode layers directly to the electrospun membrane. The high surface area to volume ratio should help to improve fuel cell performance. In addition, the membrane electrolyte assembly could potentially be manufactured in one step while electrospinning. Eventually all the acquired techniques and knowledge could be implemented to create a hybrid cylindrical fuel cell.

5.4 Acknowledgements

This work would not be possible without funding from Argonne National Laboratories and the Mechanical Engineering Department.

I would like to thank in no particular order:

- My advisor Ricky Valentin for all his support and help throughout my master.
- My colleagues Ana Lucia Vega, Alfredo Diaz and Carlos Morales.
- My undergraduate assistants Rolizmar Vega, Cyd Zamot and Alexander Marrero.
- My family for always inspiring me to improve.
- Professor Wilfredo Otaño and the University of Puerto Rico at Cayey for their valuable help.
- My University friends for providing the mental reprieve necessary to keep my mind sane.
- Last but not least, I would like to thank my lovely girlfriend Amabel Reyes for all her help and inspiration.

6. References

[1] D. J. N. Michael W. Eillis, Michael R. Von Spakovsky, "Fuel Cell Systems: Efficient, Flexible Energy Conversion for the 21st Century," *IEEE*, vol. 89, no. 12, pp. 1808-1818, 2001.

[2] S. Patrick Davis, Chalk, "DOE Hydrogen Program Record," 2006.

[3] D. of Energy, "Comparison of Fuel Cell Technologies." .

[4] "Nafion2.svg," *Wikipedia*, 2009. [Online]. Available: http://en.wikipedia.org/wiki/File:Nafion2.svg.

[5] K. a Mauritz and R. B. Moore, "State of understanding of nafion.," *Chemical reviews*, vol. 104, no. 10, pp. 4535-85, Oct. 2004.

[6] R. B. Moore, "Chemical and Morphological Properties of Solution-Cast Perfluorosulfonate Ionomers," *Macromolecules*, vol. 21, pp. 1334-1339, 1988.

[7] T. Tamura and H. Kawakami, "Aligned electrospun nanofiber composite membranes for fuel cell electrolytes.," *Nano letters*, vol. 10, no. 4, pp. 1324-8, Apr. 2010.

[8] F. B. P. R. O'Hayre, S.-W. Cha, W. Colella, *Fuel Cell Fundamentals*, Second. John Wiley & Sons, 2009.

[9] M. Unlü, J. Zhou, and P. a Kohl, "Hybrid polymer electrolyte fuel cells: alkaline electrodes with proton conducting membrane.," *Angewandte Chemie (International ed. in English)*, vol. 49, no. 7, pp. 1299-301, Feb. 2010.

[10] M. Ünlü, J. Zhou, and P. a. Kohl, "Study of Alkaline Electrodes for Hybrid Polymer Electrolyte Fuel Cells," *Journal of The Electrochemical Society*, vol. 157, no. 10, p. B1391, 2010.

[11] M. Ünlü, J. Zhou, and P. a. Kohl, "Hybrid Anion and Proton Exchange Membrane Fuel Cells," *The Journal of Physical Chemistry C*, vol. 113, no. 26, pp. 11416-11423, Jul. 2009.

[12] M. Ünlü, J. Zhou, and P. a. Kohl, "Self Humidifying Hybrid Anion-Cation Membrane Fuel Cell Operated Under Dry Conditions," *Fuel Cells*, no. 1, p. NA-NA, Sep. 2009.

[13] H. Chen, J. D. Snyder, and Y. a. Elabd, "Electrospinning and Solution Properties of Nafion and Poly(acrylic acid)," *Macromolecules*, vol. 41, no. 1, pp. 128-135, Jan. 2008.

[14] T. D. Gierke, G. E. Munn, and F. C. Wilson, "The morphology in nafion perfluorinated membrane products, as determined by wide- and small-angle x-ray studies," *Journal of Polymer Science: Polymer Physics Edition*, vol. 19, no. 11, pp. 1687-1704, 1981.

[15] J. Choi, K. M. Lee, R. Wycisk, P. N. Pintauro, and P. T. Mather, "Nanofiber Network Ion-Exchange Membranes," *Macromolecules*, vol. 41, no. 13, pp. 4569-4572, Jul. 2008.

[16] G. Gebel, “Structural evolution of water swollen perfluorosulfonated ionomers from dry membrane to solution,” *Science*, vol. 41, pp. 5829-5838, 2000.

[17] P. D. Beattie et al., “Ionic conductivity of proton exchange membranes,” *Science*, vol. 503, pp. 45-56, 2001.

[18] M. M. Nasef and A. A. Aly, “Water and charge transport models in proton exchange membranes: An overview,” *Desalination*, vol. 287, pp. 238-246, Feb. 2012.

[19] J. E. Soc, A. The, E. Society, T. E. Springer, T. A. Zawodzinski, and S. Gottesfeld, “Polymer Electrolyte Fuel Cell Model,” vol. 138, no. 8, pp. 2334-2342, 1993.

[20] R. Bajon, S. Balaji, and S. M. Guo, “Electrospun Nafion Nanofiber for Proton Exchange Membrane Fuel Cell Application,” *Journal of Fuel Cell Science and Technology*, vol. 6, no. 3, p. 031004, 2009.

[21] C. Nah, Y. Lee, B. Cho, H. Yu, B. Akle, and D. Leo, “Preparation and properties of nanofibrous Nafion mats for ionic polymer metal composites,” *Composites Science and Technology*, vol. 68, no. 14, pp. 2960-2964, Nov. 2008.

[22] J. Choi, K. M. Lee, R. Wycisk, P. N. Pintauro, and P. T. Mather, “Nanofiber Network Ion-Exchange Membranes,” *Scanning*, pp. 4569-4572, 2008.

[23] L. a Zook and J. Leddy, “Density and solubility of nafion: recast, annealed, and commercial films.,” *Analytical chemistry*, vol. 68, no. 21, pp. 3793-6, Nov. 1996.

[24] T. Tamura and H. Kawakami, “Aligned electrospun nanofiber composite membranes for fuel cell electrolytes.,” *Nano letters*, vol. 10, no. 4, pp. 1324-8, Apr. 2010.

[25] S. W. Choi, Y.-Z. Fu, Y. R. Ahn, S. M. Jo, and a. Manthiram, “Nafion-impregnated electrospun polyvinylidene fluoride composite membranes for direct methanol fuel cells,” *Journal of Power Sources*, vol. 180, no. 1, pp. 167-171, May 2008.

[26] H. Rivera, “Hands-On Fuel Cell Membrane Electrode Assembly Short Course.” 2010.

[27] E. Valenzuela et al., “Proton Charge Transport in Nafion Nanochannels,” *Journal of Nano Research*, vol. 5. pp. 31-36, 2009.

[28] T.-yung Chen and J. Leddy, “Ion Exchange Capacity of Nafion and Nafion Composites,” *Technology*, vol. 95, no. 9, pp. 2866-2871, 2000.

[29] T. Schmatko, P. Colomban, and A. Gruger, “Nanostructure of Na ® on 1 membranes at different states of hydration An IR and Raman study,” *Water*, vol. 26, 2001.

[30] A. Brent Strong, *Plastics; Materials and Processing*, Third Edit. Columbus, Ohio: Pearson Prentice Hall, 2006.

[31] K. Asaka, N. Fujiwara, K. Oguro, K. Onishi, and S. Sewa, “State of water and ionic conductivity of solid polymer electrolyte membranes in relation to polymer actuators,” *Journal of Electroanalytical Chemistry*, vol. 505, no. 1-2, pp. 24-32, Jun. 2001.

7. Appendix A: Design of Experiment Analysis

The DOE was analyzed with a regression analysis in order to determine which membrane concentration and processing variables had an effect on the water uptake, IEC and water content. Table 12 summarizes parameters chosen for the DOE factorial. The regression analysis was performed with Minitab software. All data points had two replicas for a total of 48 data points.

Table 12: DOE overview for four factors with two levels.

Factor	Levels	High	Low
Nafion Concentration (%wt)	2	85%	80%
Processing Order	2	1	0
Annealing Temperature (^{o}C)	2	120	70
Compacting Pressure (Ksi)	2	14	5

7. 1 Water Uptake Regression Analysis

```
The regression equation is
Water Uptake = 4.73 - 0.0446 Concentration + 0.210 Order - 0.000352 Temp
               - 0.00753 Pressure

Predictor            Coef    SE Coef      T      P
Constant           4.7343     0.4723  10.02  0.000
Concentration   -0.044630   0.005670  -7.87  0.000
Order             0.20951    0.02835   7.39  0.000
Temp           -0.0003520  0.0005670  -0.62  0.538
Pressure        -0.007533   0.003150  -2.39  0.021

S = 0.0982152   R-Sq = 74.0%   R-Sq(adj) = 71.6%
```

Figure 42: Minitab output for regression analysis of water uptake.

Figure 46 shows the Minitab output for the regression analysis of water uptake. It is very important to note that the P-values for the concentration and order are very small (> 0.0005). The temperature has a very high P-value indicating it is not statically significant. The pressure is borderline significant depending on the significant level that is chosen. A 5% significant level would make it statically significant while a 1% significant level would make it statically insignificant.

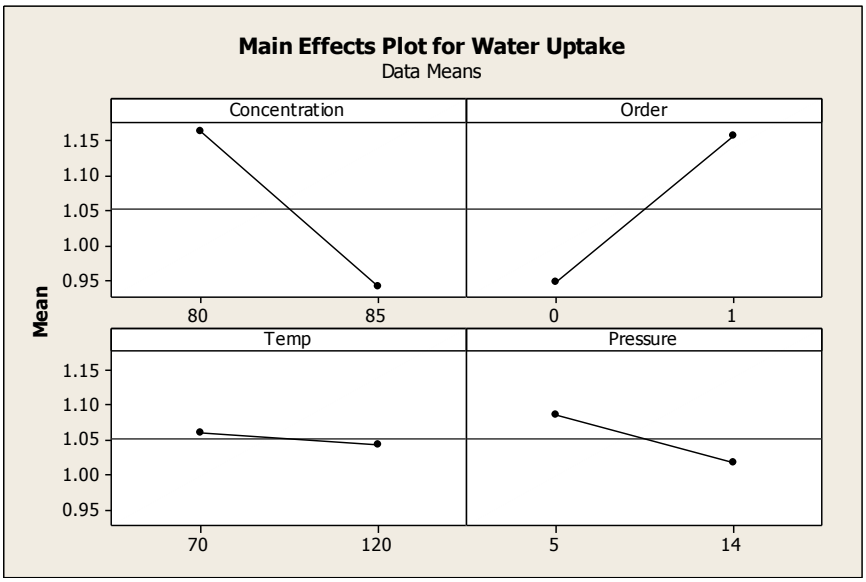

Figure 43: Main effects plot for water uptake

Figure 43 shows the main effects of four different factors on the water uptake. It is seen how concentration and order have the biggest effects on the water uptake. 80% Nafion and order 1 membranes will have higher water uptake.

7.2 Ion Exchange Capacity Regression Analysis

```
The regression equation is
Ion Exchange = 1.95 + 0.0441 Concentration + 0.575 Order + 0.00383 Temp
               + 0.0072 Pressure

Predictor          Coef   SE Coef     T      P
Constant          1.954     3.242  0.60  0.550
Concentration   0.04406   0.03892  1.13  0.264
Order            0.5750    0.1946  2.95  0.005
Temp           0.003828  0.003892  0.98  0.331
Pressure        0.00724   0.02162  0.33  0.740

S = 0.674126   R-Sq = 20.5%   R-Sq(adj) = 13.1%

Analysis of Variance

Source          DF       SS      MS     F      P
Regression       4   5.0405  1.2601  2.77  0.039
Residual Error  43  19.5412  0.4544
Total           47  24.5817
```
Figure 44: Minitab output for regression analysis of Ion Exchange Capacity.

The IEC has little correlation with the regression analysis. This is because the IEC capacity was very similar for all electrospun and commercial membranes. The only factor with a statistically significant level is the order with a P-value of 0.005, corresponding to half a percent. The whole regression has P-value of 0.039 and R^2 = 20.5% meaning it fits poorly.

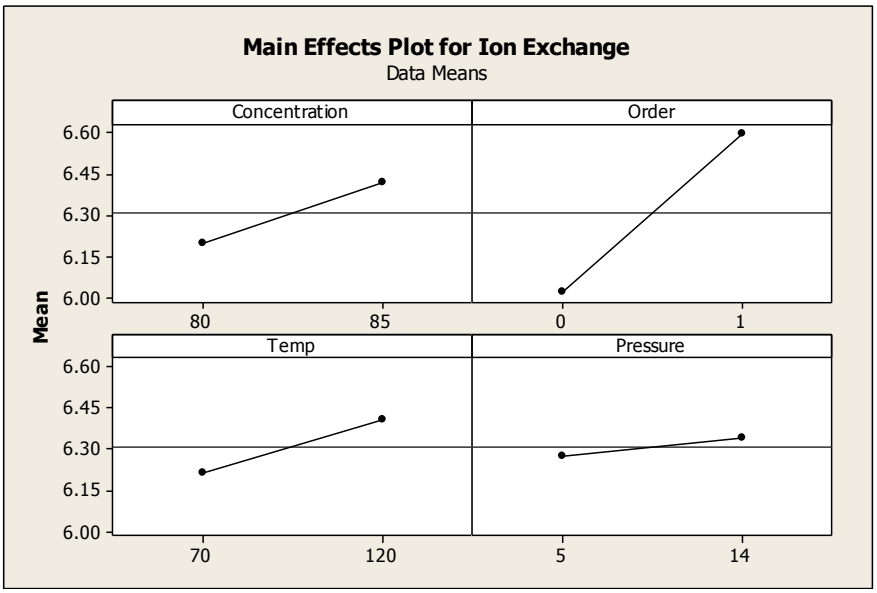

Figure 45: Main effects plots for Ion Exchange Capacity

Figure 45 shows the main effects of the four different factors on the IEC. It is seen how only order has some effect on the IEC. Order 1 membranes have more IEC.

7.3 Water Content Regression Analysis

```
The regression equation is
Water Content = 76.2 - 0.769 Concentration + 1.11 Order - 0.0141 Temp
               - 0.0447 Pressure

Predictor           Coef   SE Coef      T      P
Constant          76.218     7.460  10.22  0.000
Concentration   -0.76878   0.08957  -8.58  0.000
Order             1.1094    0.4479   2.48  0.017
Temp            -0.014098  0.008957  -1.57  0.123
Pressure         -0.04473   0.04976  -0.90  0.374

S = 1.55144   R-Sq = 65.9%   R-Sq(adj) = 62.7%
```

Figure 46: Minitab output for regression analysis of water content.

The most significant factors are the concentration and the order with P-values less than 0.0005 and 0.017 respectively. The annealing temperature and compacting pressure would not pass the null hypothesis with P-Values above 0.123 and 0.374 respectively. The whole regression has R^2 value of 65.9% and a P-value of less than 0.0005. Figure 47 shows the main effects plot for water content. Once again concentration and order have the biggest statistical significance while the temperature and pressure don't. 80% Nafion and order 1 membranes will have higher water content.

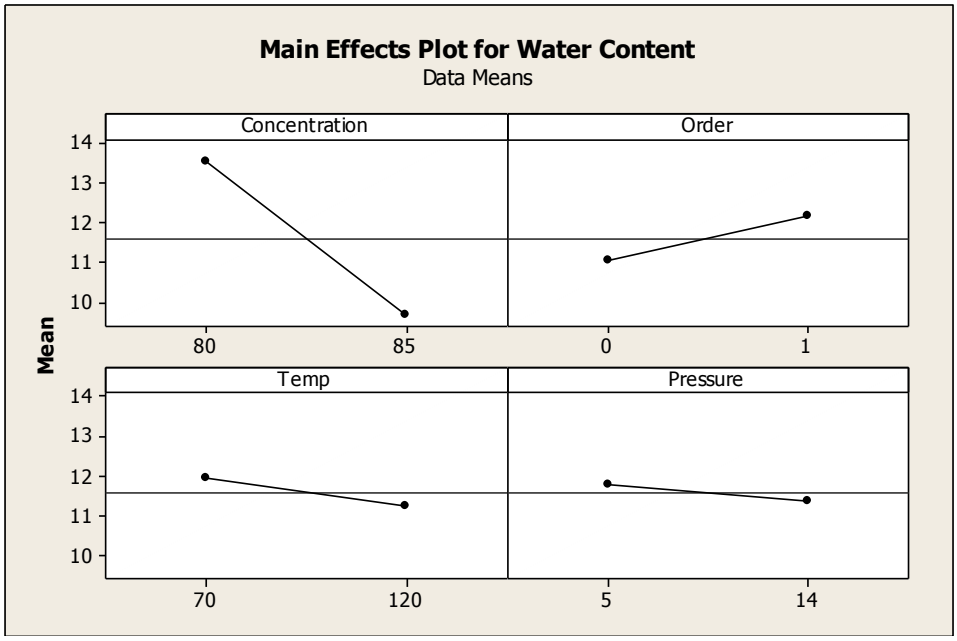

Figure 47: Main effects plot for water content.

7.4 Regression Summary

The results of the regression analysis are summarized in Table 13. These results were used through the thesis but no specific mention of the analysis was made. The P-values of the factors were examined and compared with a significance levels of 5% and 1%. The Nafion concentration had the biggest effect on water uptake and water content but it had no effect on the

IEC. The processing order had an effect on all three characterization techniques. The compacting pressure and annealing temperature had no effect on any of the three characterization techniques.

Table 13: Regression Summary

Characterization	**Statically Significant**	**Best Level**	**Statically Insignificant**	**R^2**
Water Uptake	• Concentration • Order	• 80% • 1	• Temperature • Pressure	• 74.0%
Ion Exchange Capacity	• Order	• 1	• Concentration • Temperature • Pressure	• 20%
Water Content	• Concentration • Order	• 80% • 1	• Temperature • Pressure	• 65.9%

8. Appendix B: Oscillating Drum Collector Analysis

The proposed mechanism described in this section was not constructed as specified in this appendix. The materials and time required to construct such mechanism would have been a thesis project in itself. The following analysis was performed for the sake of completeness.

8.1 Problem Description:

The polymer electrolyte was created through a process known as electrospinning. Electrospinning can create fibers with diameters between 100-2,000 nm. Typically the electrospun fibers are deposited at random on the grounded collector. The oscillating drum collector mechanism will catch the fibers at a predetermined speed and angle to construct a desired pattern.

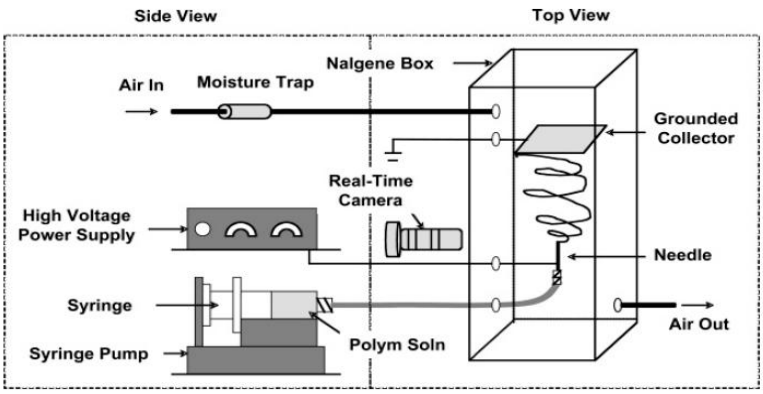

Figure 48: Typical electrospinning setup

Figure 49 illustrates the proposed mechanism. It will require two inputs. One for the spinning drum collector and another for the crank and slider mechanism.

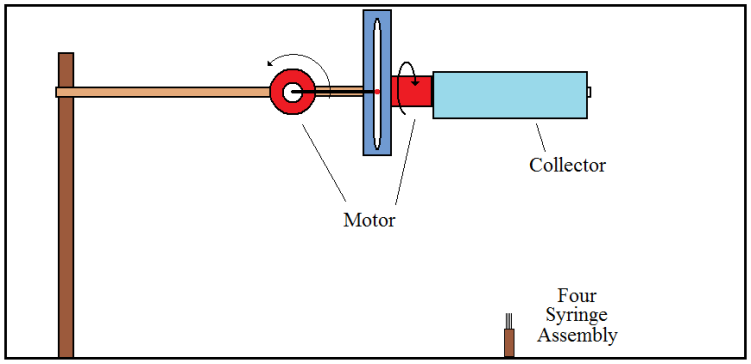

Figure 49: Proposed electrospinning setup

Fiber mat Patterns

The combinations of the two motions as illustrated in Figure 50 will allow the creation of different fiber mat patterns. Figure 51 illustrates the proposed dimensions of the cylinder. Were "D0" is the diameter of the drum collector, "h" is the length of the drum collector and "d" is the diameter of single electrospun fiber.

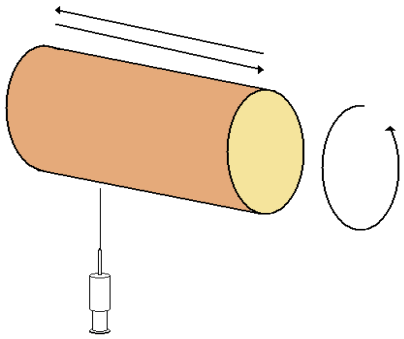

Figure 50: Possible movements of the collector

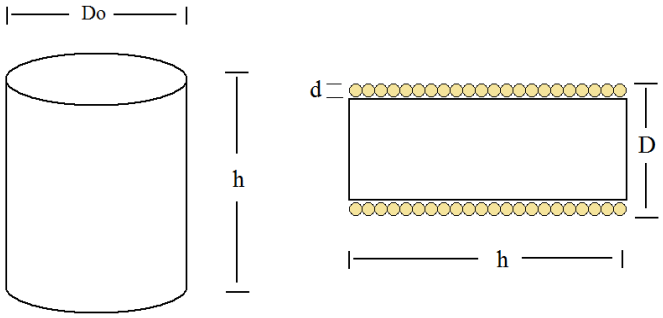

Figure 51: Dimension of the cylinder. h= 14 cm D_o= 2.54 cm d=600 nm

A desired pattern is specified by stating the angle θ. This angle determines a specific ratio between the rotational speed of the cylinder and the horizontal speed of the slider. Figure 52 shows the relations between the angle (θ), translational (Vs) and rotational (wD0/2) speeds. Were "w" is the angular velocity and "D0" is the diameter of the drum collector. Later it will be shown that the rotational speed of the cylinder collector is predetermined by the flow rate and fiber diameter. So the angle actually tells us what slider speed is required to keep a constant speed ratio.

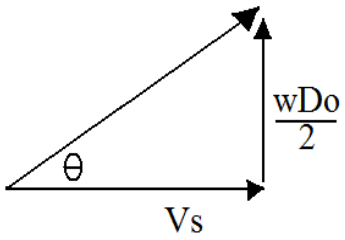

$$V_s = \frac{wD_0}{2\tan(\theta)}$$

$$\theta = \tan^{-1}\left(\frac{wD_o}{2V_s}\right)$$

Figure 52: Relations between the speeds V_s, and angle θ.

8.2 Forbidden Angles

Not all angles (θ) are possible because a situation may arise where the fibers are deposited on top of each other in just a few areas instead of the entire drum collector surface. This happens when ever the angle is such that the fiber intersects any sides at halve intervals. Figure 53 demonstrates an example with an allowed angle (A) and a second with a forbidden angle (B). In the figure the rectangular area is the surface area of the cylinder. The dots represents the first halve interval.

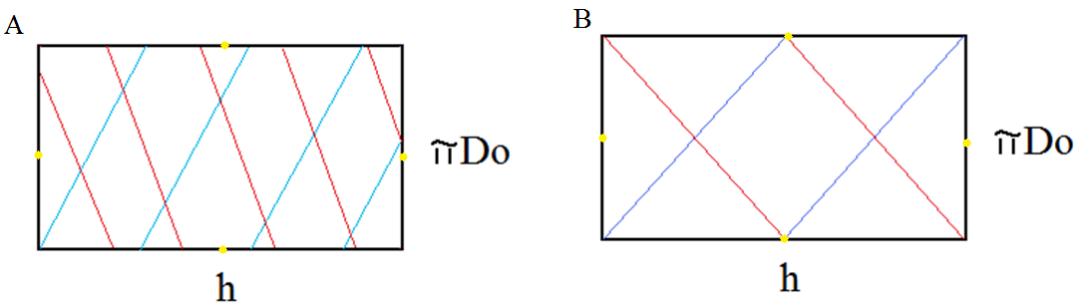

Figure 53: Examples of allowed (A) and forbidden angles (B).

It is possible to derive an equation wish calculates the values of the forbidden angle. Figure 54 graphs the forbidden angles as a function of n, were "n" represents the level of the halve interval.

$$\theta_{bad} = tan^{-1}\left(\frac{\pi D_0}{h2^n}\right)$$

Equation 15: Forbidden Angles

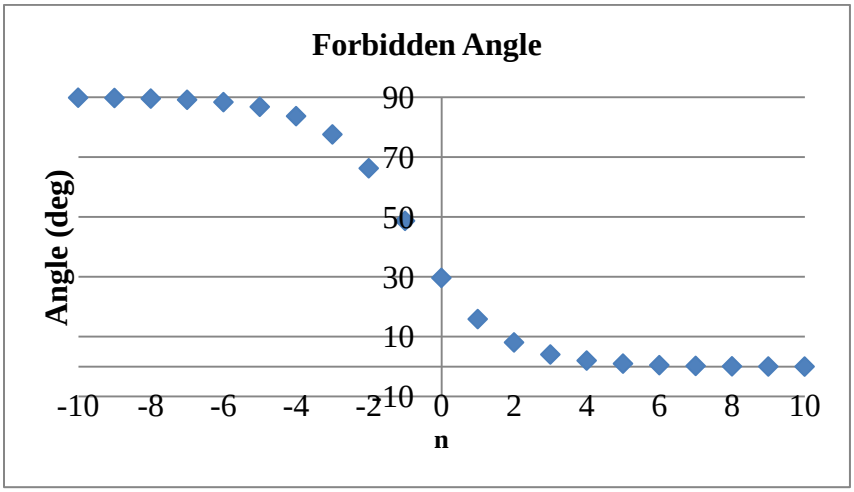

Figure 54: Forbidden angles as Function of n.

8.3 Flow rate and fiber speed velocity

The speed of the fiber is predetermined by the flow rate and the area of fibers. This in term determines the speed of the cylinder which has to match the fiber speed. The velocity of the

fiber and the angular velocity of the cylinder motor are given by Equation 16 and Equation 17. Were "Q"is the flow rate of the polymer solution through the syringe and "A_f" is the cross sectional area of the fiber. The designated flow rate will be Q=0.01 ml/h. Table 1Table 14summarizes the oscillating drum collector parameters.

$$Vel_f = \frac{Q}{A_f} = \frac{4Q}{\pi d^2}$$

Equation 16: Velocity of the fiber

$$w_1 = \frac{2Vel_f}{D_0}$$

Equation 17: Angular velocity of the drum

Table 14: Oscillating drum collector parameters.

Parameters	**Value**
Volumetric flow rate	0.01 ml/h
Velocity of the fibers	58,946 cm/min (22 mph)
Angular Velocity of the drums	W1=1,450 rpm

Using the established relations an equation of the final diameter (D) of the drum as function of time (t) can be determined as seen in Equation 18.

$$D(t) = \sqrt{\frac{4Qt}{\pi h} + D_0^2}$$

Equation 18: Diameter of the drum as function of time.

8.4 Proposed Mechanism

Our proposed mechanism has two inputs ω_1 and ω_2. ω_1 is the motor velocity for the rotating drum collector while ω_2 is the motor velocity for our crank and slider mechanism. Figure 56 shows once again the proposed mechanism with angular velocities while Figure 55 shows the crank and slider mechanism.

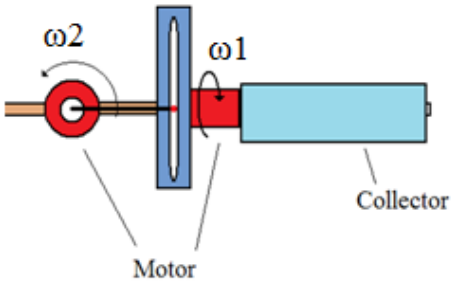

Figure 56: Proposed mechanism

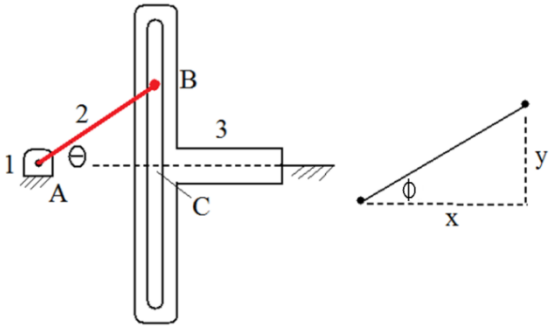

Figure 55: Crank and slider mechanism

Since ω_1 was determined from the flow rate and now we need to determine ω_2. ω_2 has to be such that the velocity of the slider (V_s) follows .

$$V_s = \frac{w_1 D_0}{2\tan(\theta)}$$

Equation 19: Velocity of the slider

Doing a mechanism analysis for the crank and slider the following equations can be constructed were "X_s" is the position of the slider, "V_s" the velocity of the slider and "$\dot{\varphi}$" is ω_2:

$$X_S = l_2 \cos(\varphi)$$

$$Vs = -l_2 \dot{\varphi} \sin(\varphi)$$

$$\varphi = \cos^{-1}\left(\frac{X_s}{l_2}\right)$$

$$\dot{\varphi} = \frac{-Vs}{l_2 \sin(\varphi)}$$

Equation 20: Angular velocity of the crank

Equation 19 and Equation 20 can be combined to obtain the direct relationship between ω_2 and our desired angle for the pattern as seen in Equation 21.

$$\omega_2 = \frac{-wD_0}{2l_2 \tan(\theta)\sin\left(\cos^{-1}\left(\frac{x}{l_2}\right)\right)}$$

Equation 21: Angular velocity of the crank as function of the desired pattern angle

8.5 Time for One Pass

Using the velocity of our slider (Vs) and the length of the cylinder (h) the time it takes to make one pass with the slider can be calculated. In the example ($\theta=75^o$) the slider has a velocity of 5,986.8 cm/min and the time it takes to make one pass is 1.38 seconds. Table 1 summarizes the values of the example. The values of ω_2 were calculated with Equation 21 and graphed as shown in Figure 57. The acceleration was also graphed. It is interesting to note that it is impossible to fallow precisely angular velocity doe to the required angular acceleration as seen in Figure 58. To solve this problem a slack will be left on the cylinder. Of the 14 cm length of the cylinder only 10 cm will be used, providing two centimeters on each side to accelerate to the required angular velocities.

Table 15: Summary of parameters

D_o (cm)	2.54
d (cm)	0.00006
h (cm)	14
Q (cm^3/h)	0.01
Amount of syringes	12
Circumference of cylinder (cm)	7.979
Fiber speed (cm/min)	58,946.28
Fiber speed mph	21.9765
w1 (rpm)	1,450
Vs (cm/min)	5,986.80

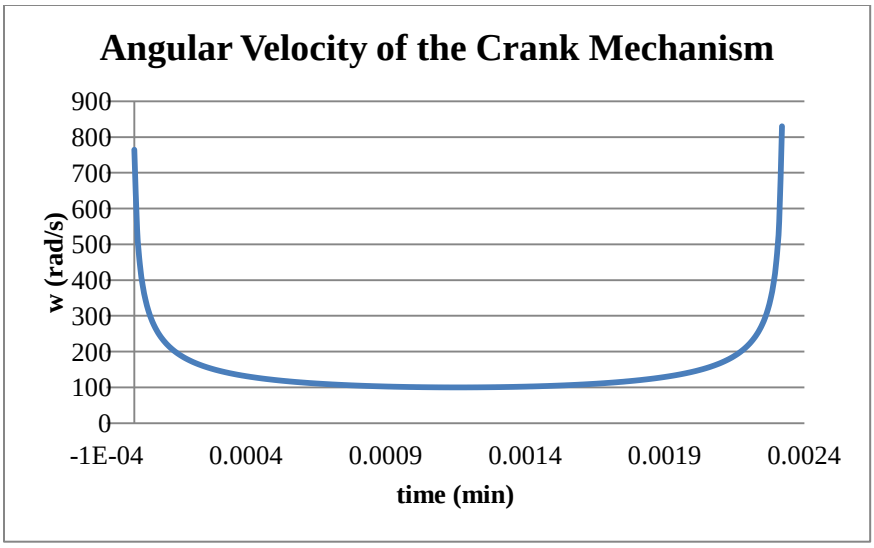

Figure 57: Angular velocity of the crank mechanism as function of time

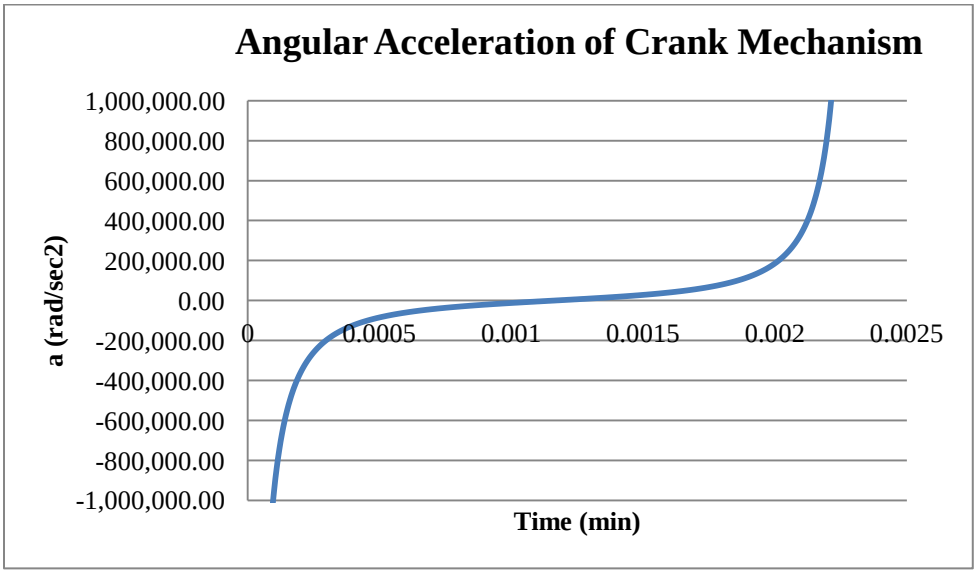

Figure 58: Angular acceleration as function of time.

A very precise motor with the appropriate software can be used to control the angular velocity of the crank mechanism. A desired pattern can be programmed and collected with the proposed mechanism.